We put science to work.™

Savannah River National Laboratory™

OPERATED BY SAVANNAH RIVER NUCLEAR SOLUTIONS

A U.S. DEPARTMENT OF ENERGY NATIONAL LABORATORY • SAVANNAH RIVER SITE • AIKEN, SC

VAPOR SPACE CORROSION TESTING SIMULATING THE ENVIRONMENT OF HANFORD DOUBLE-SHELL TANKS

J. R. Gray
B.L. Garcia-Diaz
T. H. Murphy
K. R. Hicks

December 2013

SRNL-STI-2013-00739, Revision 0

SRNL.DOE.GOV

DISCLAIMER

Printed in the United States of America

Prepared for
U.S. Department of Energy

SRNL-STI-2013-00739
Revision 0

Keywords: Carbon steel, pitting corrosion, waste tanks

Retention: *Permanent*

VAPOR SPACE CORROSION TESTING SIMULATING THE ENVIRONMENT OF HANFORD DOUBLE-SHELL TANKS

J. R. Gray
B. L. Garcia-Diaz
T. H. Murphy
K. R. Hicks

December 2013

Prepared for the U.S. Department of Energy under contract number DE-AC09-08SR22470.

Savannah River National Laboratory™

OPERATED BY SAVANNAH RIVER NUCLEAR SOLUTIONS

REVIEWS AND APPROVALS

AUTHORS:

____

J.R. Gray, Materials Science and Technology Date

____

B.L. Garcia-Diaz, Materials Science and Technology Date

____

T.H. Murphy, Materials Science and Technology Date

____

K.R. Hicks, Materials Science and Technology Date

TECHNICAL REVIEW:

____

R. E. Fuentes, Materials Science and Technology Date

APPROVALS:

____

K .E. Zeigler, Manager, Savannah River National Laboratory Date

____

K. D. Boomer, Program Manager, Washington River Protection Solutions Date

____

J. L. Castleberry, Project Manager, Double Shell/Single Shell Tank Integrity Projects Date
Washington River Protection Solutions

EXECUTIVE SUMMARY

As part of an integrated program to better understand corrosion in the high level waste tanks, Hanford has been investigating corrosion at the liquid/air interface (LAI) and at higher areas in the tank vapor space. This current research evaluated localized corrosion in the vapor space over Hanford double shell tank simulants to assess the impact of ammonia and new minimum nitrite concentration limits, which are part of the broader corrosion chemistry limits.

The findings from this study showed that the presence of ammonia gas (550 ppm) in the vapor space is sufficient to reduce corrosion over the short-term (i.e. four months) for a Hanford waste chemistry (SY102 High Nitrate). These findings are in agreement with previous studies at both Hanford and SRS which showed ammonia gas in the vapor space to be inhibitive.

The presence of ammonia in electrochemical test solution, however, was insufficient to inhibit against pitting corrosion. The effect of the ammonia appears to be a function of the waste chemistry and may have more significant effects in waste with low nitrite concentrations. Since high levels of ammonia were found beneficial in previous studies, additional testing is recommended to assess the necessary minimum concentration for protection of carbon steel.

The new minimum R value of 0.15 was found to be insufficient to prevent pitting corrosion in the vapor space. The pitting that occurred, however, did not progress over the four-month test. Pits appeared to stop growing, which would indicate that pitting might not progress through wall.

TABLE OF CONTENTS

LIST OF TABLES

LIST OF FIGURES

LIST OF ABBREVIATIONS

CPP	Cyclic Potentiodynamic Polarization
DST	Double Shell Tanks
LAI	Liquid Air Interface
mpy	mils per year
OCP	Open-Circuit Potential
sccm	standard cubic centimeters per minute
R	Nitrite/Nitrate ion ratio
SRS	Savannah River Site

1.0 Introduction

As part of an integrated program to better understand corrosion in the high level waste tanks, Hanford has been investigating corrosion at the liquid/air interface (LAI) and at higher areas in the tank vapor space [1-4]. Controlling the corrosion of the tank walls is an ongoing challenge to overcome in maintaining the structural integrity of the double shell tanks (DST) at both Hanford and the Savannah River Site (SRS). The interaction between corrosive and inhibitor species in condensates on the tank wall above the LAI and subsequent interactions with vapor phase constituents as the liquid evaporates influences the corrosion of the carbon steel tank walls. The Savannah River National Laboratory has recently completed a series of studies investigating both the LAI and vapor space corrosion [5, 6]. This report provides the experimental details and conclusion from studies of the vapor space corrosion for Hanford-based high level waste simulants with a special emphasis on the impact of ammonia on carbon steel corrosion. The results from the LAI study are reported elsewhere [7].

2.0 Background

Understanding the vapor space corrosion in Hanford DST is important under two different scenarios. The first scenario is for current DST in which previous testing results have shown that the ammonia gas that is generated from the waste may have a positive impact on reducing corrosion of the carbon steel tanks. Thermodynamic models have been used to understand the condensate chemistry and the influence of ammonia [1], which was taken into consideration for establishing test parameters for this first scenario. The second scenario is with new corrosion chemistry limits and their impact on corrosion in the vapor space.

2.1 Current Chemistry of DST

The formation and evolution of the condensate chemistry in the vapor space and on the tank wall are complex and transient due to the changing equilibria of multiple chemical species in this environment. Of these multiple chemical species, the corrosive and inhibiting species on the tank wall determine the type and degree of corrosion. Thermodynamic models based on representative Hanford DST supernates have been used to predict the chemistry of adsorbed surface condensates based on the equilibrium between key vapor space constituents and the condensate and changes that occur in the condensate chemistry due to evaporation of water [1]. Six representative Hanford DST supernates were targeted for the study: AY-101 (Segment 3), AY-101 (Segment 8), AN-102, AY-102, SY-102 (high nitrate), and SY-102 (high chloride).

The tank wall condensate was found to be primarily composed of nitrate and ammonia, and possibly carbonate and bicarbonate. Nitrite, although present, was initially in low concentration but increased with the evaporation of water. The initial low concentration of nitrite and sodium may indicate that aerosol transport does not have a significant impact on vapor space chemistry and the subsequent corrosion of the tank wall.

A major factor in controlling corrosion in waste tanks is the pH of the waste. The equilibrium of the pH in the liquid phase on the tank wall in the vapor space is dependent on carbon dioxide and ammonia, which are both dominant species in the vapor space of Hanford DST. The pH remains relatively stable (i.e., > 9) until the condensates are nearly evaporated and solids precipitation occurs. The pH changes during the final stage are a function of the initial condensate pH, the CO_2 concentration, the formation of ammonium carbamate ($NH_4CO_2NH_2$), and other predicted ammonium solids. The experimental studies showed that the final pH for the evaporated wastes was higher than that predicted for the model, which may have been due to lower humidity conditions during testing.

Electrochemical corrosion testing was performed in solutions predicted from these models at SRNL for the six simulants at three levels of evaporation [3]. The tests were conducted on carbon steel samples that were completely immersed in a bulk simulant. Cyclic potentiodynamic polarization (CPP) tests with (0.001M and 0.5M) and without ammonium salts present in the simulant were performed. The ammonium nitrate that was added rapidly equilibrates with dissolved ammonia gas in the solution. Ammonia gas has been shown to be an inhibitor for carbon steel in previous studies at both Hanford and SRS [8, 9]. The addition of the ammonia had differing responses depending on the simulant and the level of evaporation. The four different levels of response observed from the CPP tests were:

- No pitting at any level of evaporation (AY-102)
- Pitting at the 0% evaporation level, but increasing resistance at higher levels of evaporation (AN-102 and SY-102, high chloride)
- Minor pitting at the 0% evaporation level, but decreasing resistance to pitting at higher evaporation levels (AY-101, segment 3, AY-101, segment 8)
- Heavy pitting at all levels of evaporation (SY-102, high nitrate)

The addition of the low ammonia concentration had a small effect on the corrosion response. However, at the higher concentration of ammonia in the AY-101, Segment 8 simulant at 0% evaporation, the pitting resistance increased significantly. This result suggested further electrochemical studies were needed to evaluate the effect of ammonia gas on corrosion, particularly for solutions that had aggressive corrosion, i.e. AY-101 Segment 3, AY-101 Segment 8, and SY-102 high nitrate simulants.

2.2 Ammonia Test Concentrations

Ammonia is primarily of interest in the Hanford waste tanks as a flammable gas hazard and a noxious vapor [15]. Ammonia is produced predominantly in the liquid waste through thermal and radiolytically induced reactions between organic waste components and nitrate and nitrite anions. Slightly more than 70% of the tank headspaces (127 of 177) have been analyzed for ammonia. The highest measured ammonia concentration in a DST was 550 ppm in Tank SY-102. The measurements show that under normal quiescent conditions that only 3 of the 127 tanks reached more than 1% of the LFL (i.e., all were single shell tanks), while none exceeded 2% LFL.

Ammonia has been demonstrated to be beneficial from the standpoint of vapor space corrosion inhibition [8, 9]. The presence of the ammonia maintains the pH in the condensates that form thin films on the steel in the vapor phase at alkaline values that inhibit corrosion [1]. However, the presence of other aggressive species from dissolved salts on the wall (e.g., nitrate, chloride, etc.) complicates the evaluation.

The ammonia concentrations selected for these tests were 50 ppm and 550 ppm. The lower concentration level was selected to determine a minimum ammonia concentration for corrosion inhibition. The minimum concentration determined from previous tests was 100 ppm [9]. The higher concentration level was selected to be representative of the maximum ammonia concentration observed in the head space of a DST, Tank SY-102.

For the testing it was desired to establish equilibrium between the ammonia gas and the dissolved ammonia that would be in a condensate. The two concentrations are related by a Henry's Law constant that is a complex function of ionic strength and temperature [15]. Equilibrium ammonia concentrations were calculated on a spreadsheet provided by WRPS [16]. For example, for the SY-102, High Nitrate, 0% evaporation, if the ammonia gas in the vapor space is at 550 ppm, the dissolved ammonia in the liquid condensate was calculated to be 0.0132 M.

To achieve the desired dissolved ammonia concentrations in test solutions, ammonium nitrate was added to the solution. Once dissolved, the ammonium and ammonia achieve equilibrium as shown by the following equation.

$$NH4^{+} + OH^{-} + (n\text{-}1)\ H_2O\ (l) = NH_3 \bullet nH_2O\ (aq) \qquad (1)$$

The equilibrium is a complex function of temperature, pH, and ionic strength. For example, the $NH_3/(NH_3+NH_4^+)$ fraction in water at pH 10 and 40 °C is 0.94 [17]. This fraction decreases with temperature to 0.85 at a temperature of 25 °C. An increase in the ionic strength (e.g., I=1 M) for the 40 °C value would result in a decrease in the fraction to 0.92. Based on the pH, test temperature, and solution compositions, the External Panel for Optimization of Chemistry recommended that a fraction of 0.9 be utilized. For example, for the SY-102, High Nitrate, 0% evaporation, if the dissolved ammonia in the liquid condensate was calculated to be 0.0132M, the ammonium nitrate that was added to the solution was 0.0147M.

2.3 New Corrosion Limits

New corrosion chemistry limits have been recommended for the minimization of the threat of stress corrosion cracking in the DST [10]. These limits are summarized in Table 2-1. The vapor space corrosion of the steel above waste that is at the boundary of the new limits is not known so testing is required to determine if the new corrosion chemistry limits for the DST effectively mitigate vapor space corrosion. The specific limit of interest for the current testing is the minimum nitrite/nitrate ion ratio (R) of 0.15 with a minimum nitrite concentration of 0.05M.

Table 2-1 Proposed Specifications for the Control of SCC in Nitrate Ion Wastes in DST

Parameter	Limit
Maximum Temperature:	50 °C
Maximum Concentration of Nitrate Ion	6.0M
Maximum Concentration of Hydroxide Ion	6.0M
Minimum pH	11
Minimum Concentration of Nitrite Ion	0.05M
Minimum Nitrite Ion/Nitrate Ion Ratio	0.15

3.0 Experiment Procedure

The vapor space corrosion testing to study the effects of ammonia on carbon steel corrosion consisted of three tasks: electrochemical testing of the modeled condensate solutions for tanks AY101 and SY102; coupon testing in the presence of ammonia gas, and coupon testing over simulated solutions with the new corrosion-control chemistry limits (no ammonia gas).

3.1 Electrochemical Testing of Condensate Solutions

Localized corrosion in the form of pitting is of particular interest in the vapor space. Electrochemical testing was used to determine the susceptibility of carbon steel to pitting in un-evaporated and evaporated Hanford DST simulants with and without ammonia in solution. The test set up is shown in Figure 3-1. Open-circuit potential (OCP) monitoring was used to follow the sample stabilization in the test solution and was conducted for two hours. Cyclic potentiodynamic polarization (CPP) was conducted by applying a cyclic potential ramp (0.167 mV/sec) from 50 mV more negative than the OCP up to a vertex potential of 1.5 V versus the reference and back to the OCP with a current limit set at 2 mA/cm^2.

The equipment consisted of a computer-controlled Princeton Applied Research Model 273A potentiostat. A saturated calomel electrode (SCE) was used as the reference electrode, which was checked against a laboratory standard (a SCE not used for testing) before the start of each test. All potentials in this report are given versus this reference electrode. The reference electrode was place in a Luggin capillary bridge containing a 0.1M sodium nitrate solution. The counter electrode for the electrochemical cell was a graphite rod. Test solutions (600 ml) were heated to 40 ºC with a laboratory temperature-controlled hot plate. A condenser was used on the test cell to minimize evaporation. Solutions were not stirred and, for most tests, the vapor space of the test cell was air (i.e. no cover gas).

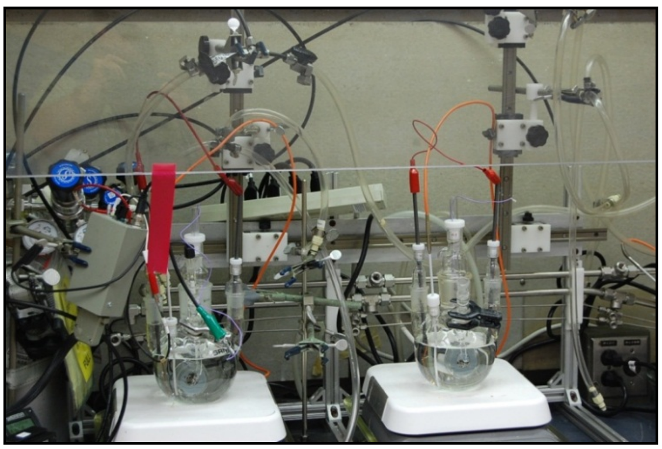

Figure 3-1 Electrochemical test cells used to evaluate Hanford DST simulants

For two tests, ammonia gas was allowed to flow into the vapor space of the corrosion test cell. The ammonia gas was added to simulate the long-term condition in which dissolved ammonia reaches equilibrium with the vapor space ammonia gas. These tests were performed to confirm a hypothesis that, over the course of the test (i. e. short-term test), ammonia gas that would be in equilibrium with dissolved ammonia in the condensate would not impact the test results.

Ammonia was procured mixed to the desired concentrations of 50 and 550 ppm in air. The gas feeds were then routed through electronic flow meters (Sierra Instruments) which were set to bleed in the cover gas at 5 standard cubic centimeters per minute (sccm). The gas lines were fed into bubblers which were filled with the same solution as was present in the test cells in order to humidify the gas prior to entering the test cell vapor space. Gas was fed on a constant basis over the duration of the test.

The electrochemical testing was performed using circular disks of A537 carbon steel, Class 1, mounted in a metallurgical mount using a two-part epoxy. The chemical composition of A537 steel is given in Table 3-1, where the balance is iron.

Table 3-1 Chemical Composition (Wt %) of A537 Carbon Steel, Class I

C	Mn	P	S	Cu	Ni	Cr	Si
0.14	1.44	0.008	0.003	0.14	0.11	0.09	0.29

Prior to mounting, multi-stranded electrical wires were attached to the back side of the sample using a silver epoxy. Each sample had a unique identifier etched into the epoxy. This carbon steel is similar in composition to the steel grade used to construct the Hanford DST. The mounting protocol was similar to that used previously [2, 3]. Bullet-shaped samples were also used in three tests to compare with the results from the disk-shaped disks. The bullets were made from plate of archived material used for the Hanford DST, similar to those used during round robin testing for the standardization of electrochemical test protocol [11]. All samples were photographed after testing to document the amount of surface corrosion.

Prior to testing, both types of samples were prepared following a similar protocol that was also used during the recent round robin testing [11]. These steps included grinding the sample surface with 600-grit silicon carbide paper to remove previous corrosion, followed by a series of distilled water and acetone rinses, blow drying and immediately placing into the test solution.

Test solutions were prepared based on chemistries from the thermodynamic modeling and used during subsequent testing. [1, 3]. Table 3-2 shows the chemistry for the unevaporated condensate simulants without ammonia addition.

Table 3-2 Composition of Unevaporated Condensate Simulants without Ammonia Addition.

Species	AY-101, Segment 3, 0% Evaporated	AY-101, Segment 3, 34% Evaporated	AY-101, Segment 3, 76% Evaporated	AY-101, Segment 8, 0% Evaporated	AY-101, Segment 8, 27% Evaporated	AY-101, Segment 8, 68% Evaporated	SY-102, High Nitrate, 0% Evaporated	SY-102, High Nitrate, 33% Evaporated
KNO3	0	0	0	0.04	0.053	0.105	0.0009	0.0012
NaBr	0.0048	0.0071	0.017	0	0	0	0.064	0.088
NaCl	0.013	0.02	0.048	0.086	0.11	0.18	0.011	0.015
NaF	0.0105	0.0156	0.038	0.0099	0.013	0.026	0.0026	0.0036
NaNO3	1.01	1.49	3.59	1.54	2.027	4.045	3.6391	5.0188
NaNO2	0.167	0.248	0.6	0.972	1.28	2.55	0.097	0.13
Na3PO4 12H2O	0.04	0.06	0.144	0.043	0.057	0.11	0.024	0.033
Na2SO4	0.0153	0.023	0.055	0.033	0.044	0.087	0.047	0.064
NaHCO3	0.0501	0.0555	0.0442	0.0532	0.0526	0.0237	0.0304	0.0285
Na2CO3	0.486	0.727	1.106	0.867	1.157	0.484	0.265	0.376
pH	10.15	10.23	10.43	10.29	10.39	10.32	10.01	10.16

For each simulant two concentrations of ammonium nitrate (0.0015M and 0.015M) were tested along with the base line solution without ammonium nitrate. These two levels were chosen to give soluble ammonia gas concentrations of 50 and 550 ppm. The chemical constituents targeted for each simulant are listed in Appendix A. All solutions were made from reagent-grade chemicals.

3.2 Coupon Testing With Ammonia Gas

Coupon exposure tests with ammonia gas in the vapor space were set up to understand the evolution of corrosion products on carbon steel and the impact on corrosion rate and morphology when ammonia gas is present. A corrosive Hanford waste chemistry was used, SY102 High Nitrate simulant at 33% evaporation. The make-up chemistry is shown in Appendix A. All solutions were made from reagent-grade chemicals.

Rectangular A537 carbon steel coupons (1 inch by 2 inch by 0.125 inch) were used in the testing with a surface prepared on 600-grit silicon carbide paper. Samples were weighed on a calibrated balance prior to testing. The tests were conducted for four months with samples removed at one-month intervals. Two samples were removed at each time interval for each solution. After removal, the samples were rinsed with distilled water and dried in air, then wrapped in protective tissue and placed within a desiccator. At the conclusion of testing, the samples were photographed and then cleaned using Clark's solution [12]. The coupons were weighed again for calculating total weight losses. Coupons were photographed again for documenting the corrosion morphology.

The test cells that were used are shown in Figure 3-2. Each test setup consisted of a thermocouple controlled hotplate set to 40°C and a borosilicate glass test cell with a solution volume of approximately 1.5L. The coupons were suspended on glass sample holders attached through a 3/16" hole drilled in the sample. Ammonia was procured mixed to the desired concentrations of 50 and 550 ppm in air. The gas feeds were then routed through electronic flow meters (Sierra Instruments) which were set to bleed in the cover gas at 5 sccm. The gas lines were fed into bubblers which were filled with the same solution as was present in the test cells in order to humidify the gas prior to entering the test cell vapor space. Gas was fed on a constant basis over the four month test duration.

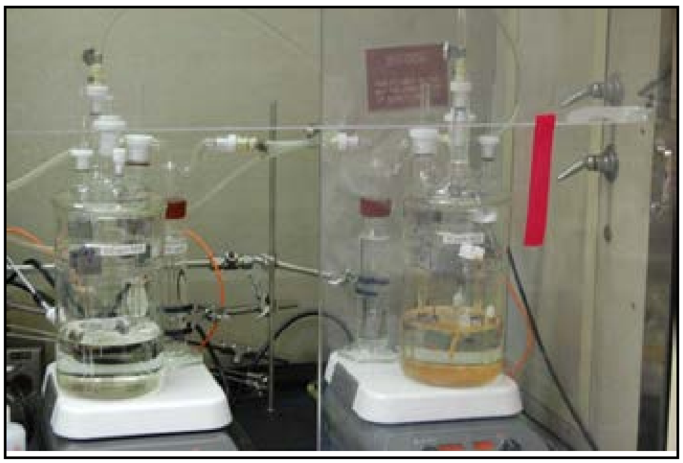

Figure 3-2 Coupon test cells for evaluating effect of ammonia gas on carbon steel corrosion over a simulated Hanford waste

3.3 Coupon Testing for New Corrosion Chemistry Limits

Coupon exposure tests were conducted in the vapor space above three waste simulants that are at the boundary of the new corrosion chemistry limits for the DST. The solutions contained three levels of nitrate, 0.4 M, 2.0 M, and 4.5 M at the minimum nitrite/nitrate ratio of 0.15. These nitrate concentrations are representative of the three tiers currently in the DST chemistry controls. The minimum nitrite concentration was 0.05M at a pH 10. The pH for these tests is actually below the new limits. Tests at pH 11, the requirement, and at pH 12 were performed at DNV. These tests were performed to understand the effect of the variation from the required pH. The major and minor constituents in the three simulants are summarized in Table 3-3. The concentrations of these constituents are within those observed for Hanford waste. All solutions were made from reagent-grade chemicals.

Table 3-3 Composition of Solutions Representative of New Corrosion Chemistry Limits

Solution Number	Initial pH	$NaNO_2$	$NaNO_3$	NaCl	NaF	Na_2SO_4	Na_2CO_3	$NaHCO_3$	Na_3PO_4
1	10	0.06	0.4	0.01	0.003	0.005	0.075	0.025	0.0005
2	10	0.3	2	0.04	0.01	0.05	0.4	0.1	0.01
3	10	0.675	4.5	0.1	0.02	0.1	0.833	0.167	0.05

Rectangular A537 carbon steel coupons (1 inch by 2 inch by 0.125 inch) were used in the testing with a surface prepared on 600-grit silicon carbide paper. Samples were weighed on a calibrated balance prior to testing. The tests were conducted for four months with samples removed at one-month intervals. Two samples were removed at each time interval for each solution. After removal, the samples were rinsed with distilled water and dried in air, then wrapped in protective tissue and placed within a desiccator. At the conclusion of testing, the samples were photographed and then cleaned using Clark's solution [12]. The coupons were weighed again for calculating total weight losses. Coupons were photographed again for documenting the corrosion morphology. Pit depths were measured using a Zeiss measuring microscope.

The test cells that were used are shown in Figure 3-3. Each test cell consisted of a thermocouple controlled hotplate set to 40°C and a borosilicate glass test cell with approximately 1.5L of solution. The coupons were suspended from rods over the test solution. As can be seen in Figure 3-3, this testing was conducted in conjunction with that for the LAI testing. In this case, the vapor space was air.

Figure 3-3 Experimental setup for performing coupon tests for new corrosion limits (testing for vapor space and LAI corrosion was conducted simultaneously)

4.0 Results and Discussion

During this current investigation, the test conditions, including the effect of ammonia and the minimum nitrite/nitrate ion ratio, did not provide any instance in which corrosion was not observed although the severity of corrosion was altered. The effect of dissolved ammonia in the electrochemical test and the ammonia gas in the coupon test differed but the presence of ammonia provided some inhibition. In the case of the new limits, the corrosion was reduced at a constant nitrite/nitrate ratio as the absolute nitrite concentration increased.

4.1 Electrochemical Testing of Condensate Solutions

The effect of ammonia gas on the corrosion behavior of carbon steel depended on the solution chemistry. A consistent effect was not observed so each solution is discussed separately. Additionally, the effects of ammonia gas as a cover gas and sample type were also evaluated with several tests and these results are also discussed separately. The OCP trends, CPP scans and post-test sample pictures for each sample are given in Appendix B.

Table 4-1 provides averages of several parameters taken from the CPP scan that were used to assess the effect of dissolved ammonia. Positive hysteresis in the CPP scan with significant attack of the surface was an indication of pitting susceptibility. Negative hysteresis with light pitting is indicative of marginal pitting susceptibility that should be investigated further. These parameters include the corrosion potential (E_{corr}), the current density in the passive region (i_{pass}), the current density of the reverse scan (i_{rev}), and a qualitative estimate of the corrosion observed after the test. i_{pass} was measured in two ways. If there was a breakdown potential, i_{pass} was taken as the current density at that potential. If a breakdown potential less than the transpassive potential was not observed, i_{pass} was taken at a potential of 0.250 V. i_{rev} was the maximum current measured during the reverse scan, although small spikes, which were commonly observed during the reverse scan, were neglected.

Pitting potentials and repassivation potentials were not included in Table 4-1 since these parameters were not identified in all the CPP scans. In all but two scans, the repassivation potential was more electronegative than E_{corr}, so it was not identified. Pitting potentials were observed with the SY102 simulant and were approximately -0.1 V, SCE, independent of ammonia. For the AY101 Segment 3 simulants pitting or breakdown potentials were identified in some cases and these will be noted below.

4.1.1 *Effects of Ammonia Gas and Sample Type*

In the Hanford tanks, ammonia is generated from thermal and radiolytic induced reactions of nitrite and nitrate ions with organic waste components. Over time, ammonia released from the waste dissolves in the condensate on the tank wall and reaches equilibrium with the ammonia gas. For the protocol used for this electrochemical testing, ammonium nitrate was added to generate and simulate the dissolved ammonia gas in the condensate. Since the testing is short in duration, ammonia gas was not used in the test cell vapor space for most tests. Sufficient time would not pass to reach equilibrium between the vapor space and bulk test solution and affect the corrosion resistance of the carbon steel samples. The protocol used is similar to that used for recent electrochemical test to evaluate the corrosion resistance of carbon steel to Hanford waste chemistries [2, 11].

Two tests conditions were used to evaluate the hypothesis that the presence of ammonia gas would not impact the electrochemical response in the short term: AY101 Segment 8, 0% evaporation, 550 ppm ammonia; AY101 Segment 3, 0% evaporation, 50 ppm ammonia. For AY101 Segment 3, the data showed that, in the presence of ammonia gas, the corrosion resistance was slightly improved as shown in Figure 4-1. The CPP scans with ammonia gas were at slightly lower current densities overall and the corrosion on the sample was less. Positive and mixed[1] hysteresis was observed with and without the use of the ammonia gas. For AY101 Segment 8 the CPP scans without ammonia cover gas had negative or no hysteresis while with ammonia cover gas a positive hysteresis was seen as shown in Figure 4-2. The conclusion from these tests was that ammonia cover gas may have a mixed effect on corrosion depending on the solution

[1] Mixed hysteresis indicates a change in the nature of hysteresis during the course of the reverse scan, i.e. starts negative then becomes positive.

chemistry, which is similar to results discussed below for each solution with dissolved ammonia present.

Table 4-1 Average Electrochemical Parameters from CPP Scans for Carbon Steel in Hanford Simulants

Solution	NH_3 (ppm)	E_{corr} (V, SCE)	i_{pass} (A/cm^2)	i_{rev} (A/cm^2)	Hysteresis (Negative or Positive?)	Corrosion observed on sample (%)*
SY102, High Nitrate, 0% Evaporation	0	-0.483	1E-4	2E-2	Positive	75
	50	-0.336	1.6E-4	5.5E-3	Positive	25
	550	-0.305	6.7E-5	3E-5	Positive	25
SY-102, High Nitrate, 0% Evaporation	0	-0.439	7.5E-5	9.25E-3	Positive	<50
	50	-0.318	3E-5	8.4E-3	Positive	<50
	550	-0.324	2.3E-5	4.2E-3	Positive	25
AY101, Segment 3, 0% Evaporation	0	-0.356	3.1E-5	3.5E-4	Positive	<10
	50	-0.302	5.5E-5	4.9E-4	Positive	5
	550	-0.294	3.6E-5	5.8E-4	Positive	10
AY101, Segment 3, 34% Evaporation	0	-0.250	2.3E-6	1.3E-4	Positive	5
	50	-0.399	8.8E-5	1.3E-4	Positive	<5
	550	-0.319	8.9E-4	9.5E-4	Positive	10
AY101, Segment 3, 76% Evaporation	0	-0.262	1.7E-5	2E-4	Positive	<10
	50	-0.329	8.8E-5	3.5E-4	Positive	<10
	550	-0.275	2.3E-5	1.1E-4	Positive	5
AY101, Segment 8, 0% Evaporation	0	-0.279	0.8E-4	4E-4	Positive	5
	50	-0.263	2.3E-5	7.9E-4	Positive	<5
	550	-0.335	3.6E-5	2E-5	Positive	<1
AY101, Segment 8, 27% Evaporation	0	-0.277	2.5E-5	None	Negative	1
	50	-0.290	4.9E-5	None	Negative	No data
	550	-0.303	5.9E-5	None	Negative	1
AY101, Segment 8, 68% Evaporation	0	-0.283	1.7E-5	4.5E-5	Positive	1
	50	-0.233	1.1E-5	1.7E-4	Positive	1
	550	-0.422	7.7E-5	None	Negative	5

* Corrosion was broadly assessed using the following percentages: 75, 50, 25, 10, 5, and 1. The < or > indicates that the corrosion appeared better or worse than the identified % but not to the next level. The corrosion given is the worse observed for that condition.

Three test conditions were used to evaluate if the sample type impacted the results: AY101 Segment 8, 68% evaporation, 550 ppm ammonia; AY101 Segment 8, 69% evaporation, no ammonia present; and SY102 High Nitrate, 0% evaporation, no ammonia present. These solutions represented electrochemical results for the flat coupons of positive and negative hystereses and a borderline case between these two hystereses. For SY102 and AY101 Segment 8 with no ammonia, both sample types displayed similar curves with positive hysteresis and mixed hysteresis, respectively, although the bullet samples were at lower current densities and higher E_{corr} values (see Appendix B for the CPP scans). In AY101 Segment 8 with 550 ppm ammonia, the bullet sample had a mixed hysteresis; whereas, the mounted disk samples had negative hysteresis as shown in Figure 4-3. The bullet sample had a lower i_{pass} and again a more electropositive E_{corr}. Both samples had evidence of pitting on the surface.

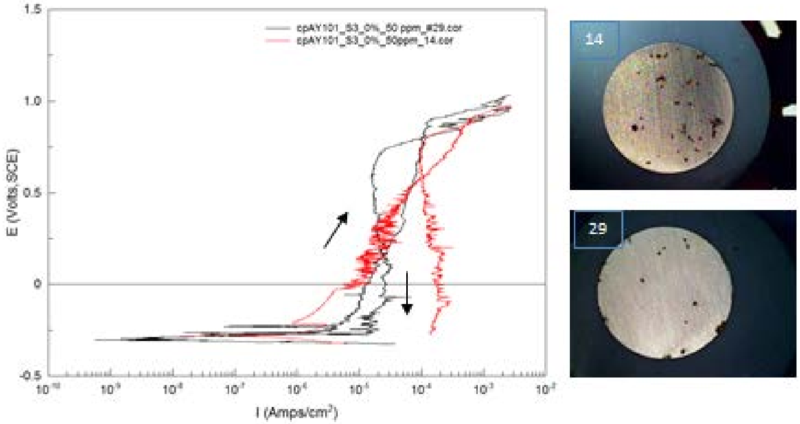

Figure 4-1 CPP scans for AY101, Segment 3, 0% evaporation, 50 ppm ammonia with (#29) and without (#14) ammonia cover gas

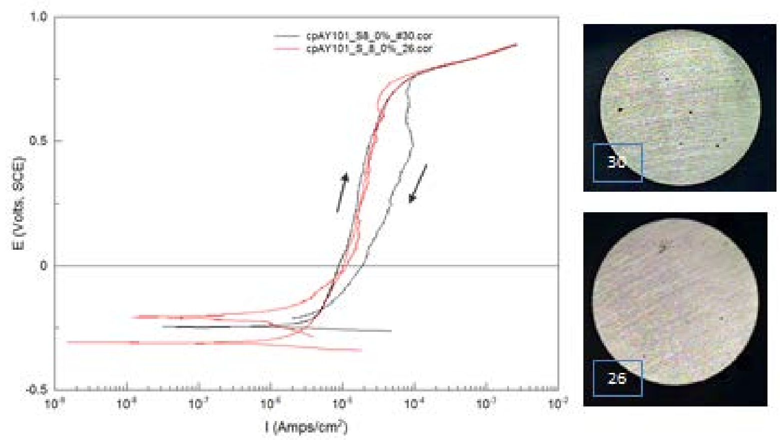

Figure 4-2 CPP scans for AY101, Segment 8, 0% evaporation, 550 ppm ammonia and with (#30) and without (#26) ammonia cover gas

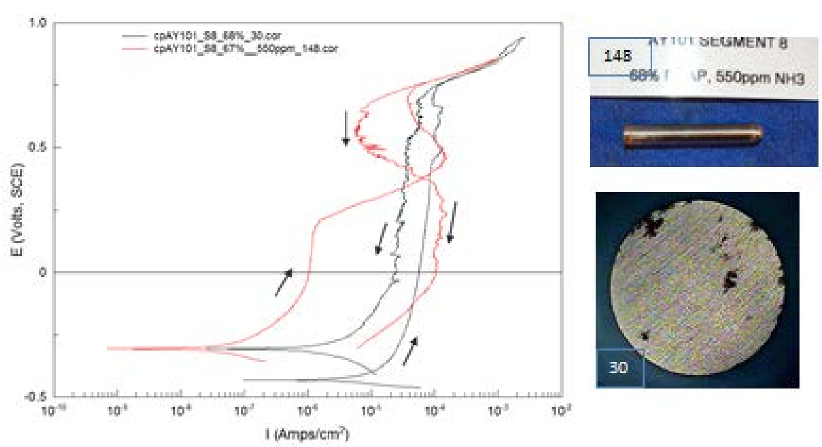

Figure 4-3 CPP scans for AY101, Segment 8, 68% evaporation, 550 ppm ammonia with mounted disk (#30) and with bullet sample (#148)

4.1.2 *SY102 High Nitrate*

The ammonia gas in the SY102, high nitrate simulant had a slightly inhibitive effect for carbon steel at both evaporation levels. Both of these solutions have high nitrate concentrations with very low concentrations of nitrite corrosion inhibitors (R=0.026). The observed changes appeared to be a function of the ammonia concentration as shown by the data in Table 4-1. For both levels of evaporation, E_{corr} became more electropositive and i_{pass} and i_{rev} decreased with increasing ammonia concentration. These changes can be seen by the CPP scans shown in Figure 4-4 for 0% evaporation. At both evaporations, large positive hysteresis loops were seen indicating high localized corrosion susceptibility. The post-test sample inspection confirmed significant pitting.

Although polarization resistance was not one of the test performed, a corrosion rate based on the polarization around E_{corr} from the cyclic polarization data showed a slight decrease in corrosion rate with the electropositive shift in potential. These factors all indicate an inhibitive effect from the presence of the ammonia. However, there was not a big difference in the observed corrosion after the test as shown in Figure 4-4. Generally, samples exposed to 550 ppm ammonia were less corroded as can be seen by the data in Appendix B.

Two postulated pathways are proposed to attempt to explain the inhibitive effect of ammonia in the waste simulants at this time. Both pathways affect the cathodic reaction driving the corrosion and involve ammonia. The first pathway, which was developed using HSC Chemistry software, results from oxidation of ammonia as shown in Equation 1[18].

$$2\ NH_3\,(aq) + 6\ OH^- \leftrightarrow N_2 + 6\ H_2O + 6e^- \qquad \text{(Eq. 1)}$$

This reaction has a low reduction potential (-1.0 V, SCE) with dissolved ammonia gas, which shifts to a lower potential (-1.2 V, SCE) when ammonia is present. The oxidation of ammonia can reduce nitrate ions to nitrite ions according to Equation 2 [18].

$$NO_3^- + H_2O + 2e^- \leftrightarrow NO_2^- + 2OH^- \qquad \text{(Eq. 2)}$$

This reaction has a reduction potential of (-0.22 V, SCE) and reduces the aggressive nitrate species into a protective nitrite species. Since SY102 has a small concentration of nitrite, the additional inhibitive species (i.e., nitrite and hydroxide) produced by the overall cell reaction between the ammonia and the nitrate ions would lead to less corrosion. This equilibrium potential would be affected by Nernstian corrections for the concentration of the individual species (nitrate, nitrite and ammonia) which may be a reason for complex trends in data for this solution and the other solutions. If this reaction led to a greater cathodic current, a positive shift in the OCP might be expected as was observed for SY-102, High Nitrate.

Nitrate can also go through a series of intermediaries, including nitrite and hydrazine, to be reduced to the ammonium ion [19]. In the presence of ammonium this chain of reactions would be limited and lead to a decrease in the reduction of nitrate and the corrosion of carbon steel. The ammonium concentration is dependent in part on the ionic strength, which for these test solutions is the highest with the SY-102, high nitrate simulant. The higher ionic strength reduced the $NH_3/(NH_3+NH_4^+)$ fraction. Therefore, to maintain this ratio constant for testing higher ionic strength solutions, a greater ammonia concentration resulted. The SY-102, high nitrate composition should give the strongest effect of ammonia on corrosion by this pathway. As can be seen from the data for SY-102, high nitrate simulant, the presence of dissolved ammonia in solution decreased the observed corrosion. Further study is required to determine the actual mechanism.

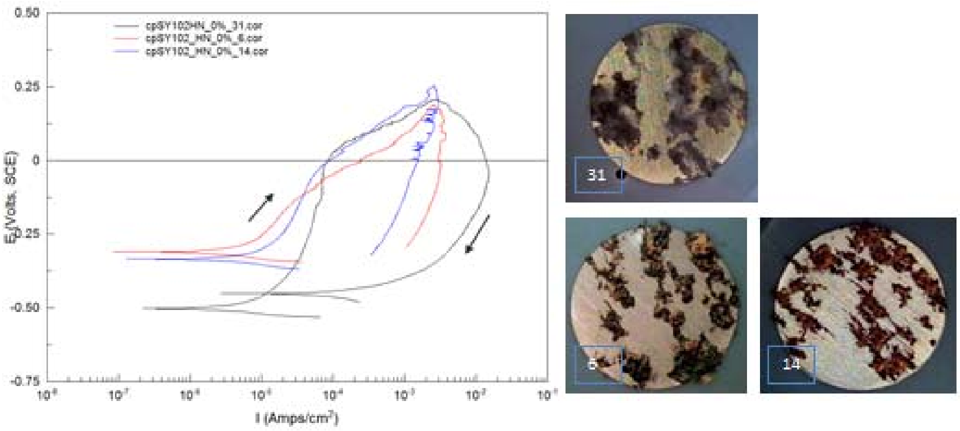

Figure 4-4 CPP scans for SY102, High Nitrate, 0% evaporation with 0 (#31), 50 ppm (#6), and 550 ppm (#14) ammonia

4.1.3 *AY101 Segment 3*

The presence of ammonia in this solution shifted the CPP scans to higher current densities as shown by the data in Table 4-1 for all evaporation levels and the CPP scans shown in Figure 4-5 for 34% evaporation. Pitting potentials were seen at 34% evaporation with no ammonia and for all conditions at 76% evaporation. The values ranged from approximately 0.1 V, SCE to 0.3 V, SCE. The scans generally had positive hysteresis, although, at the high evaporation and with ammonia present, weaving or negative/positive transitions occurred on the reverse scan. The corrosion observed on the samples also indicated that the effect of ammonia was minimal. In some cases, the corrosion was worse with ammonia present as shown by the photographs in Figure 4-5.

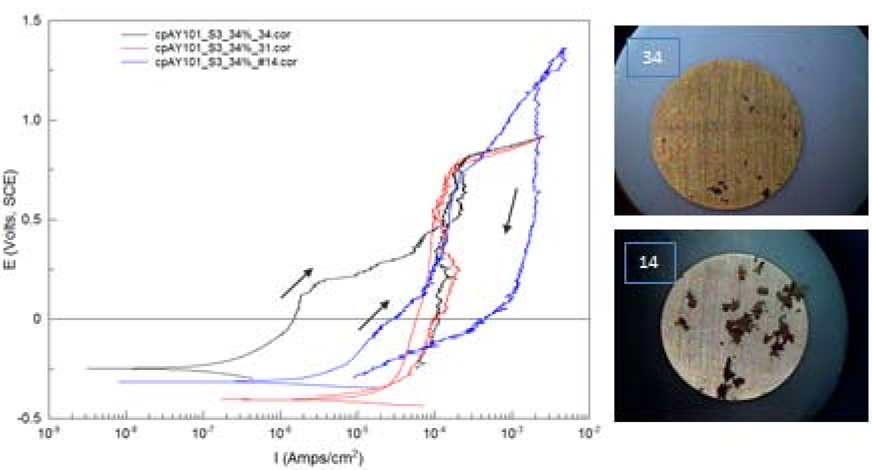

Figure 4-5 CPP scans for AY101, Segment 3, 34% evaporation with 0 (#34), 50 ppm (#31), and 550 ppm (#14) ammonia

The higher i_{pass} and i_{rev} indicate that the surface oxide is less protective in the presence of ammonia. When ammonia is not present, the passive region of the CPP scan at a potential anodic to Ecorr the current density raises to a level similar to that seen when ammonia is present. In these solutions, the addition of ammonia may be sufficient to drive the cathodic reaction in localized areas leading to a higher i_{pass}. When ammonia is not present, a higher i_{pass} requires an overall change in the oxide at a higher potential. Whereas, in the case of SY102 the reduction reaction of Equation 2 is happening over the entire surface and leads to a general decrease in i_{pass} because of increased nitrite and hydroxide concentration.

These results differ from the SY102 and AY101 Segment 8 solutions where beneficial effects were found. The AY101 Segment 3 (R=0.16) solutions had lower nitrate than SY102 (R=0.026) and AY101 Segment 8 (R=0.63), although the nitrite/nitrate ratio falls between these two solutions. Solutions that are more dilute may show more aggressive localized corrosion than concentrated solutions, so at these concentrations of ammonia, the localized cathodic polarization increases passive oxide breakdown and perhaps hinders repassivation.

4.1.4 *AY101 Segment 8*

For AY101 Segment 8 solutions, the ammonia was slightly inhibitive for carbon steel especially at the higher concentration. The data in Table 4-1 shows that i_{rev} decreased slightly with ammonia present. This reduction did not show a correlation with the concentration although the values were generally lowest at 550 ppm ammonia. i_{pass} showed mixed behavior both increasing and decreasing with ammonia concentration depending on the evaporation level. For the CPP scans, which are shown in Figure 4-6 for 68% evaporation, both positive and negative hysteresis were observed at all evaporation levels. All the CPP scans are given in Appendix B. In Figure 4-6, a negative hysteresis was observed at 550 ppm ammonia. The observed corrosion was minimal for all evaporation levels and ammonia concentrations. Previous studies have shown that molar higher concentrations ammonia were beneficial in minimizing pitting corrosion [3].

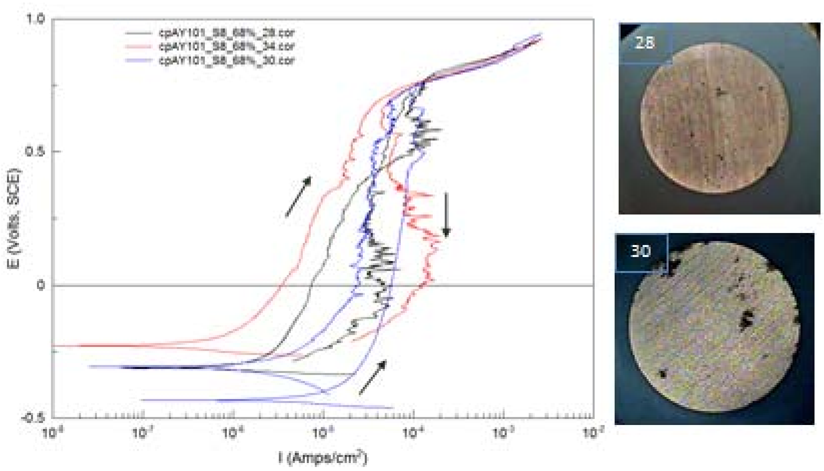

Figure 4-6 CPP scans for AY101, Segment 8, 68% evaporation with 0 (#28), 50 ppm (#34), and 550 ppm (#30) ammonia

AY101 Segment 8 solutions had the highest nitrite concentrations as well as the highest nitrite/nitrate ion ratio, R=0.63. The nitrite concentration was sufficient to maintain the surface oxide without the consequences of increasing or decreasing cathodic polarization from ammonia. The additional nitrite and hydroxide concentrations as shown by the reaction in Equation 2, when it occurs, would be beneficial to the surface oxide.

As can be seen in Table 4-1 these samples also experienced the lowest amount of corrosion and had lower i_{pass} values. The observed corrosion was a function of the amount of inhibitor with SY102, high nitrate (R=0.026) showing the most corrosion, AY101 Segment 8 (R=0.63) having the least. SY102, high nitrate was also the solution that showed the biggest effect of ammonia on the corrosion of carbon steel.

4.2 Coupon Testing With Ammonia Gas

Over the course of the four-month test, the corrosion of carbon steel was minimal for coupons exposed in the vapor space to the high ammonia gas concentration (550 ppm) with no localized corrosion observed. At the low concentration (50 ppm), the coupons experienced more general attack but some pitting. The pictures of the coupons before and after cleaning are given in Appendix C along with the tables showing the observations of surface attack and pitting for each coupon.

Although the impact of ammonia gas on localized corrosion is of primary interest, the average weight losses clearly shows the difference in vapor space corrosion resistance of carbon steel for the two gas concentrations. In Table 4-2, the average weight loss is shown for each exposure period at the two gas concentrations. These weight losses correspond to 1-2 mils per year (mpy) for the coupons exposed to 50 ppm ammonia gas and less than 1 mpy for those exposed to 550 ppm. In Figure 4-7, the difference in corrosion can be seen for Coupon #508 exposed to 50 ppm ammonia gas and Coupon #510, which was exposed to 550 ppm. These are the worse sides for each condition after the four-month exposure.

The coupons exposed in the 550 ppm ammonia gas had essentially no localized corrosion and on only one coupon (#502) was light surface attack observed after three months. This attack was less than 1 mil and covered less than 5% of the surface area. For coupons exposed in 50 ppm ammonia gas, the corrosion was greater. The corrosion appeared to occur rapidly within the first month and was stagnant after that (three- and four-month exposures). For both gas concentrations, the two-month exposure data was low although a review of the experiment did not reveal any anomalies in test operation.

Table 4-2 Average Weight Losses (g) for A537 Coupons Exposed to SY102 Simulant with Ammonia Cover Gas

Ammonia (ppm)	**Months Exposure**			
	1	**2**	**3**	**4**
50	0.276	0.077	0.27	0.297
550	0.025	0.015	0.089	0.11

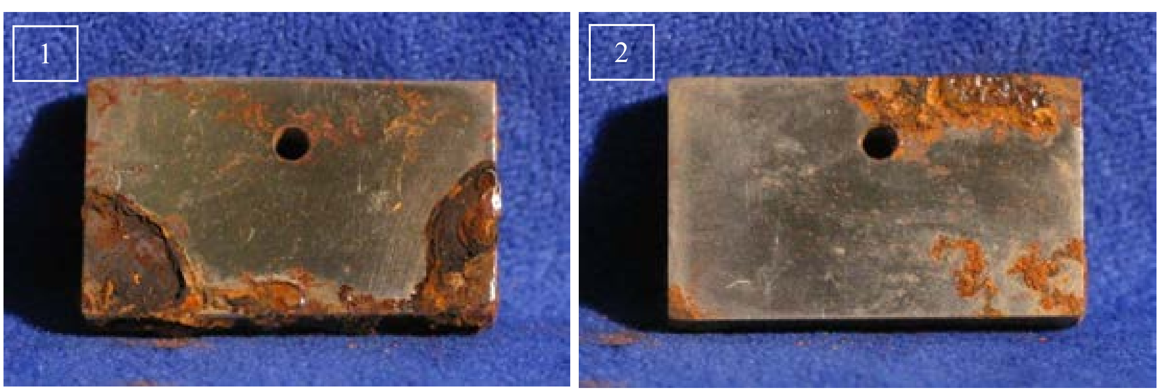

Figure 4-7 Photographs of coupons exposed to ammonia cover gas of 50 ppm concentration (1) and 550 ppm concentration (2) prior to cleaning

For the first two months, pitting was not observed, only areas of surface attack, which were generally less than 1 mil and covered at most approximately 10% of the coupon. At three and four months for these coupons the deepest pits were noted with depths ranging from 1.7 mils up to 5.9 mils. Areas of broad surface attack overlapped this range (1-5 mils). Some of the measured attack may be associated with the initial storage after test in which the coupons were not completely dry. The pictures of these coupons in Appendix C show remnants of the paper towels that they were stored in sticking to the coupon surface.

These data compare well with previous test results from both Hanford and SRS [8, 9]. In the Hanford research, coupon tests in the vapor space were performed over solutions containing 3.7M nitrate and 1.3M nitrite (R=0.35) with (100 ppm) or without ammonia cover gas [8]. The general corrosion rate dropped by an order of magnitude with ammonia present and only incipient pitting was observed. Without the ammonia cover gas, pits up to 0.003 inch were measured after a three month exposure. Similar results were observed in SRS coupon testing. In either a 0.1% or 1% ammonia concentration, only a few small spots were observed in vapor exposed samples over dilute waste simulants; whereas, in ammonia free environments pits measured 0.002 to 0.005 inch [9].

4.3 Coupon Testing for Vapor Space Corrosion with the New Corrosion Chemistry Limits

The solutions for this coupon testing were at the new minimum R value of 0.15, which is part of the new chemistry limits. The three test solutions differed in nitrate concentration, 0.4, 2.0 and 4.5M. The solutions did not contain ammonia nor was ammonia gas used during the testing. The complete solution chemistries are given in Appendix A.

All the carbon steel coupons suffered from some general attack as well as pitting corrosion. The photographs of each coupon before- and after-cleaning are shown in Appendix D along with the coupon weight loss data, pit depth measurements and qualitative assessments of the degree of corrosion. A first measure of the degree of corrosion can be seen in the weight loss data. Average corrosion losses are given in Table 4-3 for each solution and each exposure period. The worst corroded side after the four-month exposure for each solution is shown in Figure 4-8 for comparison. The solutions can be ranked in order of most aggressive as 1 ≈2 >3.

Table 4-3 Average Weight Losses (g) for A537 Coupons Exposed to Hanford Simulants at New Corrosion Chemistry Limits

Solution	**Months Exposure**			
	1	**2**	**3**	**4**
#1	0.15	0.246	0.2913	0.324
#2	0.237	0.291	0.137	0.301
#3	0.0219	0.051	0.109	0.139

Figure 4-8 Photographs of coupons after four month exposure in solutions with new minimal nitrite/nitrate ratio (R=0.15): 1) Coupon #15, 0.4M nitrate; 2) Coupon #457, 2.0M nitrate; and 3) Coupon #449, 4.5M nitrate

The localized corrosion observations are summarized in Table 4-4 for each sample and monthly exposure. The range of pit depths and depth/diameter ratios, and qualitative assessments are given.

The pitting was found to initiate quickly in these solutions, which had low concentrations of the inhibitor nitrite, and did not grow with time. The depth/diameter ratios showed a range of pit dimensions, but again did not change over the course of the four-month test. The pit depths and dimensions did not appear to be a function of the solution chemistry. The exposure however, did increase the degree of localized general attack and the depth of this attack, especially for Solutions #1 and #2. Coupons above Solution #3 were clearly the least attacked. The ranking, 1 ≈2 >3, which was given above, would be the same based on the localized corrosion assessment.

Table 4-4 Summary of localized corrosion observed from the vapor space coupon test of new corrosion chemistry limits

Solution	Month	Depth (mils)	Depth/Diameter	Comment*
#1	1	1.7-2.8	0.16-0.48	GA, Pits near GA
	2	1.8-2.8	0.21-0.54	GA-1, Pits within GA
	3	2.1-2.7	0.17-0.28	GA-3, Edge pits, Pits within GA
	4	2-3.6	0.11-0.5	GA-4, Pits near and within GA
#2	1	1.4-2.7	0.21-0.52	GA-4, Pits near and within GA
	2	1.6-2.6	0.26-.52	GA-4, Edge, Pits
	3	1.8-2.3	0.3-0.43	GA-3, Edge,
	4	1.5-4.3	0.23-0.49	SGA-3,
#3	1	1.6-3.3	0.23-0.5	GA
	2	**	**	GA-1
	3	1.3-3.5	0.21-0.59	GA, Pits coalescing
	4	2.2-3.5	0.2-0.57	GA

* GA is general attack and number indicates depth, SGA is general attack over a large percentage of coupons.

** Pitting was noted but difficult to measure because they were located within areas of general attack.

The pitting depths observed in these vapor space coupon tests fall at the lower end of pit depths measured from previous studies. These depths from both Hanford and SRS testing are summarized in Table 4-5. Those tests performed with ammonia gas are included for comparison. The pits from the current testing ranged from 0.001 to 0.004 inches. Pit depths from previous testing range from 0.002 to 0.041 inch. The deeper pits are either in inhibitor-free solutions or those with a low concentration of nitrite. The inhibitor concentrations for the current testing ranged from 0.05 to 0.67M versus 0 to 1.3M for the previous testing.

Table 4-5 Summary of localized corrosion observed with vapor space coupon tests from previous studies *

Concentration (M)		pH	Temperature (°C)	Time (months)	Depth (mils)	Ammonia	Ref
Nitrate	Nitrite						
0.08	ND	12.8/9.5	40	4	2-5	No	9
0.08	ND	12.8/9.5	40	4	None	Yes	9
5	0	ND	40	2	11	No	13
5	0	ND	40	4	41	No	13
1.5	0.45	ND	40	4	None	No	13
3.7	1.3	ND	50	3	3	No	8
3.7	1.3	ND	50	3	None	Yes	8
0.02	0.04	13/10	40	4	37	No	14
0.02	0.1	13/10	40/65	4	7/26	No	14
0.02	0.2	13/10	40	11	None	No	14

1. * ND – no data

5.0 Conclusions

This current research evaluated the localized corrosion in the vapor space over Hanford DST simulants to assess the impact on corrosion of ammonia and new minimum nitrite concentration limits, which are part of the broader corrosion chemistry limits. The findings from this study showed that the presence of ammonia gas in the vapor is sufficient to reduce corrosion over the short-term (i.e. four months) at a concentration of 550 ppm. These findings are in agreement with previous studies at both Hanford and SRS which showed ammonia gas in the vapor space to be inhibitive [8, 9].

The presence of ammonia in electrochemical test solutions, however, was insufficient to inhibit against pitting corrosion. The effect of the ammonia appears to be a function of the waste chemistry and may have more significant effects in waste with low nitrite concentrations. Since high levels of ammonia were found beneficial in previous studies, additional testing is recommended to assess the necessary minimum concentration for protection of carbon steel.

The new minimum R value of 0.15 was found to be insufficient to prevent pitting corrosion in the vapor space. The pitting that occurred, however, did not progress over the four-months. Pits appeared to stop growing, which would indicate that pitting might not progress through wall.

6.0 Acknowledgements

The authors wish to acknowledge the assistance of J. I. Mickalonis in completing this task.

7.0 References

1. A.R. Felmy, O. Qafoku, B. Arey, K.D. Boomer, “Chemical Species in the Vapor Phase of Hanford Double-Shell Tanks: Potential Impacts on Waste Tank Corrosion Processes” PNNL-19767, September 2010
2. Elizabeth N. Hoffman, “Corrosion Testing in Simulated Tank Solutions,” SRNL-STI-2010-00509, September 2010
3. Elizabeth N. Hoffman, “Testing Vapor Space and Liquid-Air Interface Corrosion In Simulated Environments of Hanford Double-Shelled Tanks,” SRNL-STI-2011-00494, September 2011
4. RPP-RPT-31129, “Expert Panel Workshop on Double-Shell Tank Vapor Space Corrosion Testing,” CH2M Hill Hanford Group, Inc., Richland, WA, 2006
5. J. R. Gray and B. L. Garcia Diaz, “Task Technical Plan for Vapor Space Corrosion Testing Simulating Environment of Hanford Double-Shell Tanks,” SRNL-STI-2013-00087, Revision 0, April 2013
6. J. R. Gray and B. L. Garcia Diaz, “Task Technical Plan for Liquid-Air Interface Corrosion Testing Simulating Environment of Hanford Double-Shell Tanks,” SRNL-STI-2013-00272, Revision 0, May 2013
7. J. R. Gray and B. L. Garcia Diaz, “Liquid-Air Interface Corrosion Testing Simulating the Environment of Hanford Double-Shell Tanks,” SRNL-STI-2013-00943, Revision 0, December 2013
8. R. P. Anantatmula, “DST Pitting Annual Report,” WHC-SD-WM-PRS-016, Rev 0, Westinghouse Hanford Company, Richland, WA, September 26, 1996
9. J. .W Congdon, “Evaluation of Corrosion Inhibitors for Washed Precipitate – Coupon Test Results,” DPST-86-721, Savannah River Laboratory, Aiken SC, October 15, 1986
10. L. M. Stock, J. R. Follett, and E. C. Shallman, “Specifications for the Minimization of the Stress Corrosion Cracking Threat in Double-Shell Tank Wastes,” RPP-RPT-47337, Washington River Protection Solutions, March 2011
11. Hongbo Cong, Kathleen M. Sherer, Kavitha Tummaia, C. Sean Brossia, Shane Finneran, and Narasi Sridhar, “FY2013 DNV DST and SST Corrosion and Stress Corrosion Cracking Testing Report,” in draft
12. ASTM G1-03 Standard Practice for Preparing, Cleaning, and Evaluating Corrosion Test Specimens, ASTM International, Conshohochen PA, 2011
13. K. Subramanian and P. E. Zapp, “Pitting Corrosion in the Vapor Sapce and Liquid/Air Interface of High Level Radioactive Waste Tank,” WSRC-MS-2003-00883
14. A. F. Riechman, “In-Tank Processing: Corrosion Phenomena Due to Storage of Dilute Waste Solutions,” DPST-86-236, Savannah River Laboratory, January 20, 1986
15. R. J. Yarbrough, “Steady-State Flammable Gas Release Rate Calculation and Lower Flammability Level Evaluation for Hanford Tank Waste”, RPP-5926, Rev. 12, September 26, 2012
16. “RPP-5926 Ammonia Evaluation, v. 1.0”, SVF-1549, Washington River Protection Solutions, Richland, WA, 2008
17. R. V. Thurston, et.al, “Aqueous Ammonia Equilibrium”, EPA-600/3-79-091, August, 1979
18. HSC Chemistry 7.1, Outotec, Pori, FI, 2012
19. John Emsley, The Elements, First edition, Oxford University Press, UK, 1990

APPENDIX A

Solution Compositions for Electochemical and Coupon Tests

SY102 High Nitrate – 0% Evaporation – 0 ppm NH_3

Solution Volume	2.0000	L		
SY102 high nitrate 0%	CHECK pH before starting electrochemical test, pH=10.01			
	Molecular weight	**Experimental Conc (M)**	**Experimental Mass (g)**	**Measured Mass**
KNO3	101.1100	0.0009	0.1820	
Na2OAl2O3 3H2O	217.9900	0	0.0000	
NaBr	102.8900	0.064	13.1699	
NaCl	58.4400	0.011	1.2857	
NaCrO4		0	0.0000	
NaF	41.9900	0.0026	0.2183	
NaNO3	84.9900	3.6391	618.5742	
NaNO2	69.0000	0.097	13.3860	
Na3PO4 12H2O	380.1200	0.024	18.2458	
Na2SO4	142.0400	0.047	13.3518	
NaHCO3	84.0100	0.0304	5.1099	
Na2CO3	105.9900	0.265	56.0873	
NH4NO3	80.0520	0	0.0000	

SY102 High Nitrate – 32.81% Evaporation – 0 ppm NH_3

Solution Volume	2.0000	L		
SY102 high nitrate 32.81%	CHECK pH before starting electrochemical test, pH=10.16			
	Molecular weight	**Experimental Conc (M)**	**Experimental Mass (g)**	**Measured Mass**
KNO3	101.1100	0.0012	0.2427	
Na2OAl2O3 3H2O	217.9900	0	0.0000	
NaBr	102.8900	0.088	18.1086	
NaCl	58.4400	0.015	1.7532	
NaCrO4		0	0.0000	
NaF	41.9900	0.0036	0.3023	
NaNO3	84.9900	5.0188	853.0956	
NaNO2	69.0000	0.13	17.9400	
Na3PO4 12H2O	380.1200	0.033	25.0879	
Na2SO4	142.0400	0.064	18.1811	
NaHCO3	84.0100	0.0285	4.7921	
Na2CO3	105.9900	0.376	79.8060	
NH4NO3	80.0520	0	0.0000	

SY102 High Nitrate – 0% Evaporation – 50 ppm NH_3

Solution Volume	2.0000	L		
SY102 high nitrate 0%, 50 ppm	CHECK pH before starting electrochemical test, pH=10.01			
	Molecular weight	**Experimental Conc (M)**	**Experimental Mass (g)**	**Measured Mass**
KNO3	101.1100	0.0009	0.1820	
Na2OAl2O3 3H2O	217.9900	0	0.0000	
NaBr	102.8900	0.064	13.1699	
NaCl	58.4400	0.011	1.2857	
NaCrO4		0	0.0000	
NaF	41.9900	0.0026	0.2183	
NaNO3	84.9900	3.64	618.3514	
NaNO2	69.0000	0.097	13.3860	
Na3PO4 12H2O	380.1200	0.024	18.2458	
Na2SO4	142.0400	0.047	13.3518	
NaHCO3	84.0100	0.0304	5.1099	
Na2CO3	105.9900	0.265	56.0873	
NH4NO3	80.0520	0.00131	0.2099	

SY102 High Nitrate – 32.81% Evaporation – 50 ppm NH_3

Solution Volume	2.0000	L		
SY102 high nitrate 32.81%, 50 ppm	CHECK pH before starting electrochemical test, pH=10.16			
	Molecular weight	**Experimental Conc (M)**	**Experimental Mass (g)**	**Measured Mass**
KNO3	101.1100	0.0012	0.2427	
Na2OAl2O3 3H2O	217.9900	0	0.0000	
NaBr	102.8900	0.088	18.1086	
NaCl	58.4400	0.015	1.7532	
NaCrO4		0	0.0000	
NaF	41.9900	0.0036	0.3023	
NaNO3	84.9900	5.02	852.8312	
NaNO2	69.0000	0.13	17.9400	
Na3PO4 12H2O	380.1200	0.033	25.0879	
Na2SO4	142.0400	0.064	18.1811	
NaHCO3	84.0100	0.0285	4.7921	
Na2CO3	105.9900	0.376	79.8060	
NH4NO3	80.0520	0.00156	0.2491	

SY102 High Nitrate – 0% Evaporation – 550 ppm NH_3

Solution Volume	2.0000	L		
SY102 high nitrate 0%, 550 ppm	CHECK pH before starting electrochemical test, pH=10.01			
	Molecular weight	**Experimental Conc (M)**	**Experimental Mass (g)**	**Measured Mass**
KNO3	101.1100	0.0009	0.1820	
Na2OAl2O3 3H2O	217.9900	0	0.0000	
NaBr	102.8900	0.064	13.1699	
NaCl	58.4400	0.011	1.2857	
NaCrO4		0	0.0000	
NaF	41.9900	0.0026	0.2183	
NaNO3	84.9900	3.62	616.0812	
NaNO2	69.0000	0.097	13.3860	
Na3PO4 12H2O	380.1200	0.024	18.2458	
Na2SO4	142.0400	0.047	13.3518	
NaHCO3	84.0100	0.0304	5.1099	
Na2CO3	105.9900	0.265	56.0873	
NH4NO3	80.0520	0.0147	2.3482	

SY102 High Nitrate – 32.81% Evaporation – 550 ppm NH_3

Solution Volume	2.0000	L		
SY102 high nitrate 32.81%, 550 ppm	CHECK pH before starting electrochemical test, pH=10.16			
	Molecular weight	**Experimental Conc (M)**	**Experimental Mass (g)**	**Measured Mass**
KNO3	101.1100	0.0012	0.2427	
Na2OAl2O3 3H2O	217.9900	0	0.0000	
NaBr	102.8900	0.088	18.1086	
NaCl	58.4400	0.015	1.7532	
NaCrO4		0	0.0000	
NaF	41.9900	0.0036	0.3023	
NaNO3	84.9900	5.00	850.1871	
NaNO2	69.0000	0.13	17.9400	
Na3PO4 12H2O	380.1200	0.033	25.0879	
Na2SO4	142.0400	0.064	18.1811	
NaHCO3	84.0100	0.0285	4.7921	
Na2CO3	105.9900	0.376	79.8060	
NH4NO3	80.0520	0.0171	2.7396	

AY101 Segment 3 – 0% Evaporation – 0 ppm NH_3

Solution Volume	2.0000	L		
AY101 segment 3 0%	CHECK pH before starting electrochemical test, pH=10.15			
	Molecular weight	**Experimental Conc (M)**	**Experimental Mass (g)**	**Measured Mass**
KNO3	101.1100	0	0.0000	
Na2OAl2O3 3H2O	217.9900	0	0.0000	
NaBr	102.8900	0.0048	0.9877	
NaCl	58.4400	0.013	1.5194	
NaCrO4		0	0.0000	
NaF	41.9900	0.0105	0.8818	
NaNO3	84.9900	1.01	171.6798	
NaNO2	69.0000	0.167	23.0460	
Na3PO4 12H2O	380.1200	0.04	30.4096	
Na2SO4	142.0400	0.0153	4.3464	
NaHCO3	84.0100	0.0501	8.4167	
Na2CO3	105.9900	0.486	103.0025	
NH4NO3	80.0000	0	0.0000	

AY101 Segment 3 – 34.37% Evaporation – 0 ppm NH_3

Solution Volume	2.0000	L		
AY101 Segment 3 34.37%	CHECK pH before starting electrochemical test, pH=10.23			
	Molecular weight	**Experimental Conc (M)**	**Experimental Mass (g)**	**Measured Mass**
KNO3	101.1100	0	0.0000	
Na2OAl2O3 3H2O	217.9900	0	0.0000	
NaBr	102.8900	0.0071	1.4610	
NaCl	58.4400	0.02	2.3376	
NaCrO4		0	0.0000	
NaF	41.9900	0.0156	1.3101	
NaNO3	84.9900	1.49	253.2702	
NaNO2	69.0000	0.248	34.2240	
Na3PO4 12H2O	380.1200	0.06	45.6144	
Na2SO4	142.0400	0.023	6.5338	
NaHCO3	84.0100	0.0555	9.3186	
Na2CO3	105.9900	0.727	154.0117	
NH4NO3	80.0000	0	0.0000	

AY101 Segment 3 – 76.03% Evaporation – 0 ppm NH_3

Solution Volume	2.0000	L		
AY101 Segment 3 76.03%	CHECK pH before starting electrochemical test, pH=10.43			
	Molecular weight	**Experimental Conc (M)**	**Experimental Mass (g)**	**Measured Mass**
KNO3	101.1100	0	0.0000	
Na2OAl2O3 3H2O	217.9900	0	0.0000	
NaBr	102.8900	0.017	3.4983	
NaCl	58.4400	0.048	5.6102	
NaCrO4		0	0.0000	
NaF	41.9900	0.038	3.1912	
NaNO3	84.9900	3.59	610.2282	
NaNO2	69.0000	0.6	82.8000	
Na3PO4 12H2O	380.1200	0.144	109.4746	
Na2SO4	142.0400	0.055	15.6244	
NaHCO3	84.0100	0.0442	7.4317	
Na2CO3	105.9900	1.106	234.4010	
NH4NO3	80.0000	0	0.0000	

AY101 Segment 3 – 0% Evaporation – 50 ppm NH_3

Solution Volume	2.0000	L		
AY101 segment 3 0%, 50 ppm	CHECK pH before starting electrochemical test, pH=10.15			
	Molecular weight	**Experimental Conc (M)**	**Experimental Mass (g)**	**Measured Mass**
KNO3	101.1100	0	0.0000	
Na2OAl2O3 3H2O	217.9900	0	0.0000	
NaBr	102.8900	0.0048	0.9877	
NaCl	58.4400	0.013	1.5194	
NaCrO4		0	0.0000	
NaF	41.9900	0.0105	0.8818	
NaNO3	84.9900	1.01	171.4777	
NaNO2	69.0000	0.167	23.0460	
Na3PO4 12H2O	380.1200	0.04	30.4096	
Na2SO4	142.0400	0.0153	4.3464	
NaHCO3	84.0100	0.0501	8.4167	
Na2CO3	105.9900	0.486	103.0025	
NH4NO3	80.0000	0.00119	0.1902	

AY101 Segment 3 – 34.37% Evaporation – 50 ppm NH_3

Solution Volume	2.0000	L		
AY101 Segment 3 34.37%, 50 ppm	CHECK pH before starting electrochemical test, pH=10.23			
	Molecular weight	**Experimental Conc (M)**	**Experimental Mass (g)**	**Measured Mass**
KNO3	101.1100	0	0.0000	
Na2OAl2O3 3H2O	217.9900	0	0.0000	
NaBr	102.8900	0.0071	1.4610	
NaCl	58.4400	0.02	2.3376	
NaCrO4		0	0.0000	
NaF	41.9900	0.0156	1.3101	
NaNO3	84.9900	1.49	253.0757	
NaNO2	69.0000	0.248	34.2240	
Na3PO4 12H2O	380.1200	0.06	45.6144	
Na2SO4	142.0400	0.023	6.5338	
NaHCO3	84.0100	0.0555	9.3186	
Na2CO3	105.9900	0.727	154.0117	
NH4NO3	80.0000	0.00114	0.1831	

AY101 Segment 3 – 76.03% Evaporation – 50 ppm NH_3

Solution Volume	2.0000	L		
AY101 Segment 3 76.03%, 50 ppm	CHECK pH before starting electrochemical test, pH=10.43			
	Molecular weight	**Experimental Conc (M)**	**Experimental Mass (g)**	**Measured Mass**
KNO3	101.1100	0	0.0000	
Na2OAl2O3 3H2O	217.9900	0	0.0000	
NaBr	102.8900	0.017	3.4983	
NaCl	58.4400	0.048	5.6102	
NaCrO4		0	0.0000	
NaF	41.9900	0.038	3.1912	
NaNO3	84.9900	3.59	610.0544	
NaNO2	69.0000	0.6	82.8000	
Na3PO4 12H2O	380.1200	0.144	109.4746	
Na2SO4	142.0400	0.055	15.6244	
NaHCO3	84.0100	0.0442	7.4317	
Na2CO3	105.9900	1.106	234.4010	
NH4NO3	80.0000	0.00102	0.1636	

AY101 Segment 3 – 0% Evaporation – 550 ppm NH_3

Solution Volume	2.0000	L		
AY101 segment 3 0%, 550 ppm	CHECK pH before starting electrochemical test, pH=10.15			
	Molecular weight	**Experimental Conc (M)**	**Experimental Mass (g)**	**Measured Mass**
KNO3	101.1100	0	0.0000	
Na2OAl2O3 3H2O	217.9900	0	0.0000	
NaBr	102.8900	0.0048	0.9877	
NaCl	58.4400	0.013	1.5194	
NaCrO4		0	0.0000	
NaF	41.9900	0.0105	0.8818	
NaNO3	84.9900	1.00	169.4512	
NaNO2	69.0000	0.167	23.0460	
Na3PO4 12H2O	380.1200	0.04	30.4096	
Na2SO4	142.0400	0.0153	4.3464	
NaHCO3	84.0100	0.0501	8.4167	
Na2CO3	105.9900	0.486	103.0025	
NH4NO3	80.0000	0.0131	2.0978	

AY101 Segment 3 – 34.37% Evaporation – 550 ppm NH_3

Solution Volume	2.0000	L		
AY101 Segment 3 34.37%, 550 ppm	CHECK pH before starting electrochemical test, pH=10.23			
	Molecular weight	**Experimental Conc (M)**	**Experimental Mass (g)**	**Measured Mass**
KNO3	101.1100	0	0.0000	
Na2OAl2O3 3H2O	217.9900	0	0.0000	
NaBr	102.8900	0.0071	1.4610	
NaCl	58.4400	0.02	2.3376	
NaCrO4		0	0.0000	
NaF	41.9900	0.0156	1.3101	
NaNO3	84.9900	1.48	251.1360	
NaNO2	69.0000	0.248	34.2240	
Na3PO4 12H2O	380.1200	0.06	45.6144	
Na2SO4	142.0400	0.023	6.5338	
NaHCO3	84.0100	0.0555	9.3186	
Na2CO3	105.9900	0.727	154.0117	
NH4NO3	80.0000	0.0126	2.0089	

AY101 Segment 3 – 76.03% Evaporation – 550 ppm NH_3

Solution Volume	2.0000	L		
AY101 Segment 3 76.03%, 550 ppm	CHECK pH before starting electrochemical test, pH=10.43			
	Molecular weight	**Experimental Conc (M)**	**Experimental Mass (g)**	**Measured Mass**
KNO3	101.1100	0	0.0000	
Na2OAl2O3 3H2O	217.9900	0	0.0000	
NaBr	102.8900	0.017	3.4983	
NaCl	58.4400	0.048	5.6102	
NaCrO4		0	0.0000	
NaF	41.9900	0.038	3.1912	
NaNO3	84.9900	3.58	608.3206	
NaNO2	69.0000	0.6	82.8000	
Na3PO4 12H2O	380.1200	0.144	109.4746	
Na2SO4	142.0400	0.055	15.6244	
NaHCO3	84.0100	0.0442	7.4317	
Na2CO3	105.9900	1.106	234.4010	
NH4NO3	80.0000	0.0112	1.7956	

AY101 Segment 8 – 0% Evaporation – 0 ppm NH_3

Solution Volume	2.0000	L		
AY101 segment 8 0%	CHECK pH before starting electrochemical test, pH=10.29			
	Molecular weight	**Experimental Conc (M)**	**Experimental Mass (g)**	**Measured Mass**
KNO3	101.1100	0.04	8.0888	
Na2OAl2O3 3H2O	217.9900	0	0.0000	
NaBr	102.8900	0	0.0000	
NaCl	58.4400	0.086	10.0517	
NaCrO4		0	0.0000	
NaF	41.9900	0.0099	0.8314	
NaNO3	84.9900	1.54	261.7692	
NaNO2	69.0000	0.972	134.1360	
Na3PO4 12H2O	380.1200	0.043	32.6903	
Na2SO4	142.0400	0.033	9.3746	
NaHCO3	84.0100	0.0532	8.9352	
Na2CO3	105.9900	0.867	183.7487	
NH4NO3	80.0000	0	0.0000	

AY101 Segment 8 – 27.36% Evaporation – 0 ppm NH_3

Solution Volume	2.0000	L		
AY101 Segment 8 27.36%	CHECK pH before starting electrochemical test, pH=10.39			
	Molecular weight	**Experimental Conc (M)**	**Experimental Mass (g)**	**Measured Mass**
KNO3	101.1100	0.053	10.7177	
Na2OAl2O3 3H2O	217.9900	0	0.0000	
NaBr	102.8900	0	0.0000	
NaCl	58.4400	0.11	12.8568	
NaCrO4		0	0.0000	
NaF	41.9900	0.013	1.0917	
NaNO3	84.9900	2.027	344.5495	
NaNO2	69.0000	1.28	176.6400	
Na3PO4 12H2O	380.1200	0.057	43.3337	
Na2SO4	142.0400	0.044	12.4995	
NaHCO3	84.0100	0.0526	8.8393	
Na2CO3	105.9900	1.157	245.3438	
NH4NO3	80.0000	0	0.0000	

AY101 Segment 8 – 67.95% Evaporation – 0 ppm NH_3

Solution Volume	2.0000	L		
AY101 Segment 8 67.95%	CHECK pH before starting electrochemical test, pH=10.32			
	Molecular weight	**Experimental Conc (M)**	**Experimental Mass (g)**	**Measured Mass**
KNO3	101.1100	0.105	21.2331	
Na2OAl2O3 3H2O	217.9900	0	0.0000	
NaBr	102.8900	0	0.0000	
NaCl	58.4400	0.18	10.5192	
NaCrO4		0	0.0000	
NaF	41.9900	0.026	1.0917	
NaNO3	84.9900	4.045	343.7846	
NaNO2	69.0000	2.55	175.9500	
Na3PO4 12H2O	380.1200	0.11	41.8132	
Na2SO4	142.0400	0.087	12.3575	
NaHCO3	84.0100	0.0237	1.9943	
Na2CO3	105.9900	0.484	51.3269	
NH4NO3	80.0000	0	0.0000	

AY101 Segment 8 – 0% Evaporation – 50 ppm NH_3

Solution Volume	2.0000	L		
AY101 segment 8 0%, 50 ppm	CHECK pH before starting electrochemical test, pH=10.29			
	Molecular weight	**Experimental Conc (M)**	**Experimental Mass (g)**	**Measured Mass**
KNO3	101.1100	0.04	8.0888	
Na2OAl2O3 3H2O	217.9900	0	0.0000	
NaBr	102.8900	0	0.0000	
NaCl	58.4400	0.086	10.0517	
NaCrO4		0	0.0000	
NaF	41.9900	0.0099	0.8314	
NaNO3	84.9900	1.54	261.5917	
NaNO2	69.0000	0.972	134.1360	
Na3PO4 12H2O	380.1200	0.043	32.6903	
Na2SO4	142.0400	0.033	9.3746	
NaHCO3	84.0100	0.0532	8.9352	
Na2CO3	105.9900	0.867	183.7487	
NH4NO3	80.0000	0.00104	0.1671	

AY101 Segment 8 – 27.36% Evaporation – 50 ppm NH_3

Solution Volume	2.0000	L		
AY101 Segment 8 27.36%, 50 ppm	CHECK pH before starting electrochemical test, pH=10.39			
	Molecular weight	**Experimental Conc (M)**	**Experimental Mass (g)**	**Measured Mass**
KNO3	101.1100	0.053	10.7177	
Na2OAl2O3 3H2O	217.9900	0	0.0000	
NaBr	102.8900	0	0.0000	
NaCl	58.4400	0.11	12.8568	
NaCrO4		0	0.0000	
NaF	41.9900	0.013	1.0917	
NaNO3	84.9900	2.03	344.3908	
NaNO2	69.0000	1.28	176.6400	
Na3PO4 12H2O	380.1200	0.057	43.3337	
Na2SO4	142.0400	0.044	12.4995	
NaHCO3	84.0100	0.0526	8.8393	
Na2CO3	105.9900	1.157	245.3438	
NH4NO3	80.0000	0.000933	0.1493	

AY101 Segment 8 – 27.95% Evaporation – 50 ppm NH_3

Solution Volume	2.0000	L		
AY101 Segment 8 67.95%, 50 ppm	CHECK pH before starting electrochemical test, pH=10.32			
	Molecular weight	**Experimental Conc (M)**	**Experimental Mass (g)**	**Measured Mass**
KNO3	101.1100	0.105	21.2331	
Na2OAl2O3 3H2O	217.9900	0	0.0000	
NaBr	102.8900	0	0.0000	
NaCl	58.4400	0.18	10.5192	
NaCrO4		0	0.0000	
NaF	41.9900	0.026	1.0917	
NaNO3	84.9900	4.04	343.6967	
NaNO2	69.0000	2.55	175.9500	
Na3PO4 12H2O	380.1200	0.11	41.8132	
Na2SO4	142.0400	0.087	12.3575	
NaHCO3	84.0100	0.0237	1.9943	
Na2CO3	105.9900	0.484	51.3269	
NH4NO3	80.0000	0.00103	0.0827	

AY101 Segment 8 – 0% Evaporation – 550 ppm NH_3

Solution Volume	2.0000	L		
AY101 segment 8 0%, 550 ppm	CHECK pH before starting electrochemical test, pH=10.29			
	Molecular weight	**Experimental Conc (M)**	**Experimental Mass (g)**	**Measured Mass**
KNO3	101.1100	0.04	8.0888	
Na2OAl2O3 3H2O	217.9900	0	0.0000	
NaBr	102.8900	0	0.0000	
NaCl	58.4400	0.086	10.0517	
NaCrO4		0	0.0000	
NaF	41.9900	0.0099	0.8314	
NaNO3	84.9900	1.53	259.8239	
NaNO2	69.0000	0.972	134.1360	
Na3PO4 12H2O	380.1200	0.043	32.6903	
Na2SO4	142.0400	0.033	9.3746	
NaHCO3	84.0100	0.0532	8.9352	
Na2CO3	105.9900	0.867	183.7487	
NH4NO3	80.0000	0.0114	1.8311	

AY101 Segment 8 – 27.36% Evaporation – 550 ppm NH_3

Solution Volume	2.0000	L		
AY101 Segment 8 27.36%, 550 ppm	CHECK pH before starting electrochemical test, pH=10.39			
	Molecular weight	**Experimental Conc (M)**	**Experimental Mass (g)**	**Measured Mass**
KNO3	101.1100	0.053	10.7177	
Na2OAl2O3 3H2O	217.9900	0	0.0000	
NaBr	102.8900	0	0.0000	
NaCl	58.4400	0.11	12.8568	
NaCrO4		0	0.0000	
NaF	41.9900	0.013	1.0917	
NaNO3	84.9900	2.02	342.7930	
NaNO2	69.0000	1.28	176.6400	
Na3PO4 12H2O	380.1200	0.057	43.3337	
Na2SO4	142.0400	0.044	12.4995	
NaHCO3	84.0100	0.0526	8.8393	
Na2CO3	105.9900	1.157	245.3438	
NH4NO3	80.0000	0.0103	1.6533	

AY101 Segment 8 – 67.95% Evaporation – 550 ppm NH_3

Solution Volume	2.0000	L		
AY101 Segment 8 67.95%, 550 ppm	CHECK pH before starting electrochemical test, pH=10.32			
	Molecular weight	**Experimental Conc (M)**	**Experimental Mass (g)**	**Measured Mass**
KNO3	101.1100	0.105	21.2331	
Na2OAl2O3 3H2O	217.9900	0	0.0000	
NaBr	102.8900	0	0.0000	
NaCl	58.4400	0.18	21.0384	
NaCrO4		0	0.0000	
NaF	41.9900	0.026	2.1835	
NaNO3	84.9900	4.03	685.6427	
NaNO2	69.0000	2.55	351.9000	
Na3PO4 12H2O	380.1200	0.11	83.6264	
Na2SO4	142.0400	0.087	24.7150	
NaHCO3	84.0100	0.0237	3.9885	
Na2CO3	105.9900	0.484	102.6538	
NH4NO3	80.0000	0.0113	1.8133	

VSC/LAI Solution 1

Solution Volume	2.0000	L		
VSC/LAI Solution 1 - SRNL	CHECK pH before starting electrochemical test, pH=10			
	Molecular weight	**Experimental Conc (M)**	**Experimental Mass (g)**	**Measured Mass**
KNO3	101.1100	0	0.0000	
Na2OAl2O3 3H2O	217.9900	0	0.0000	
NaBr	102.8900	0	0.0000	
NaCl	58.4400	0.01	1.1688	
NaCrO4	161.9700	0.0001	0.0324	
NaF	41.9900	0.003	0.2519	
NaNO3	84.9900	0.40	67.9920	
NaNO2	69.0000	0.05	6.9000	
Na3PO4 12H2O	380.1200	0.0005	0.3801	
Na2SO4	142.0400	0.005	1.4204	
NaHCO3	84.0100	0.0250	4.2005	
Na2CO3	105.9900	0.075	15.8985	
NH4NO3	80.0000	0.00104	0.1671	

VSC/LAI Solution 2

Solution Volume	2.0000	L		
VSC/LAI Solution 2 - SRNL	CHECK pH before starting electrochemical test, pH=10			
	Molecular weight	**Experimental Conc (M)**	**Experimental Mass (g)**	**Measured Mass**
KNO3	101.1100	0	0.0000	
Na2OAl2O3 3H2O	217.9900	0	0.0000	
NaBr	102.8900	0	0.0000	
NaCl	58.4400	0.04	4.6752	
NaCrO4	161.9700	0.001	0.3239	
NaF	41.9900	0.01	0.8398	
NaNO3	84.9900	2.00	339.9600	
NaNO2	69.0000	0.3	41.4000	
Na3PO4 12H2O	380.1200	0.01	7.6024	
Na2SO4	142.0400	0.05	14.2040	
NaHCO3	84.0100	0.1000	16.8020	
Na2CO3	105.9900	0.400	84.7920	
NH4NO3	80.0000	0.000000	0.0000	

VSC/LAI Solution 3

Solution Volume	2.0000	L		
VSC/LAI Solution 3 - SRNL	CHECK pH before starting electrochemical test, pH=10			
	Molecular weight	**Experimental Conc (M)**	**Experimental Mass (g)**	**Measured Mass**
KNO3	101.1100	0	0.0000	
Na2OAl2O3 3H2O	217.9900	0	0.0000	
NaBr	102.8900	0	0.0000	
NaCl	58.4400	0.1	11.6880	
NaCrO4	161.9700	0.01	3.2394	
NaF	41.9900	0.02	1.6796	
NaNO3	84.9900	4.50	764.9100	
NaNO2	69.0000	0.675	93.1500	
Na3PO4 12H2O	380.1200	0.05	38.0120	
Na2SO4	142.0400	0.1	28.4080	
NaHCO3	84.0100	0.1667	28.0089	
Na2CO3	105.9900	0.833	176.6429	
NH4NO3	80.0000	0.00000	0.0000	

APPENDIX B

Electrochemical Data

The electrochemical data presented on the following pages of Appendix B are set up in the same manner. The top graph shows the open-circuit potential (OCP) data during the initial two-hour stabilization prior to performing the cyclic potentiodynamic polarization (CPP). The graph shows the OCP as measured against the Ag/AgCl reference electrode versus stabilization time (seconds). The bottom graph is the CPP scan; a plot of potential as measured against the Ag/AgCl reference electrode versus the logarithm of the current density (A/cm^2). The post-test photographs of the sample are shown along the bottom of the page. Images include a low magnification photograph of the entire sample and two higher magnification pictures highlighting the features in the center of the sample and along the edge of the sample. For bullet samples, the two photographs are shown; one photograph shows the entire sample and the other shows the bulleted end of the sample.

AY101 - Segment 3 – 0% Evaporation – 0 ppm NH_3
No Cover Gas – Sample 19

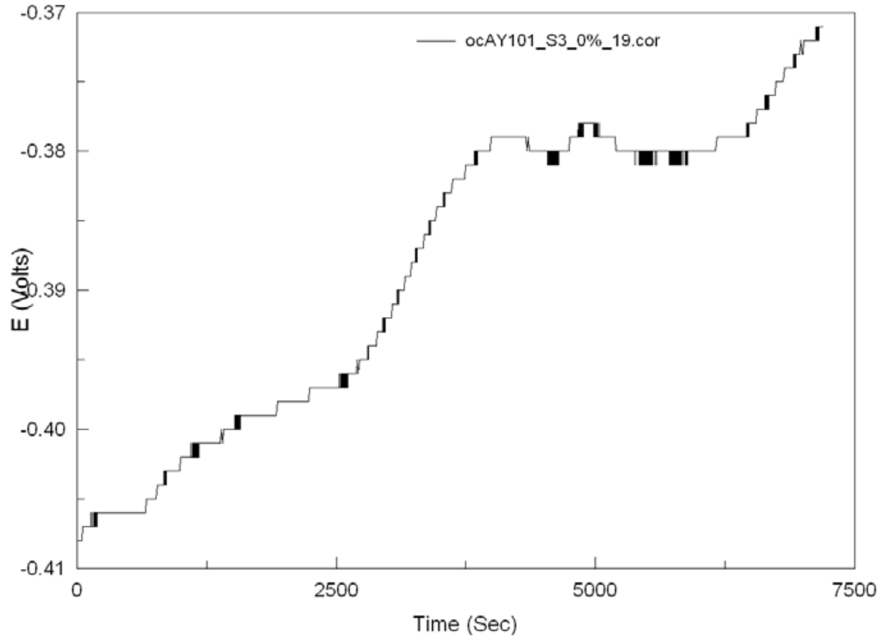

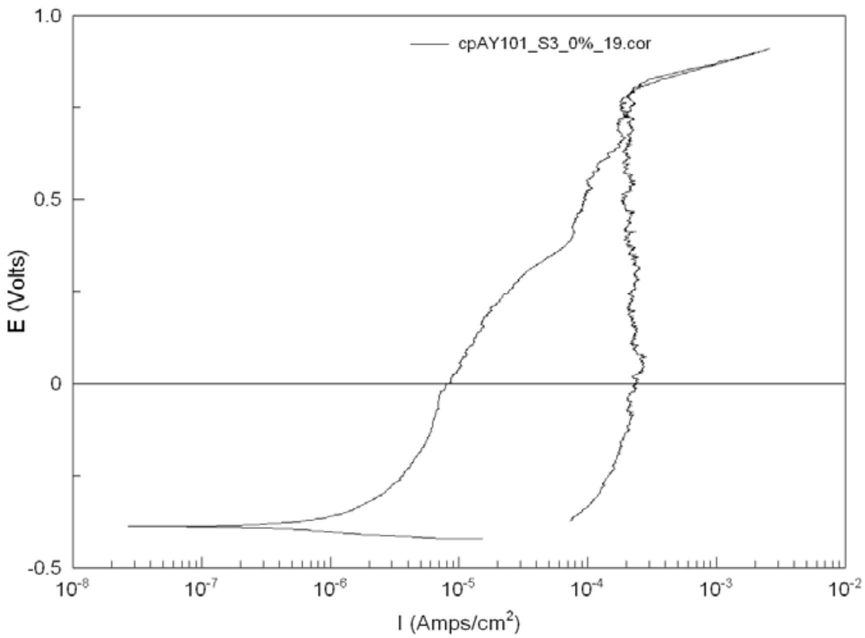

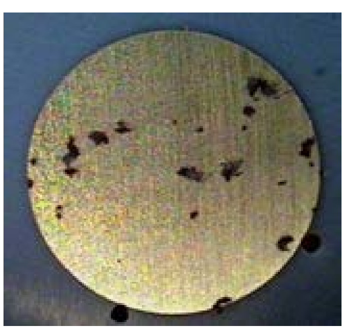

AY101 - Segment 3 – 0% Evaporation – 0 ppm NH_3
No Cover Gas – Sample 20

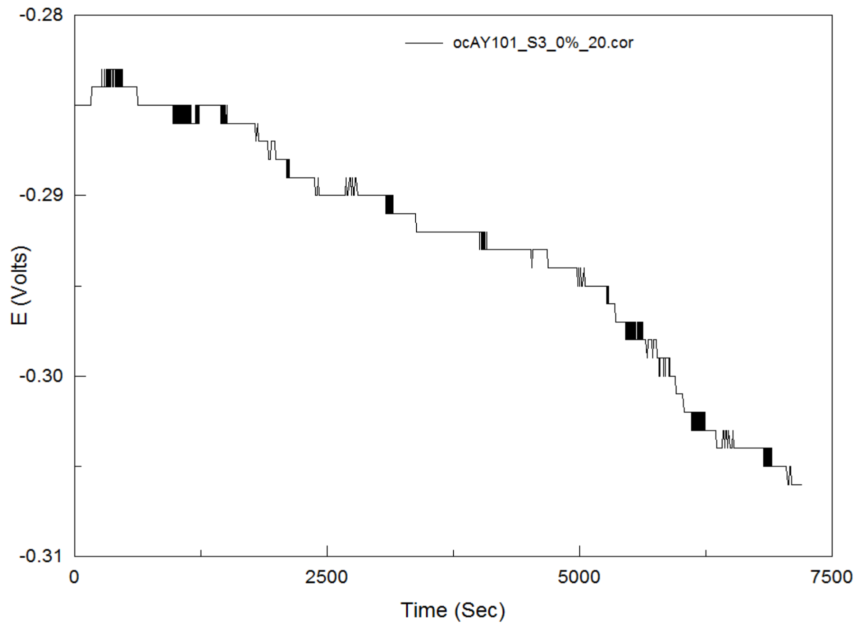

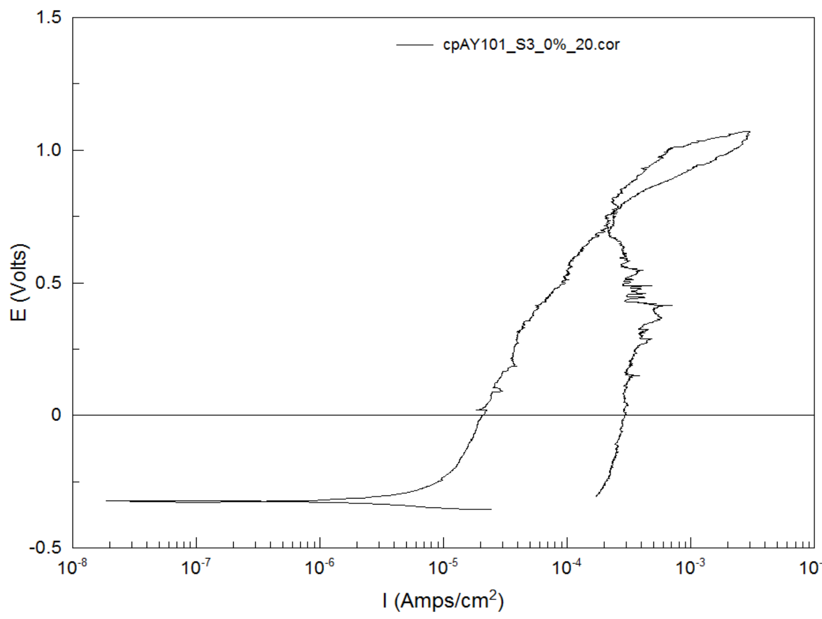

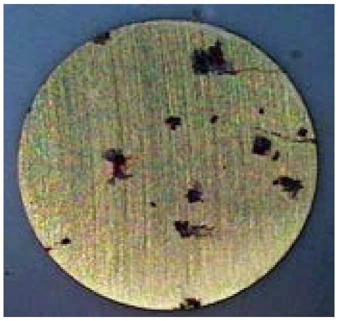

AY101 - Segment 3 – 0% Evaporation – 50 ppm NH_3
No Cover Gas – Sample 12

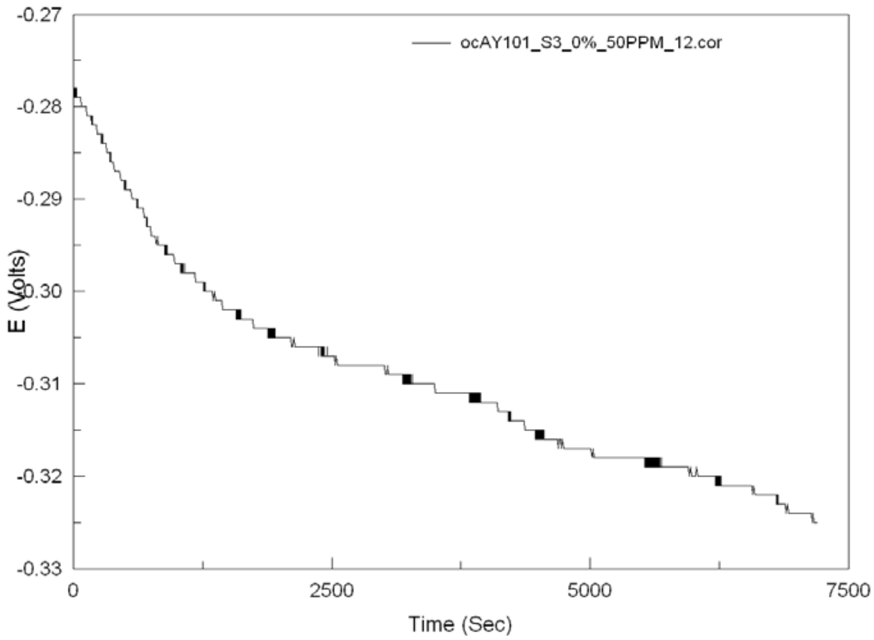

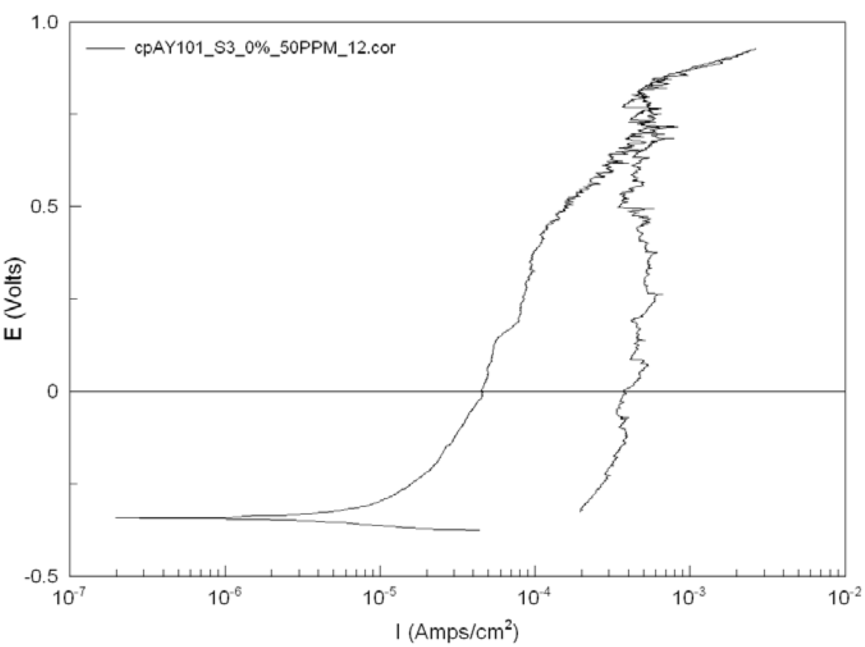

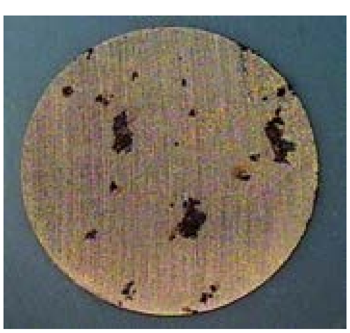
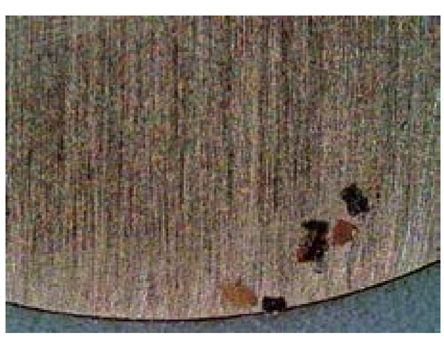


**AY101 - Segment 3 – 0% Evaporation – 50 ppm NH_3
No Cover Gas – Sample 14**

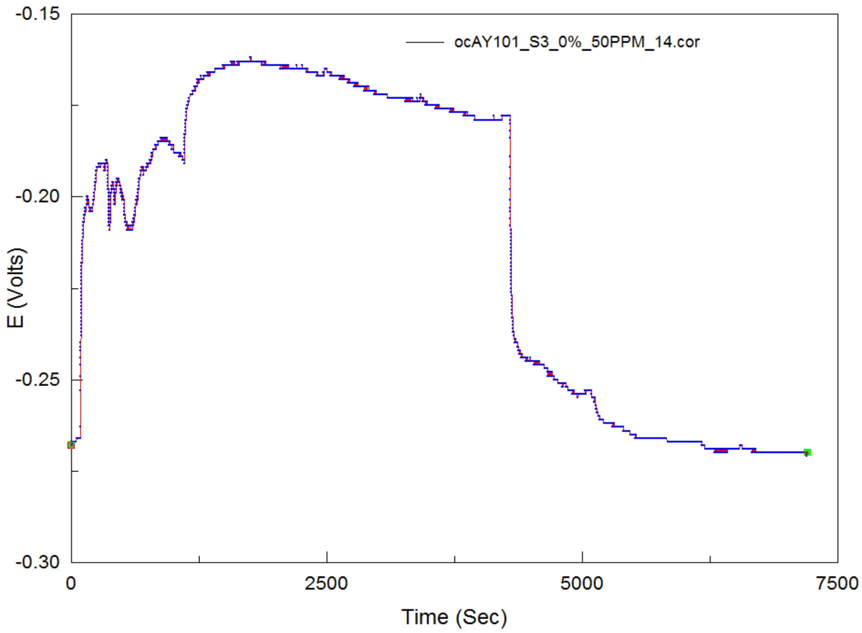

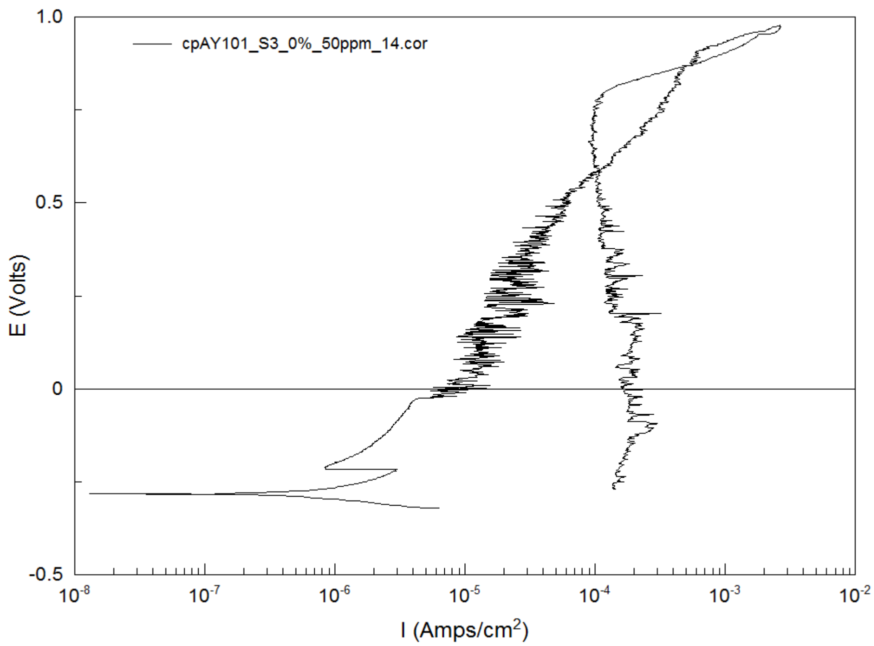

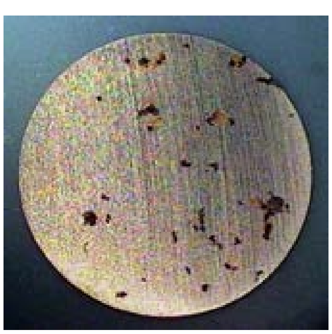

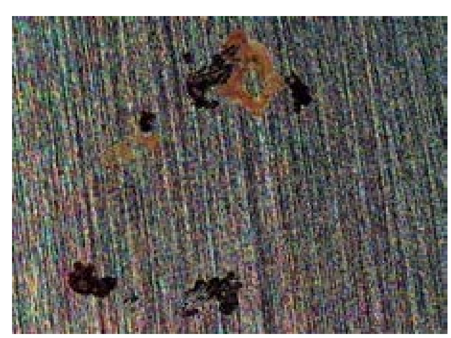

AY101 - Segment 3 – 0% Evaporation – 550 ppm NH_3
No Cover Gas – Sample 12

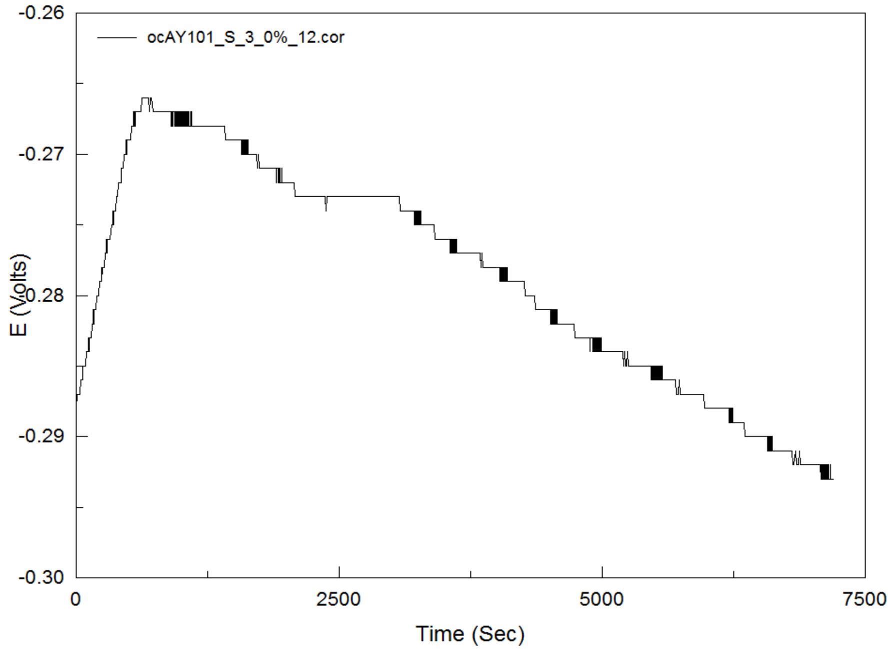

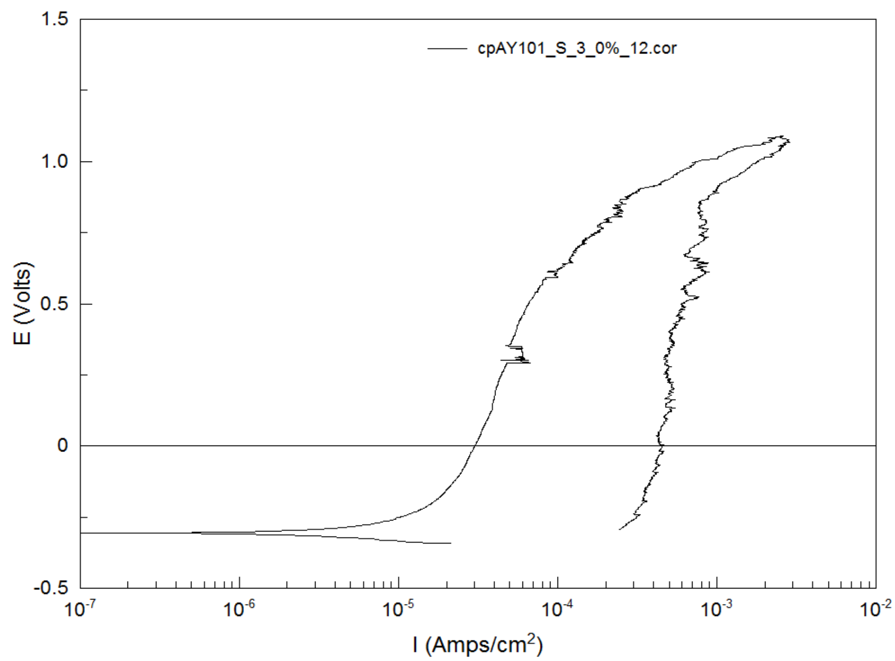



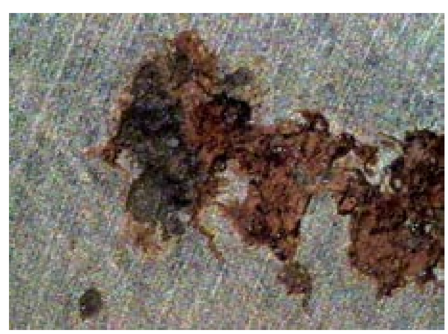

AY101 - Segment 3 – 0% Evaporation – 550 ppm NH_3
No Cover Gas – Sample 14

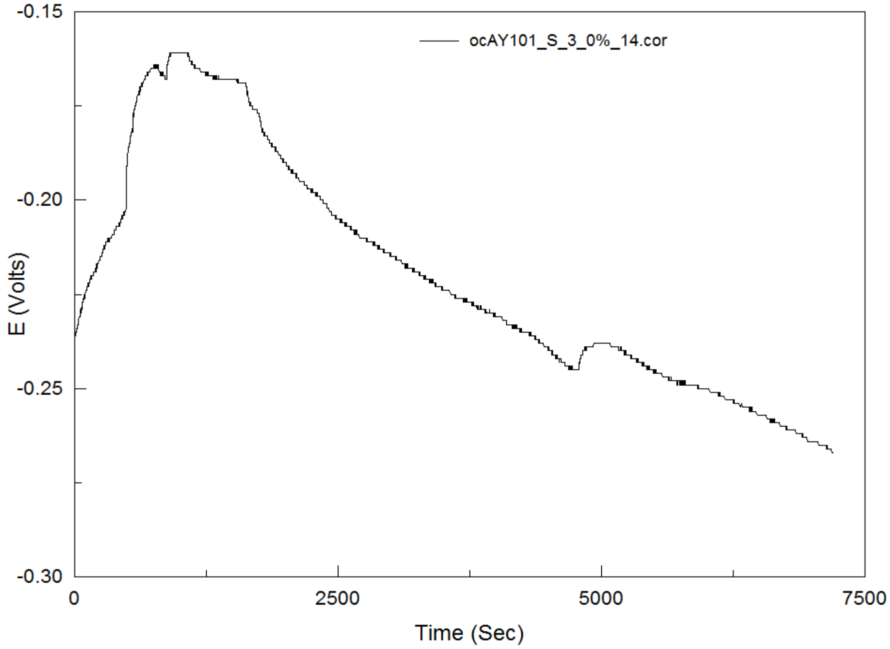

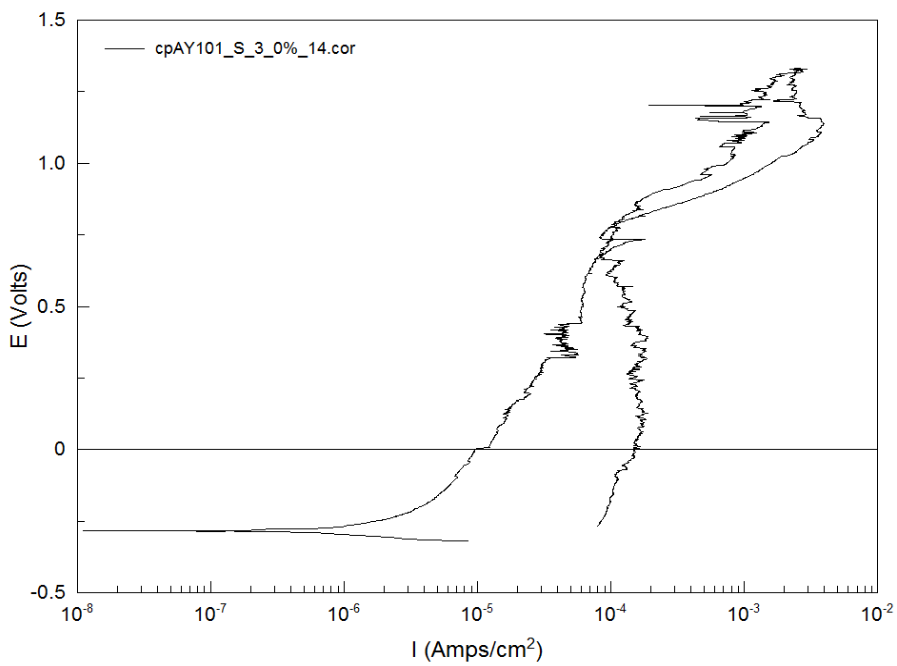

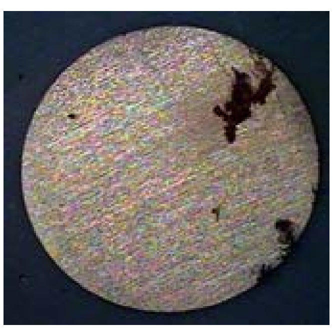
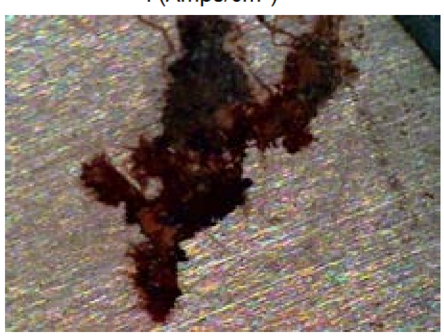
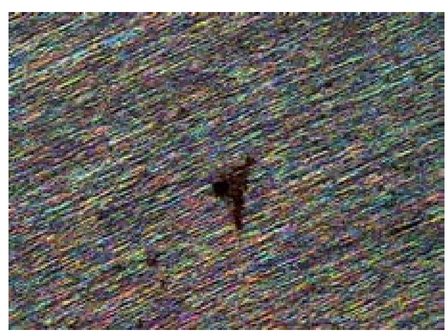

AY101 - Segment 3 – 34% Evaporation – 0 ppm NH_3
No Cover Gas – Sample 34

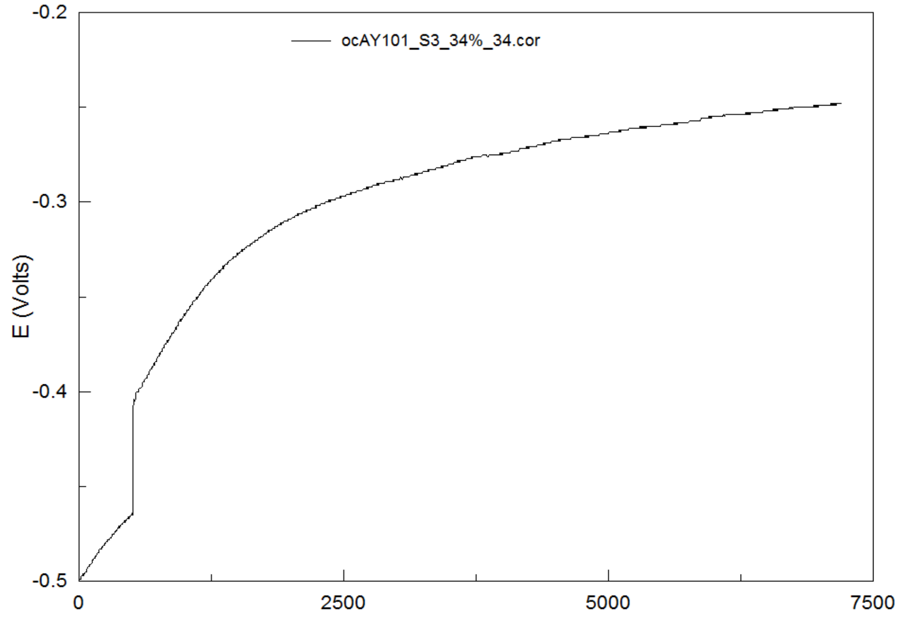

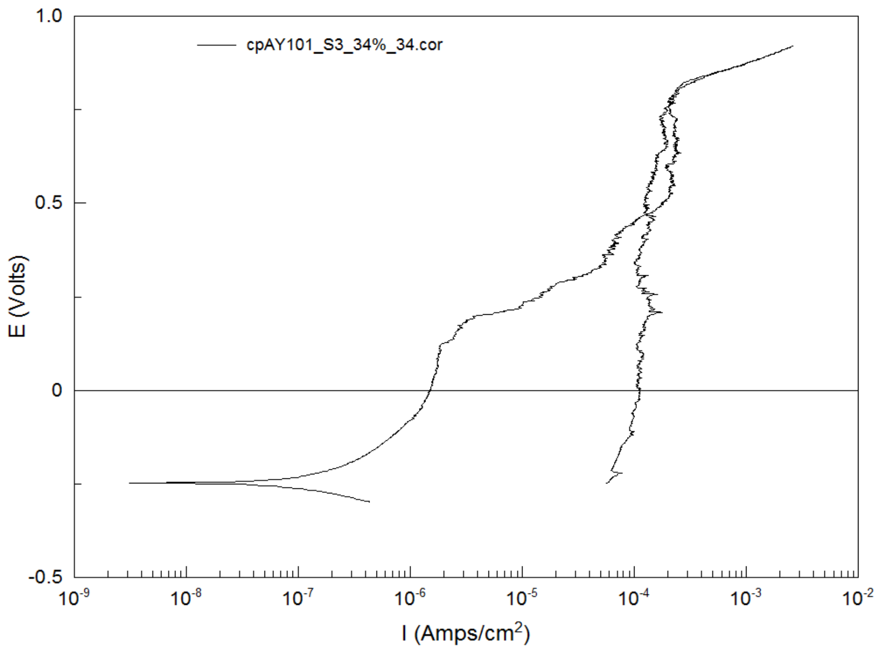


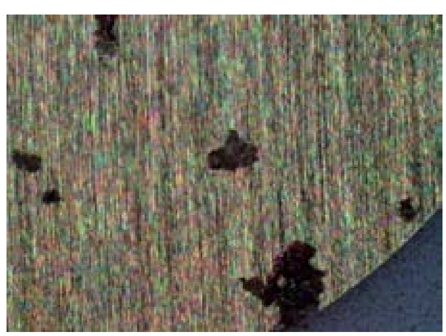
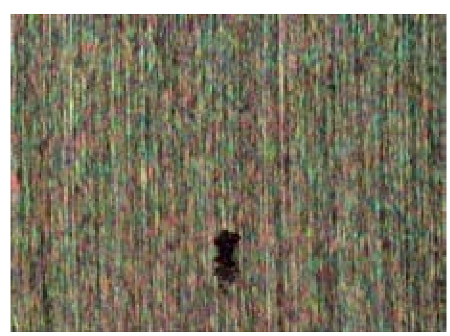

AY101 - Segment 3 – 34% Evaporation – 0 ppm NH_3
No Cover Gas – Sample 35

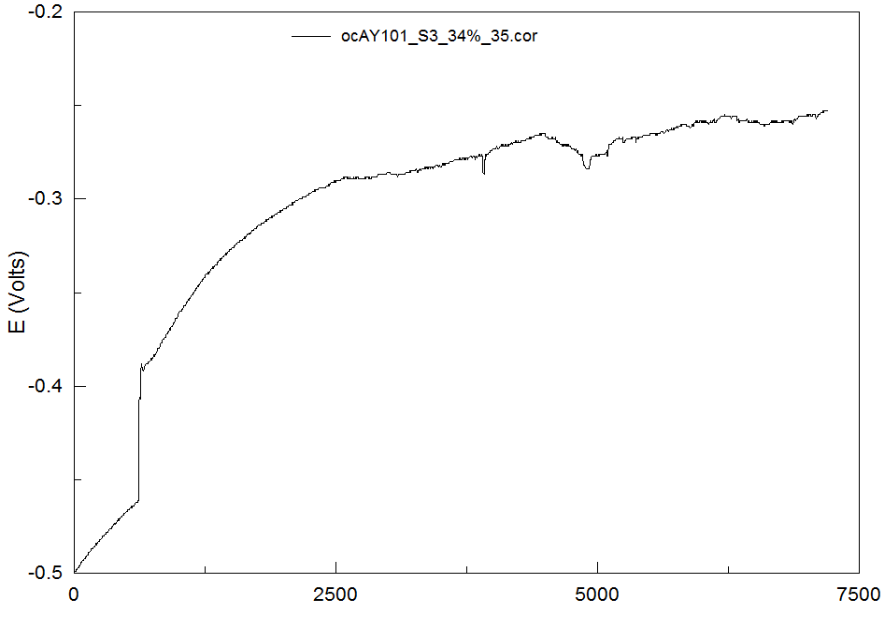

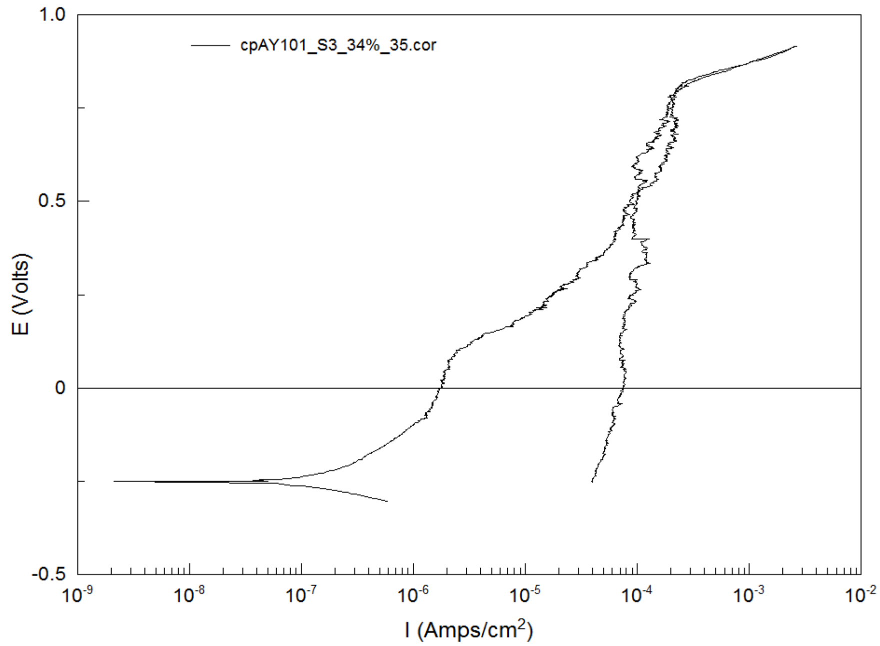

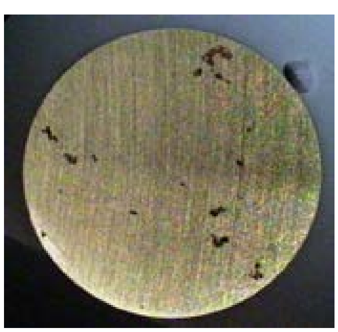

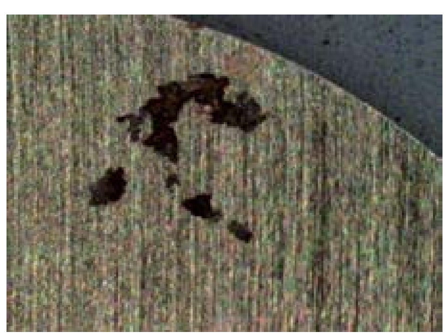

**AY101 - Segment 3 – 34% Evaporation – 50 ppm NH_3
No Cover Gas – Sample 30**

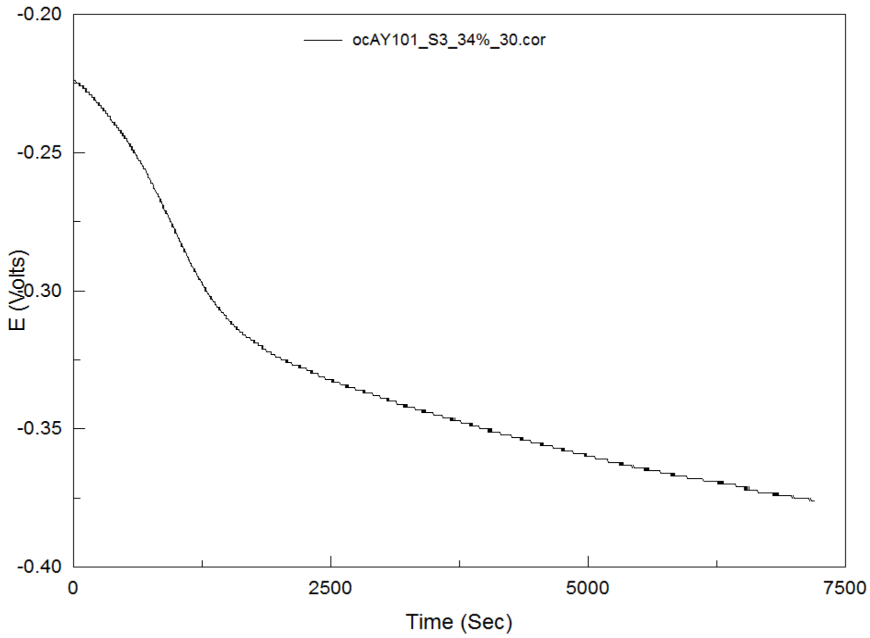

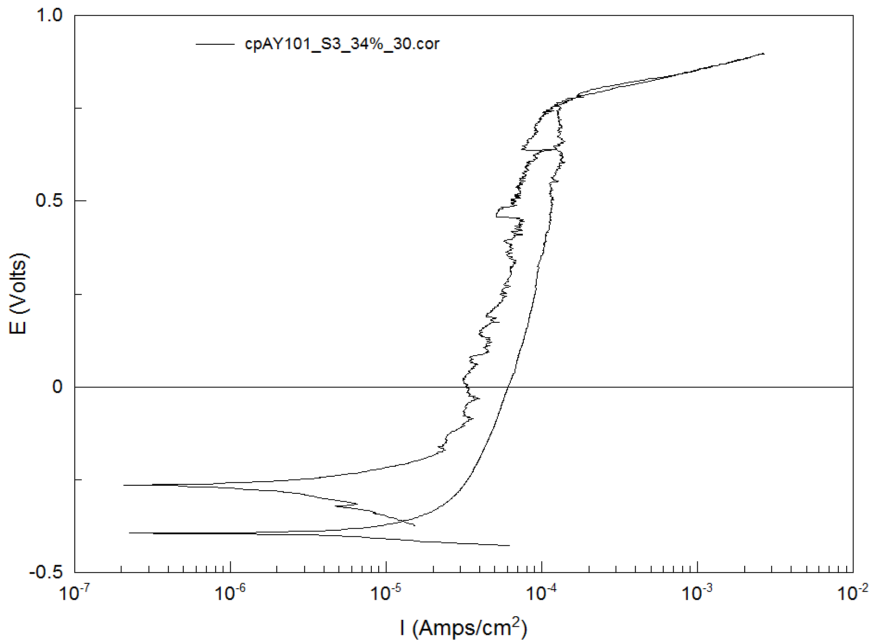

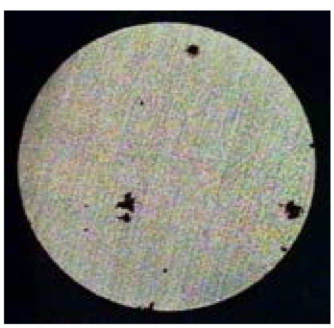

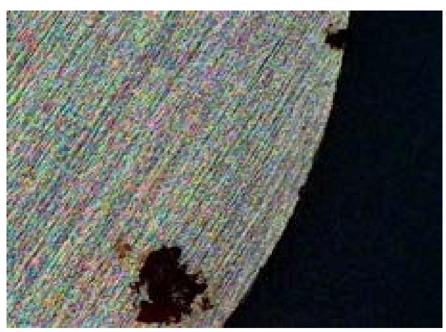

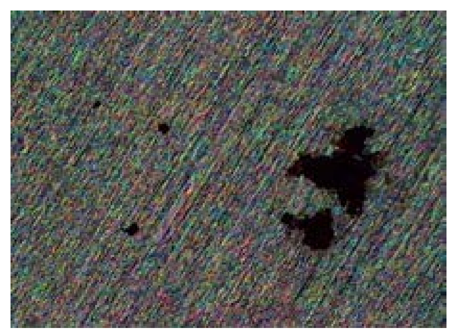

AY101 - Segment 3 – 34% Evaporation – 50 ppm NH_3
No Cover Gas – Sample 31

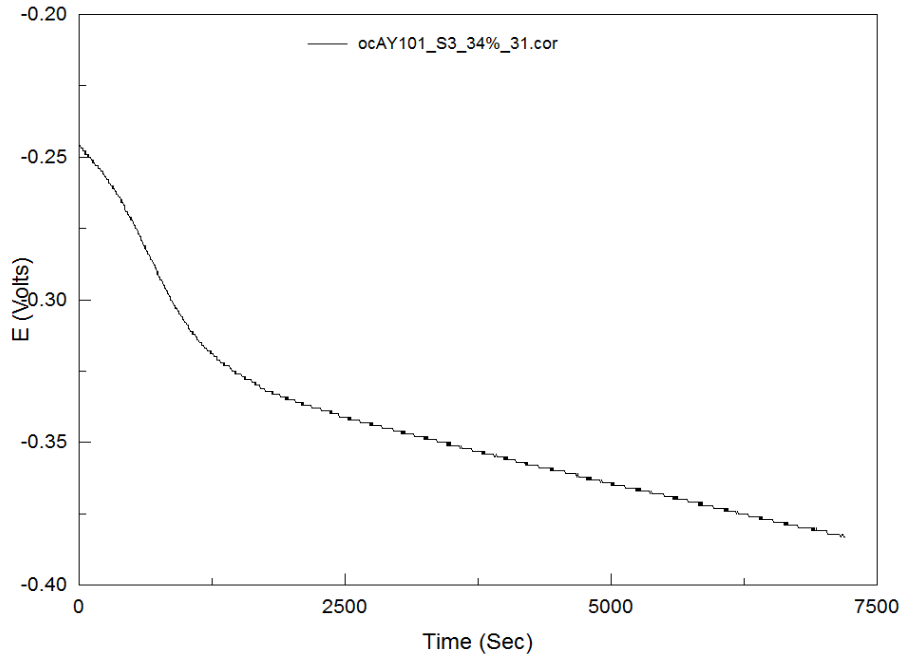

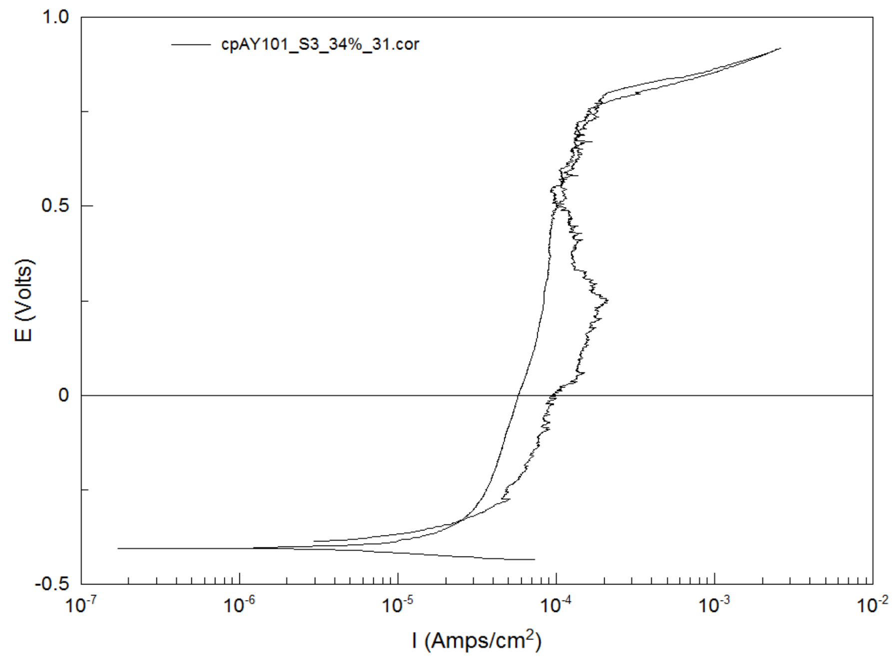

AY101 - Segment 3 – 34% Evaporation – 550 ppm NH_3
No Cover Gas – Sample 12

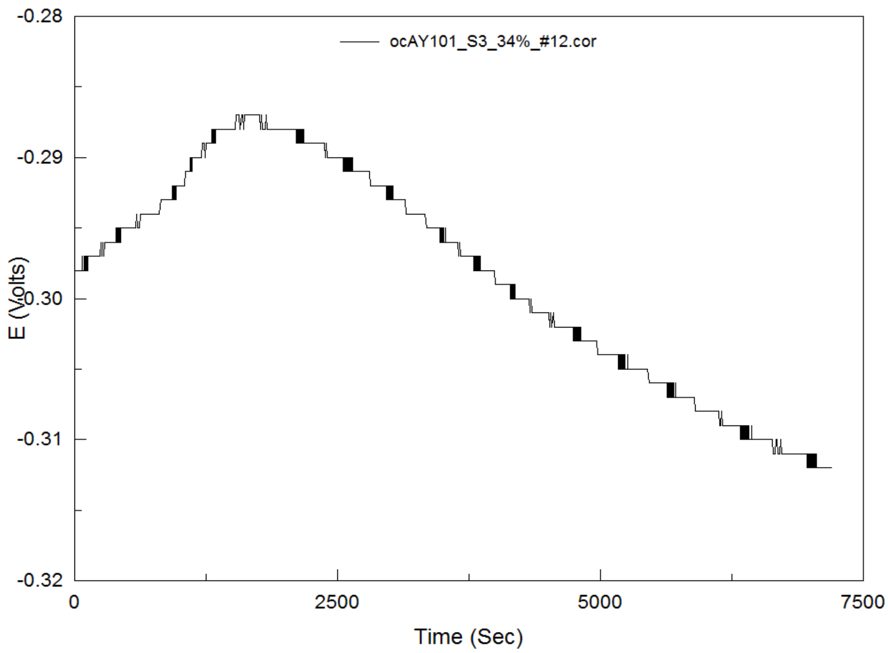

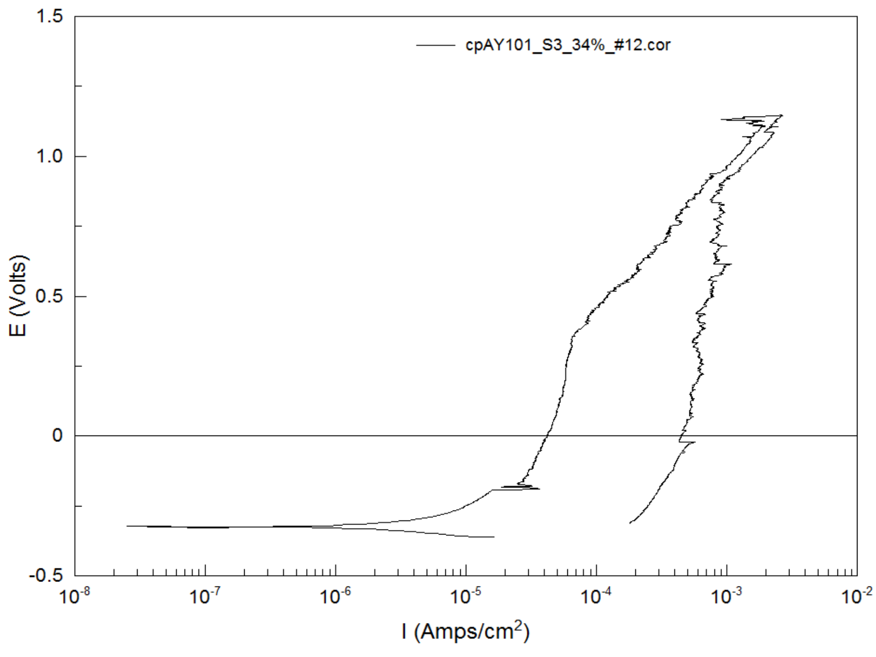

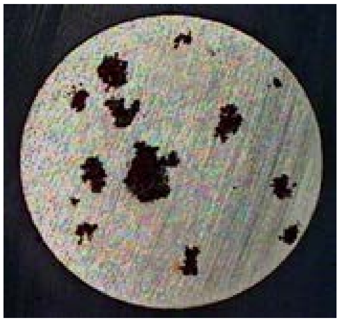

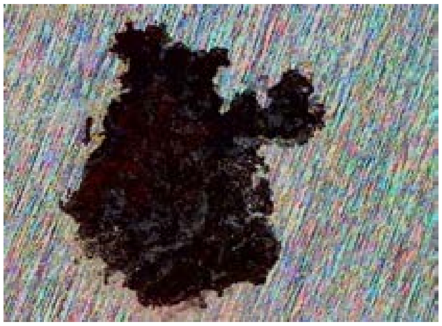

**AY101 - Segment 3 – 34% Evaporation – 550 ppm NH_3
No Cover Gas – Sample 14**

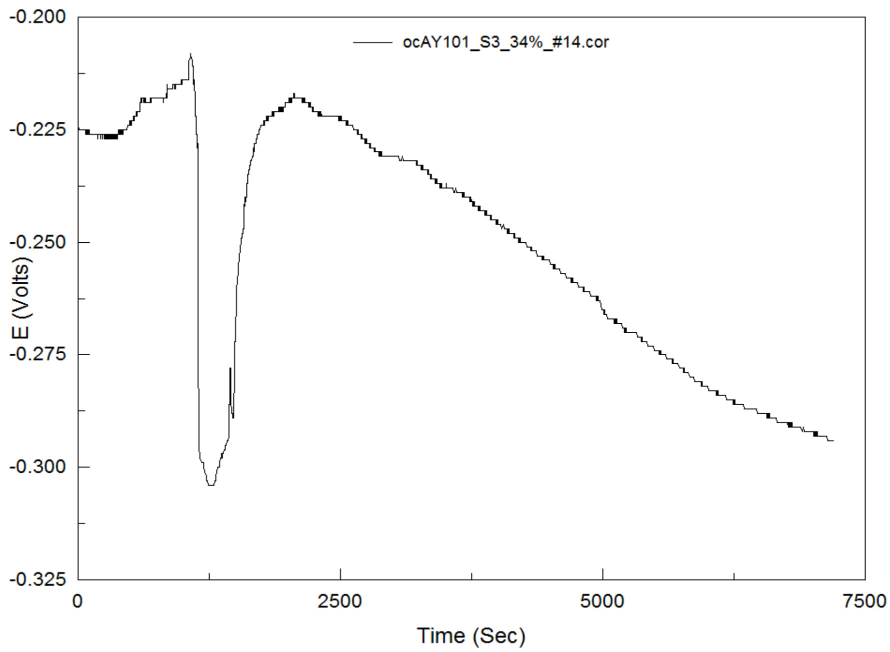

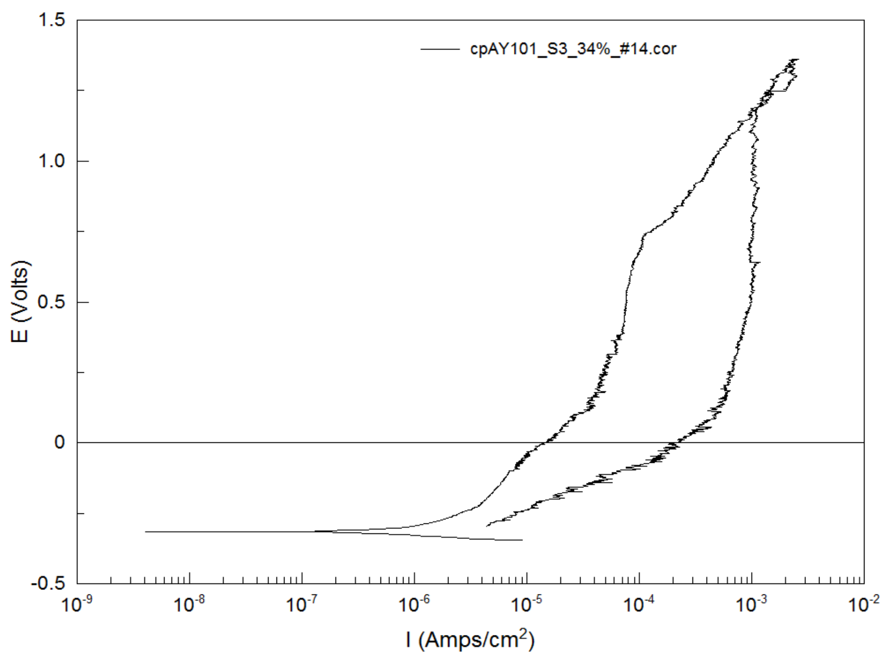

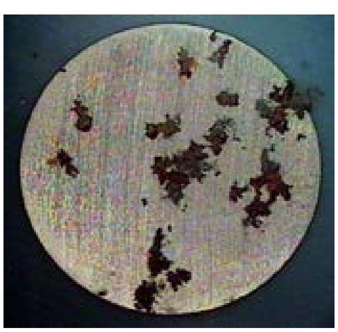

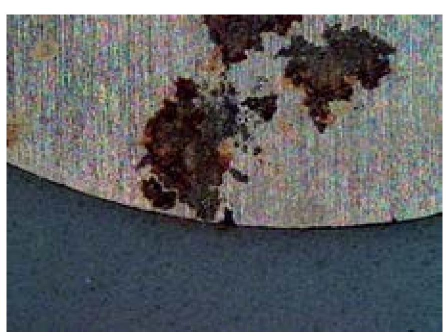

AY101 - Segment 3 – 76% Evaporation – 0 ppm NH_3
No Cover Gas – Sample 12

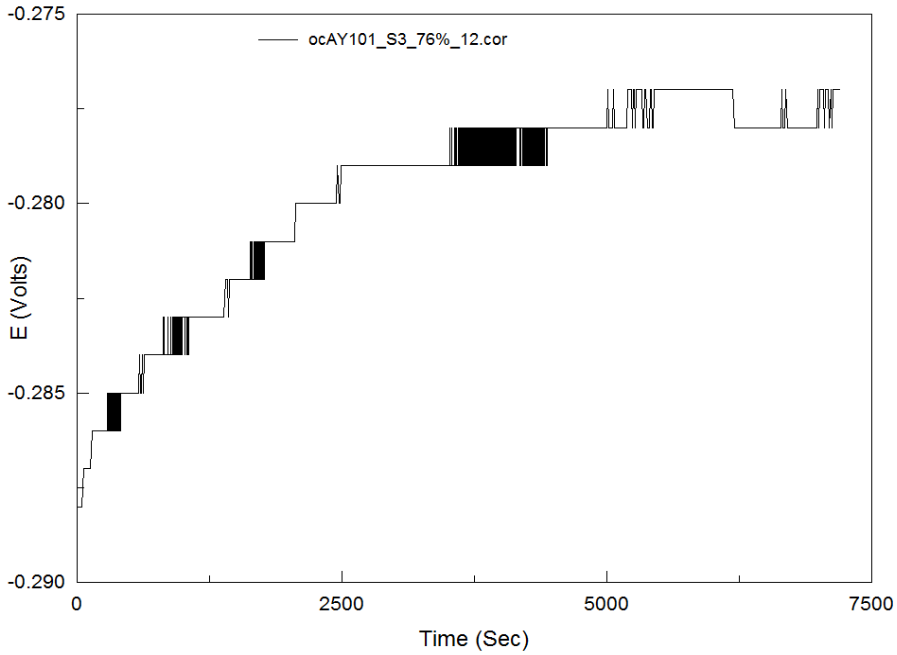

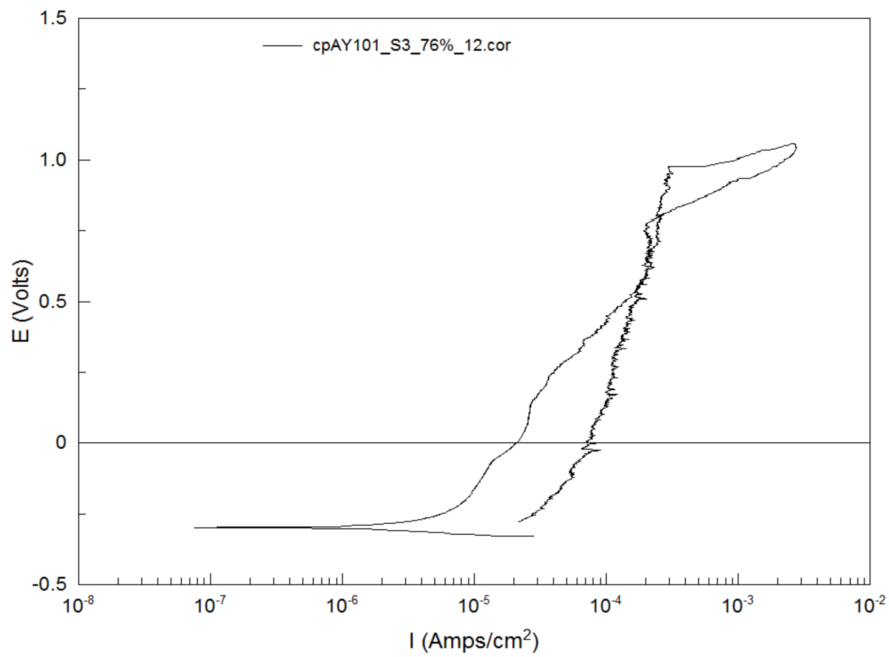

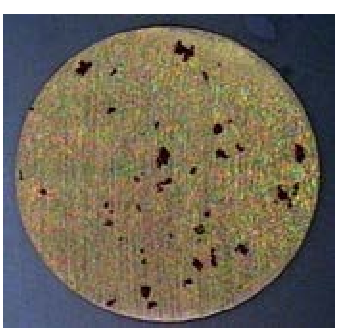

AY101 - Segment 3 – 76% Evaporation – 0 ppm NH_3
No Cover Gas – Sample 14

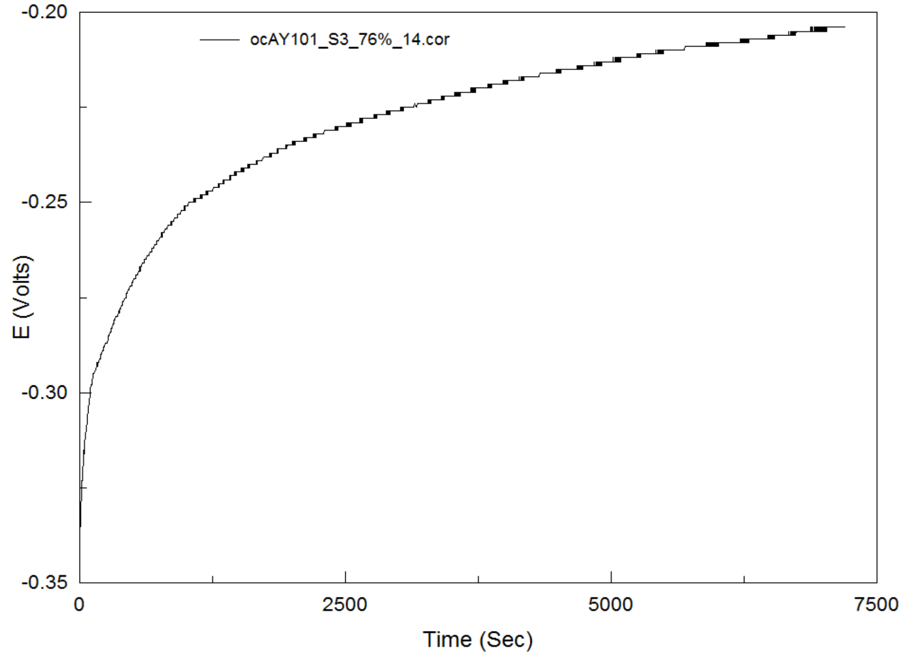

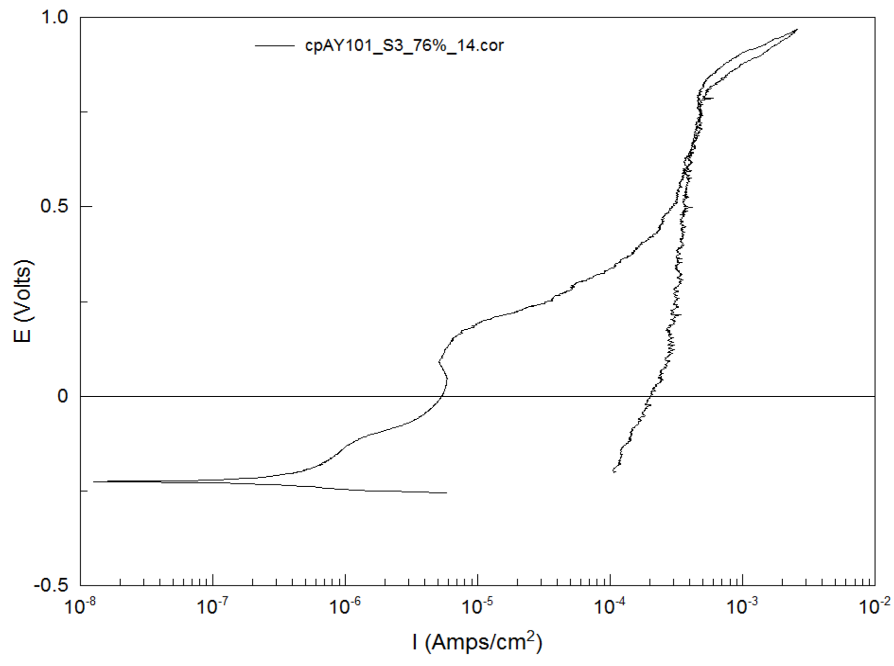

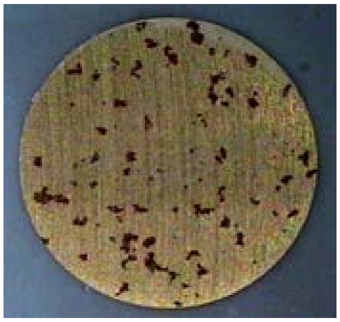

AY101 - Segment 3 – 76% Evaporation – 50 ppm NH_3
No Cover Gas – Sample 3

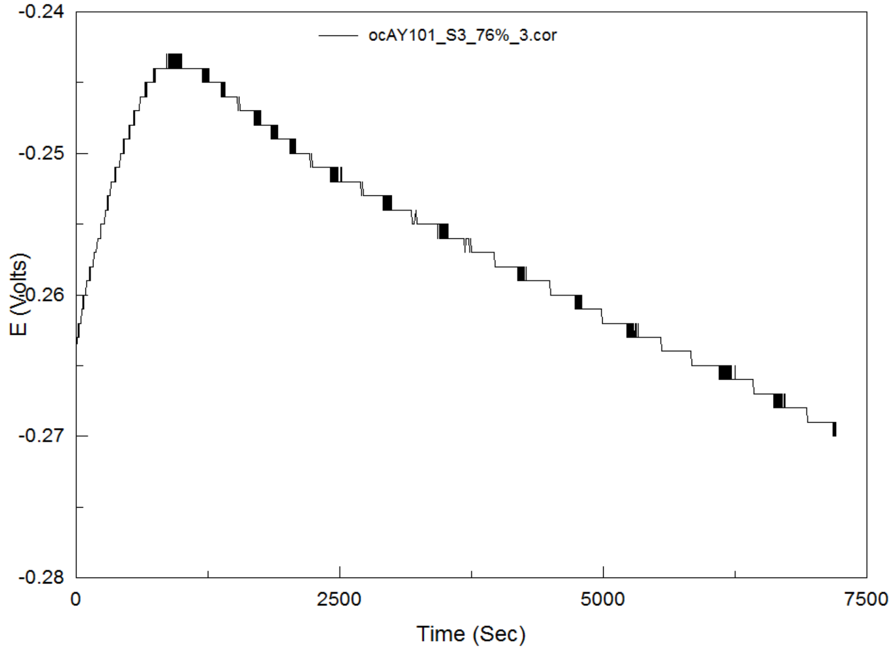

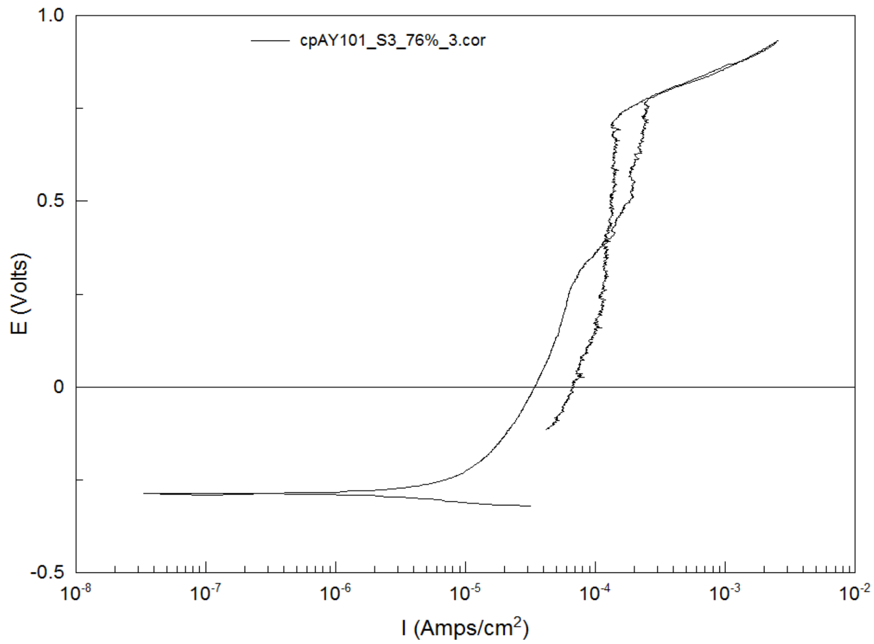

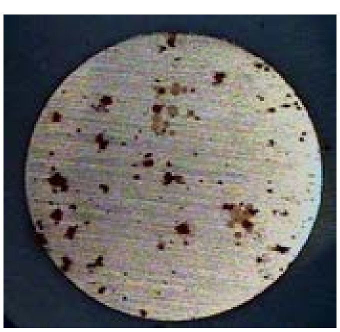

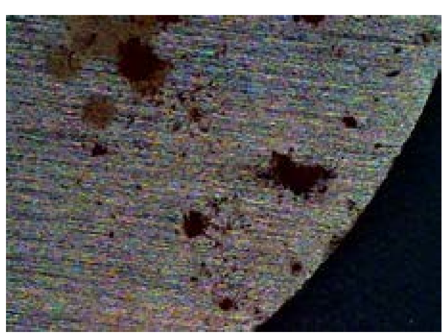

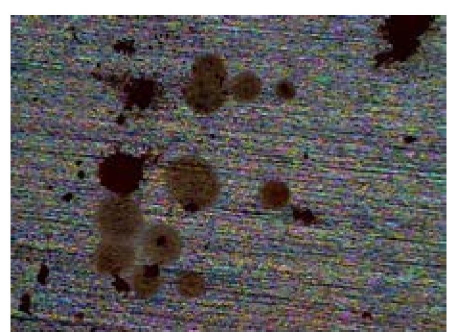

**AY101 - Segment 3 – 76% Evaporation – 50 ppm NH_3
No Cover Gas – Sample 6**

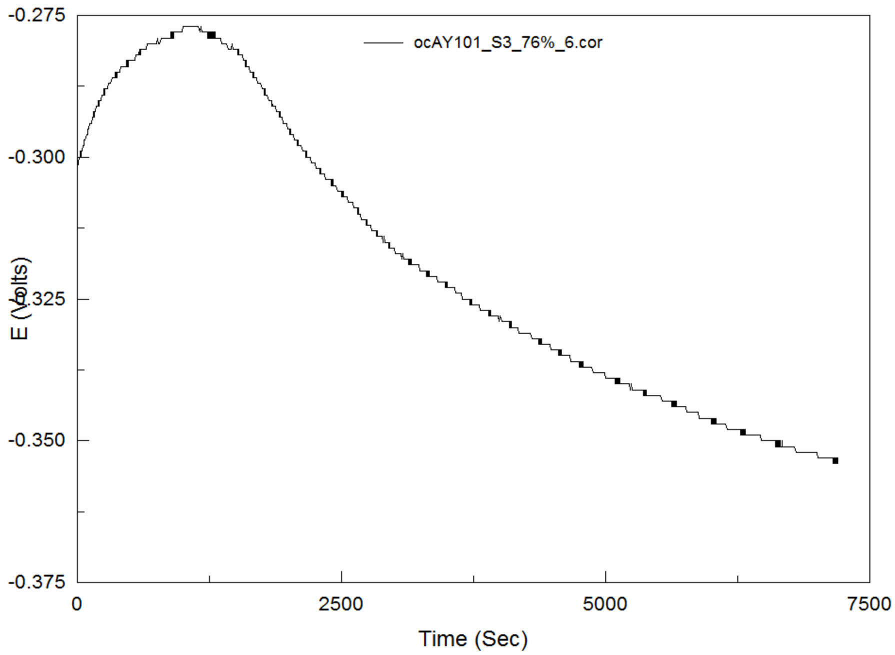

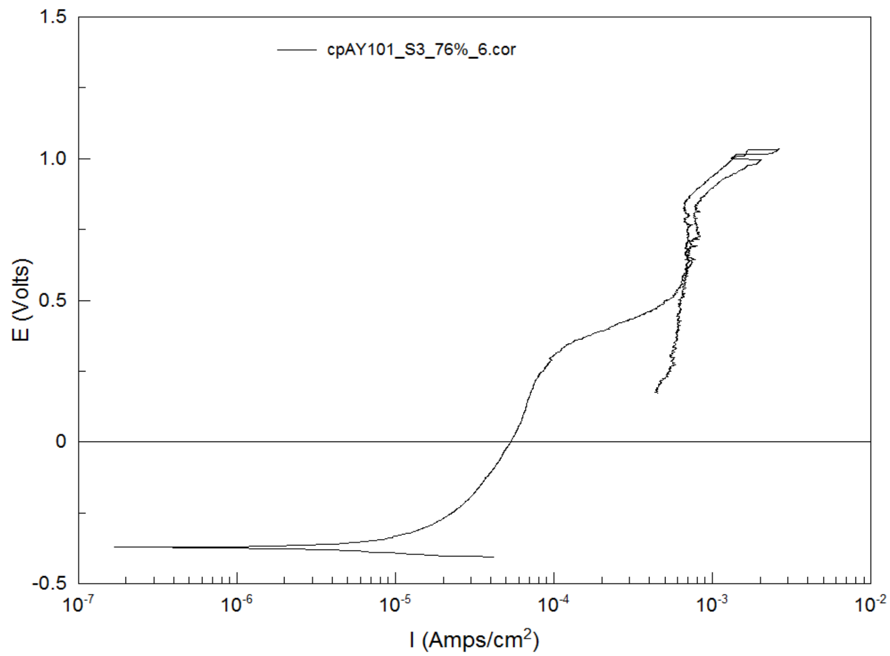

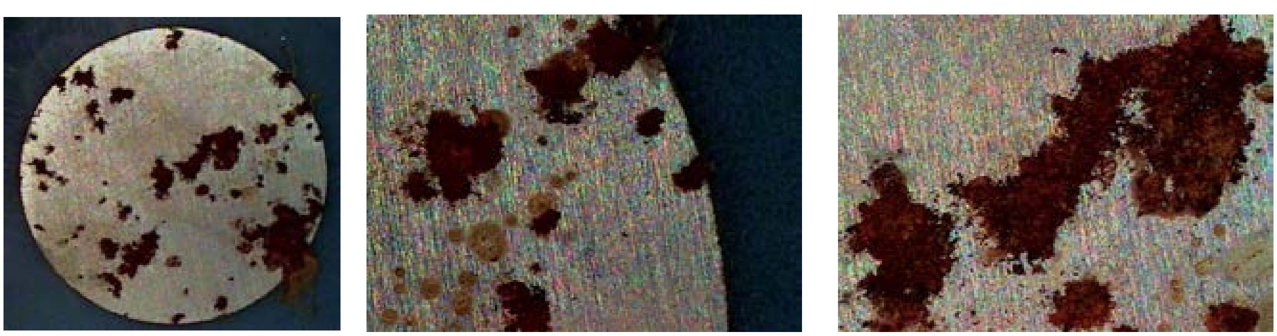

AY101 - Segment 3 – 76% Evaporation – 550 ppm NH_3
No Cover Gas – Sample 26

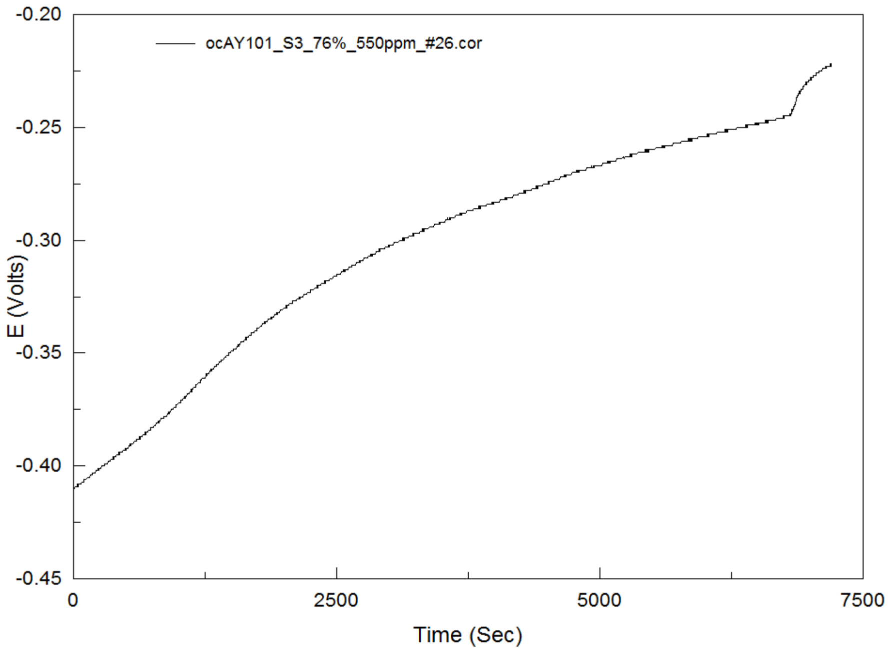

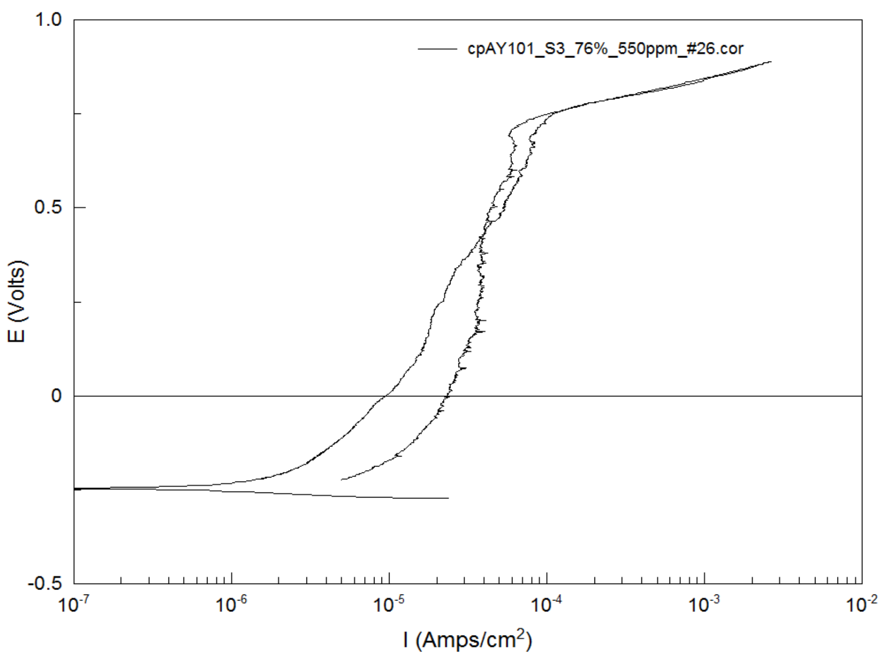

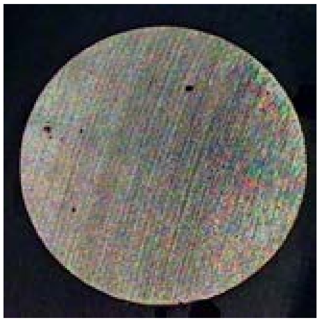
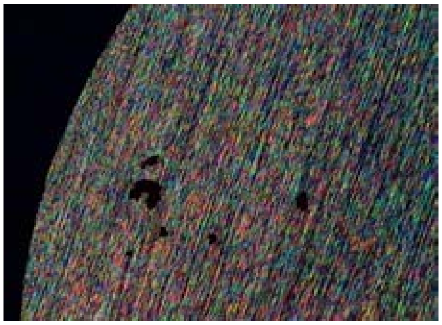
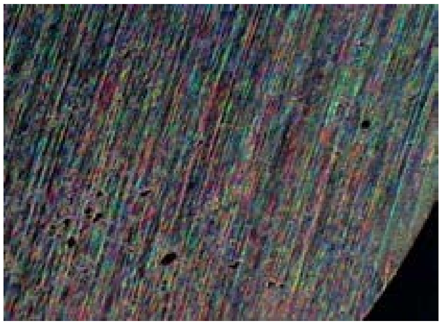

AY101 - Segment 3 – 76% Evaporation – 550 ppm NH_3
No Cover Gas – Sample 27

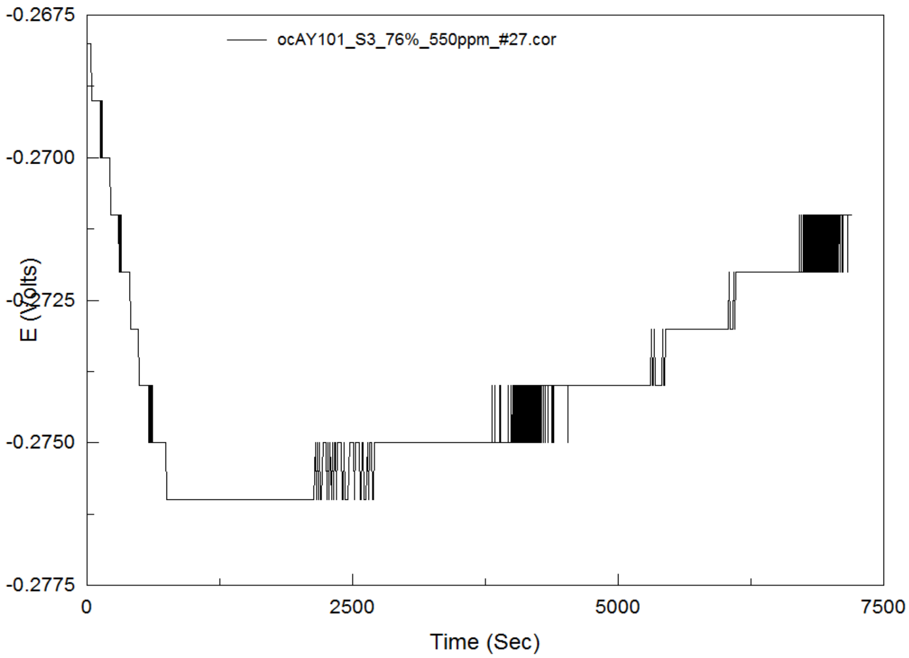

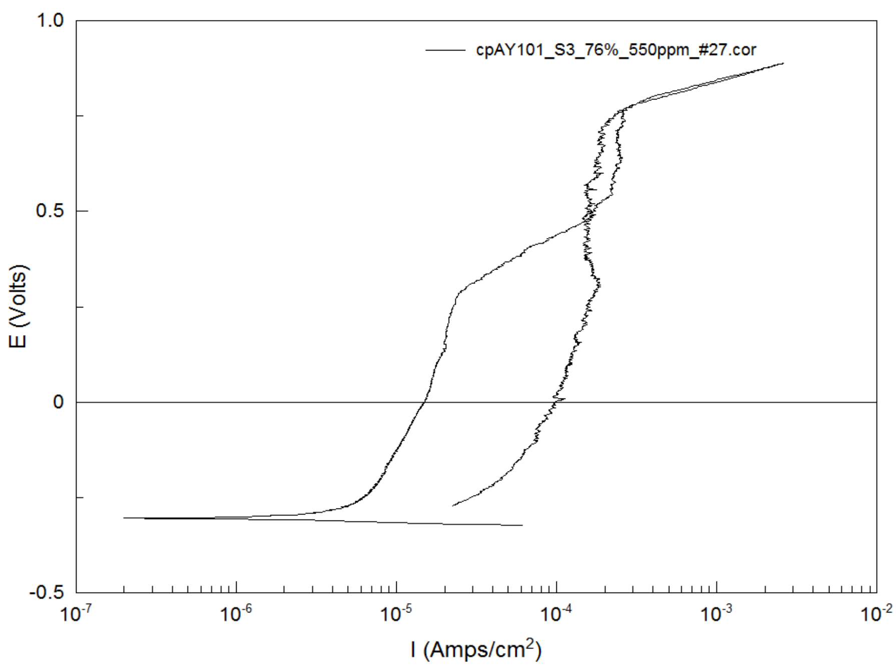

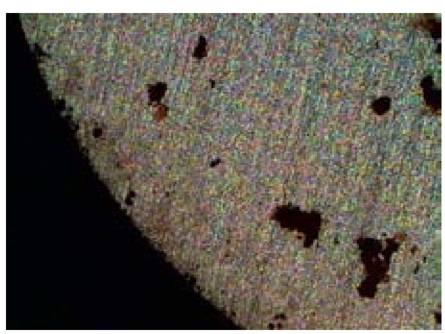

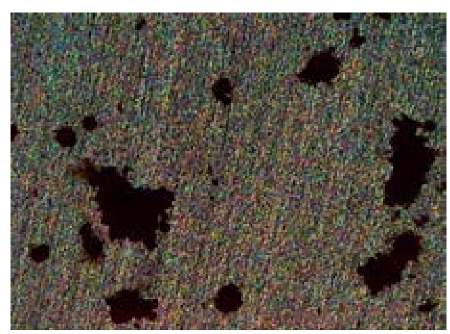

**AY101 - Segment 8 – 0% Evaporation – 0 ppm NH_3
No Cover Gas – Sample 16**

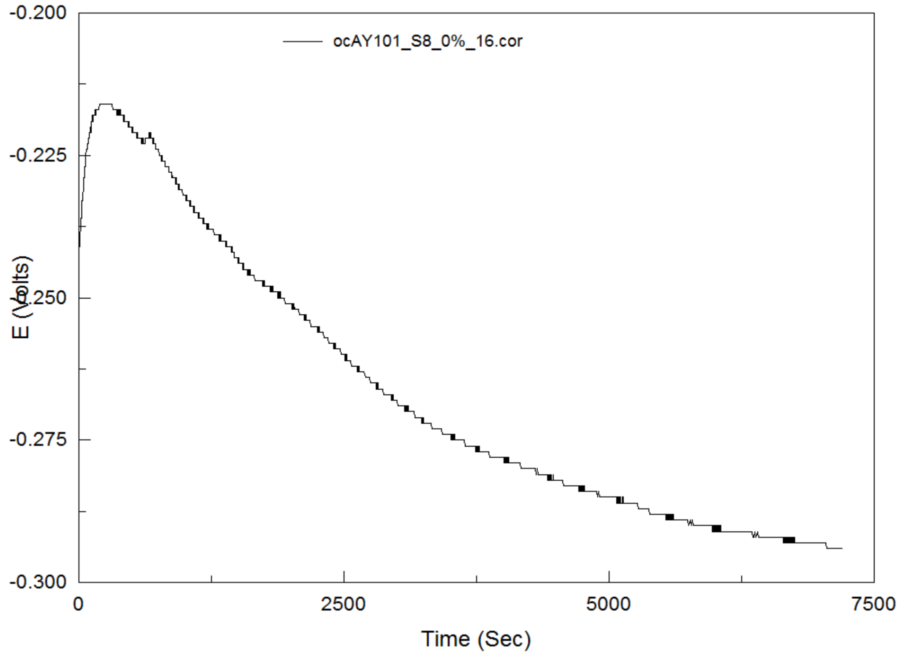

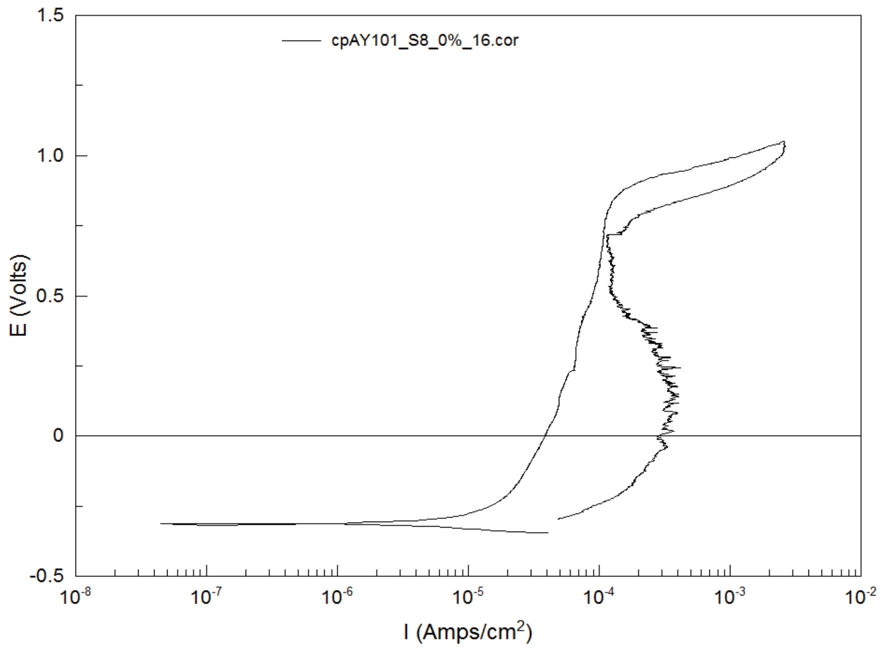

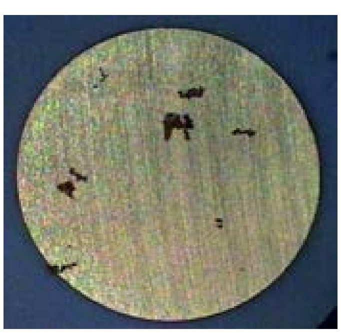

AY101 - Segment 8 – 0% Evaporation – 0 ppm NH_3
No Cover Gas – Sample 22

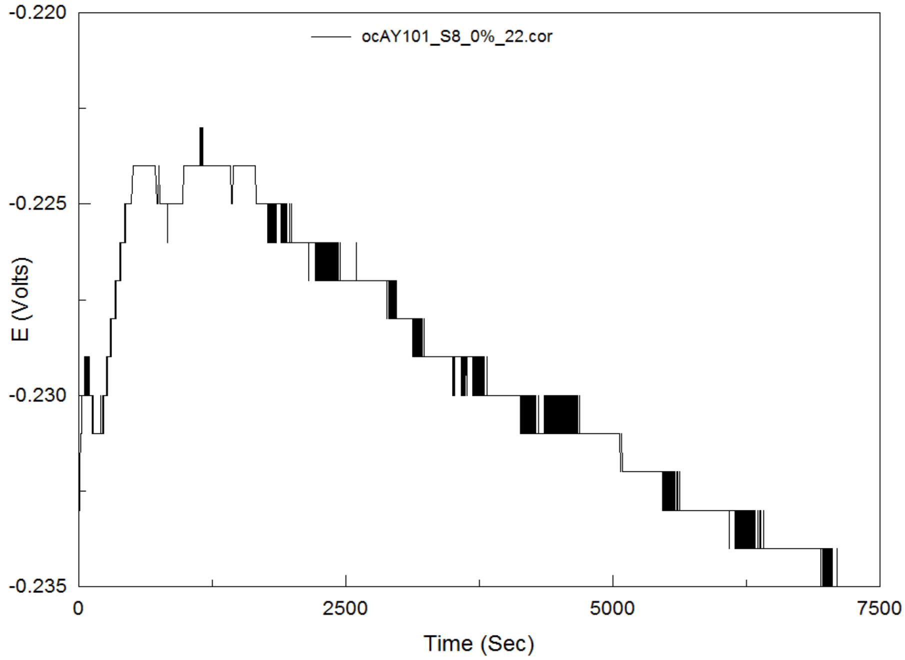

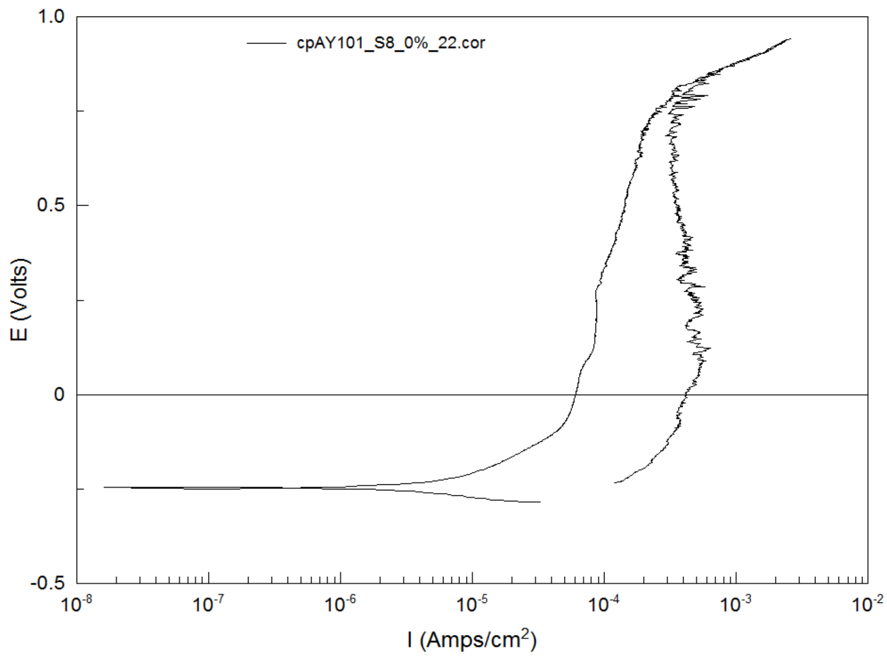

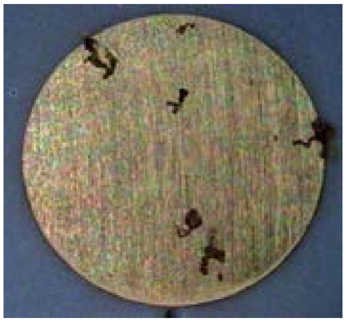

AY101 - Segment 8 – 0% Evaporation – 50 ppm NH_3
No Cover Gas – Sample 19

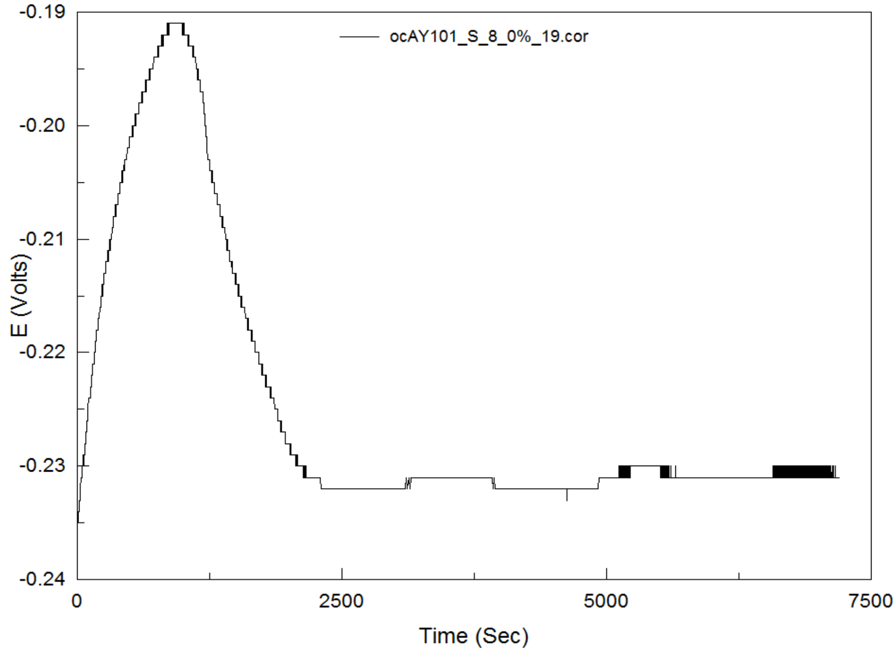

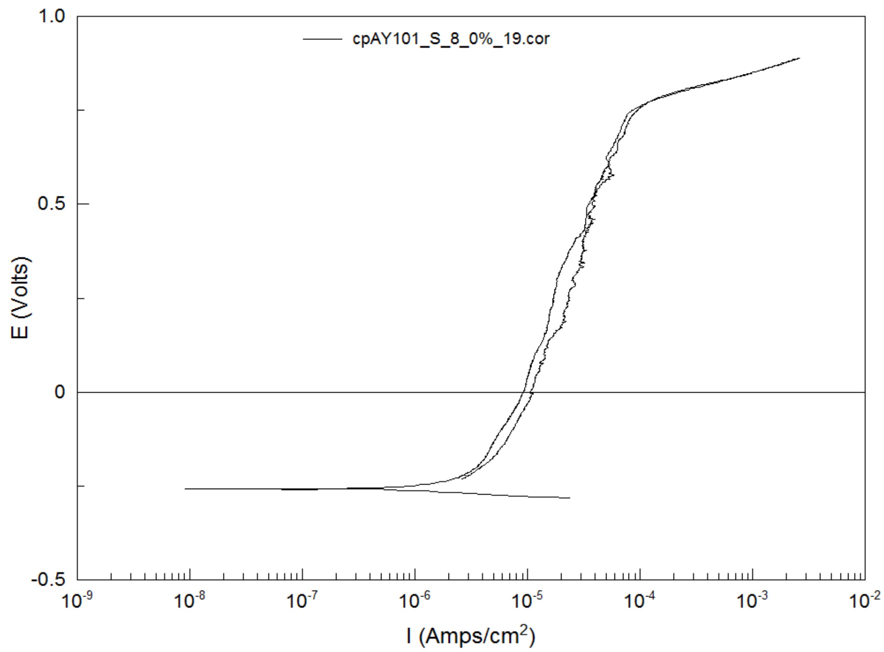

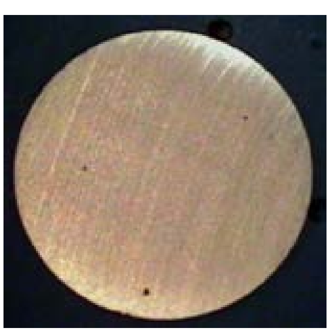

AY101 - Segment 8 – 0% Evaporation – 50 ppm NH_3
No Cover Gas – Sample 20

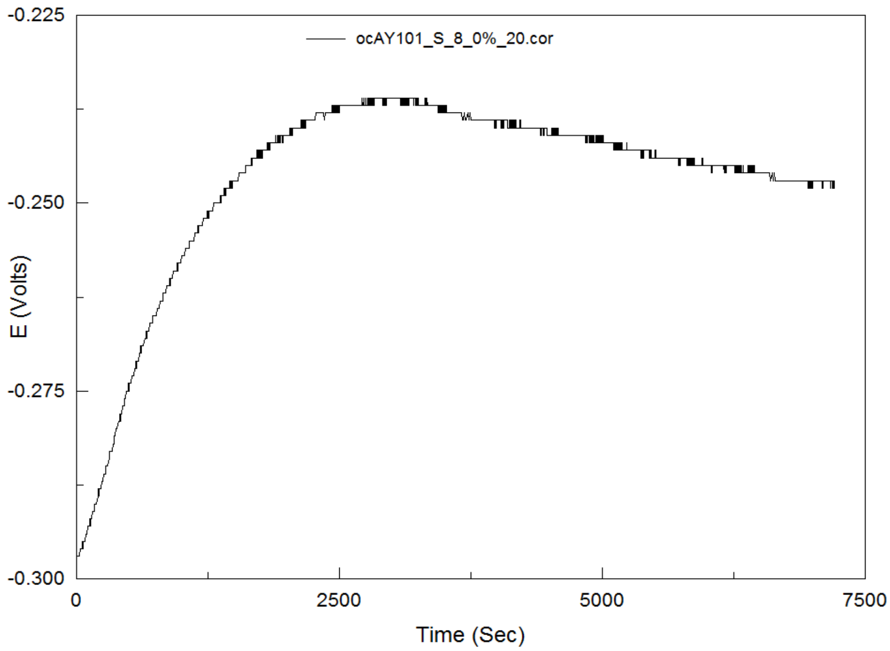

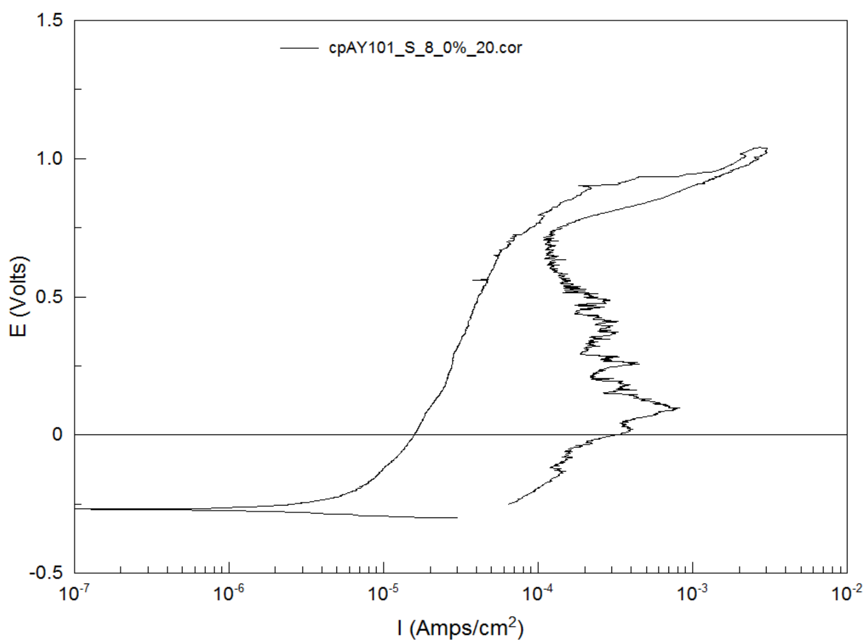

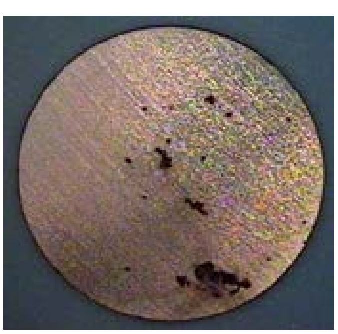
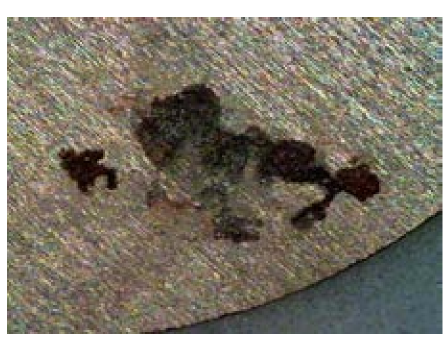
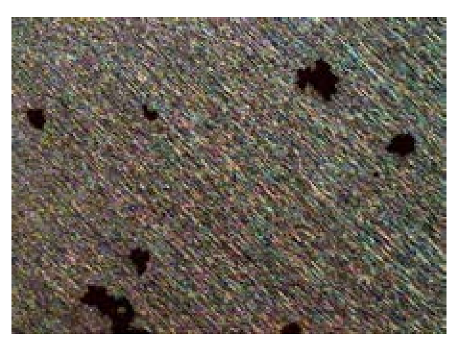

AY101 - Segment 8 – 0% Evaporation – 550 ppm NH_3
No Cover Gas – Sample 26

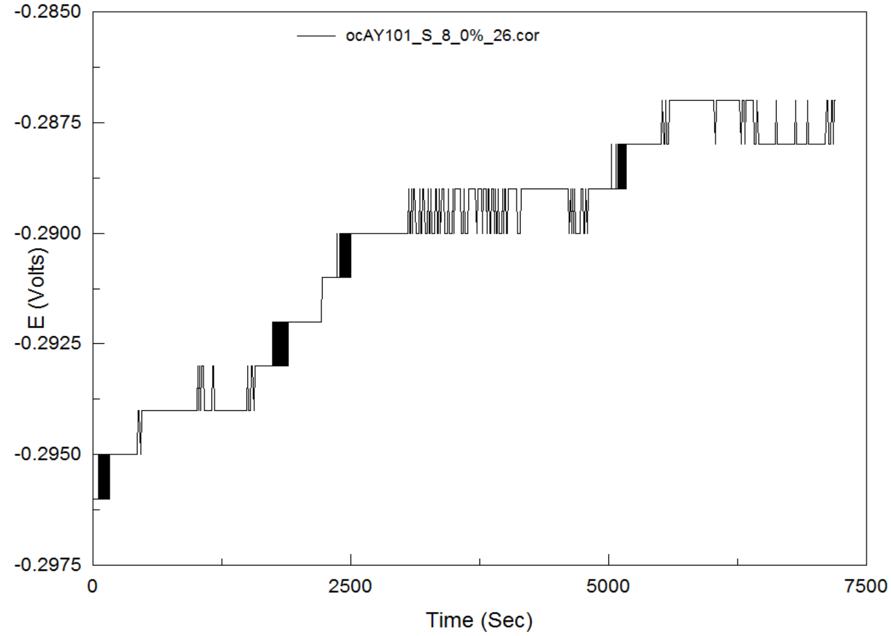

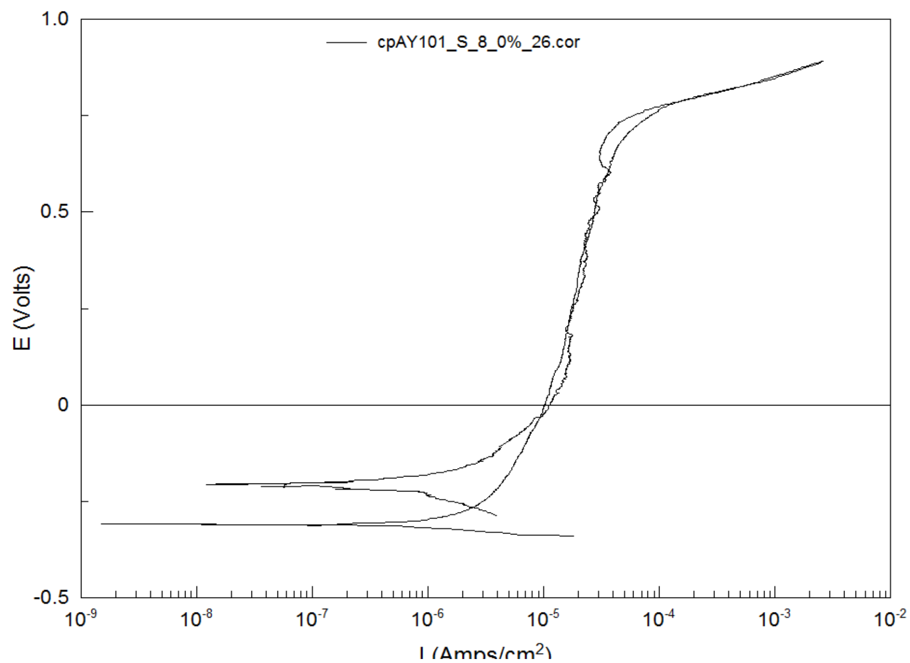

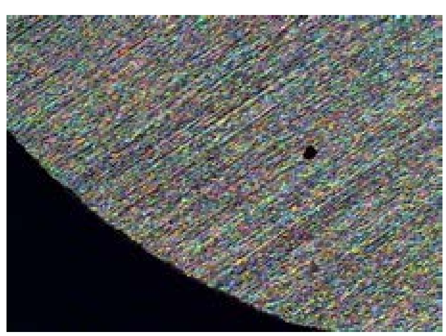

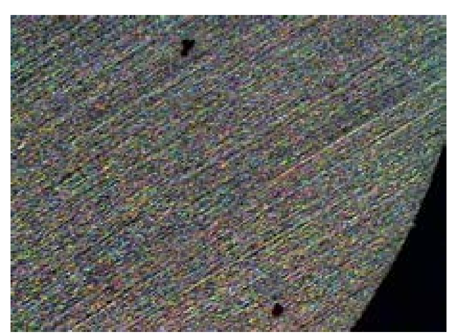

AY101 - Segment 8 – 0% Evaporation – 550 ppm NH_3
No Cover Gas – Sample 28

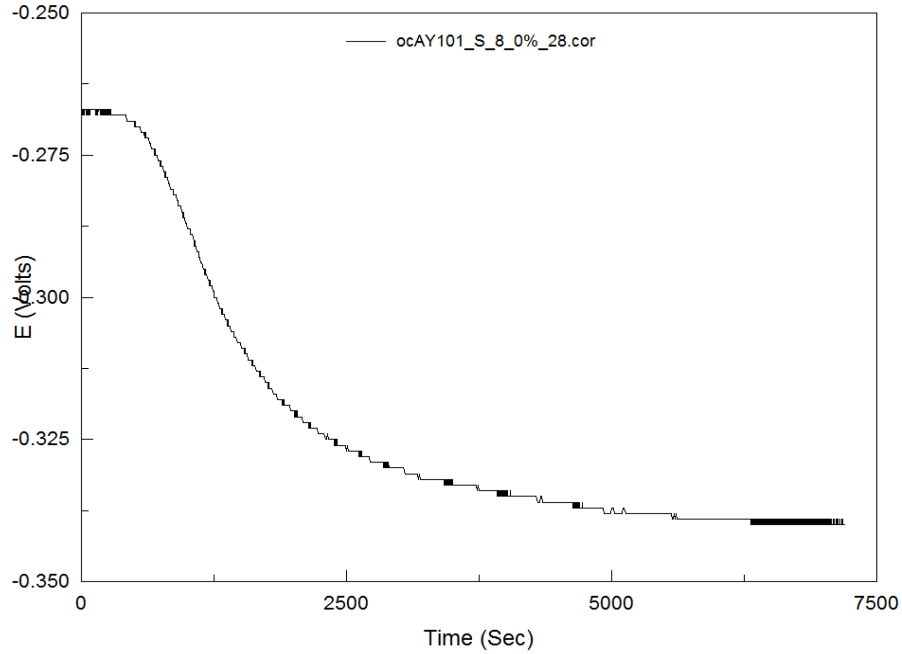

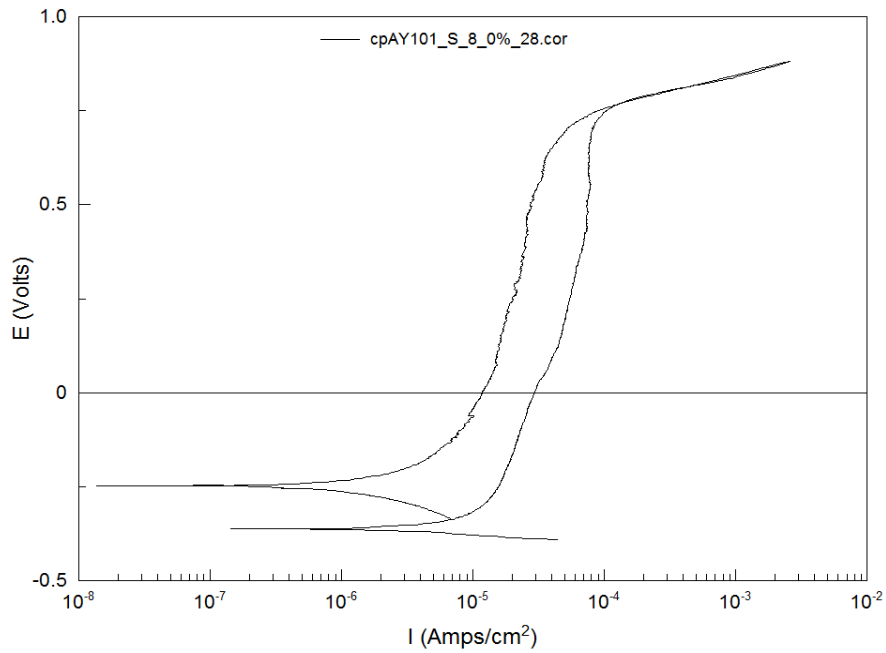

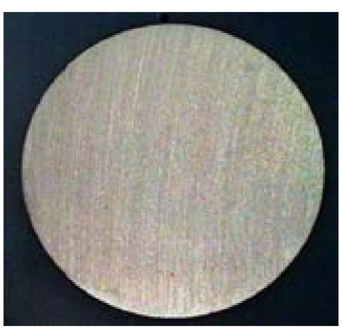

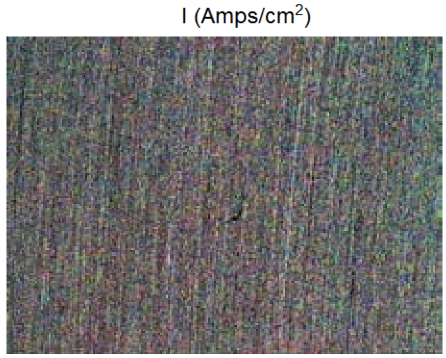

AY101 - Segment 8 – 27% Evaporation – 0 ppm NH_3
No Cover Gas – Sample 26

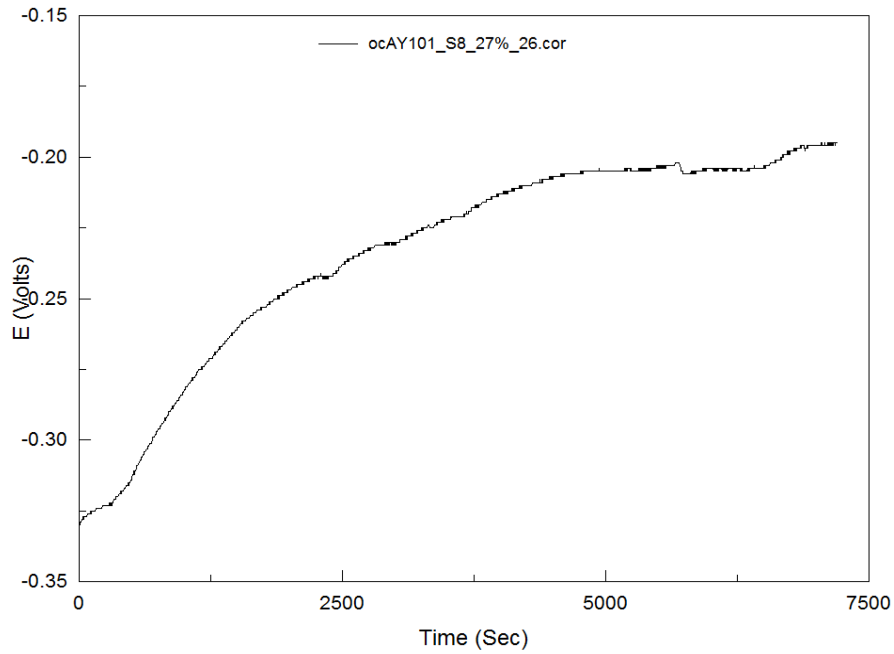

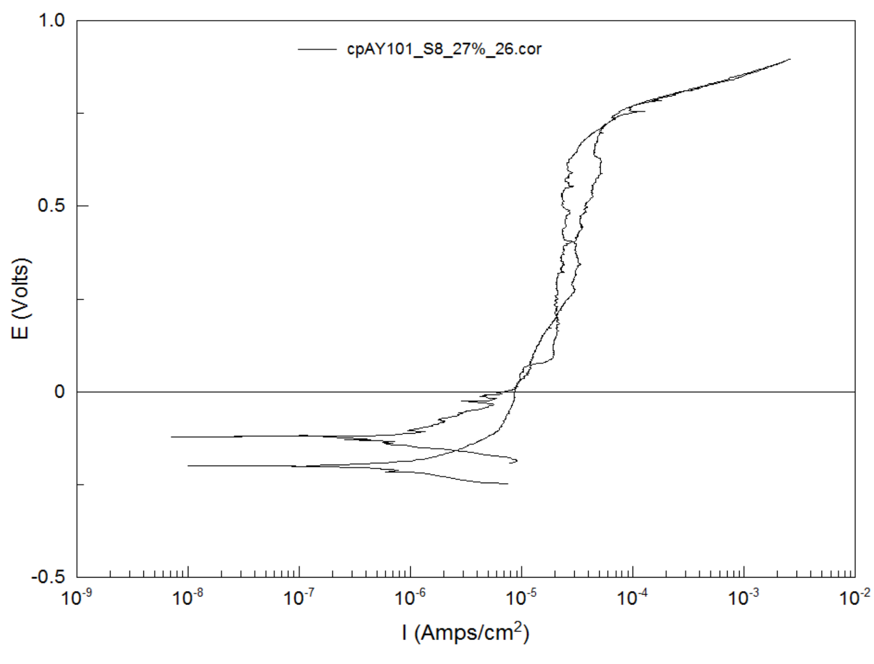

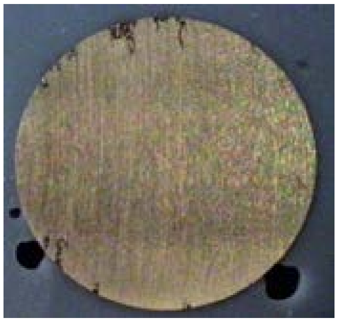

**AY101 - Segment 8 – 27% Evaporation – 0 ppm NH_3
No Cover Gas – Sample 27**

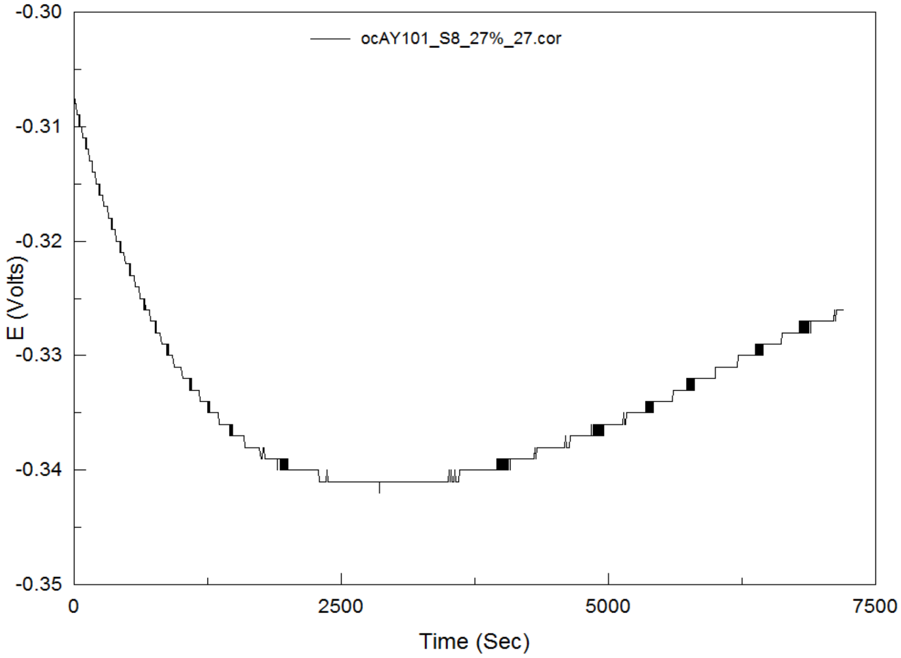

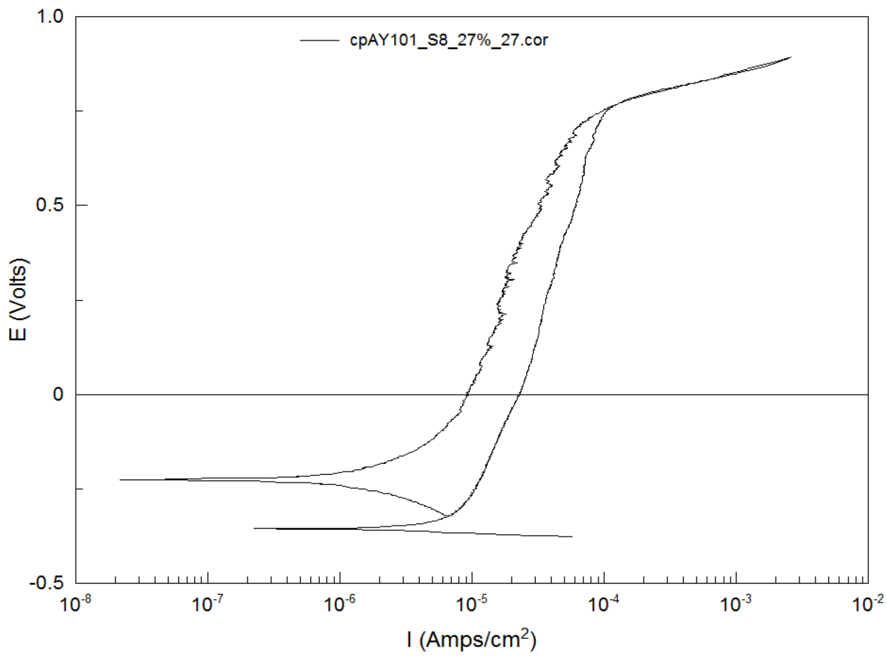

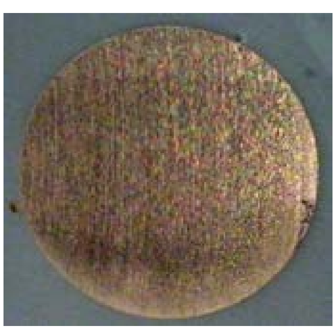
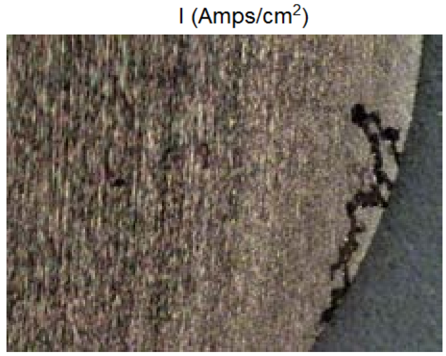


AY101 - Segment 8 – 27% Evaporation – 50 ppm NH_3
No Cover Gas – Sample 3

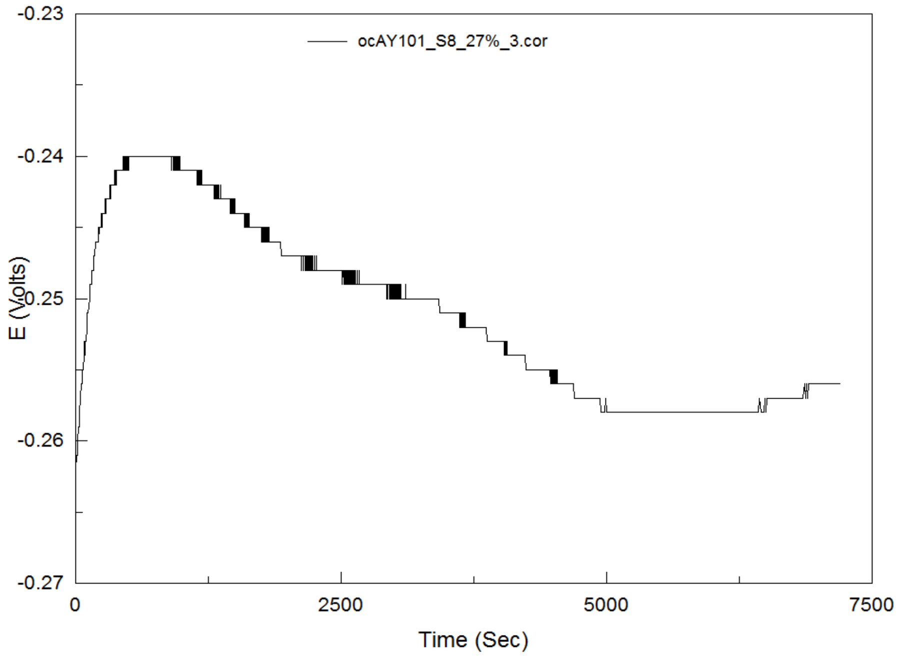

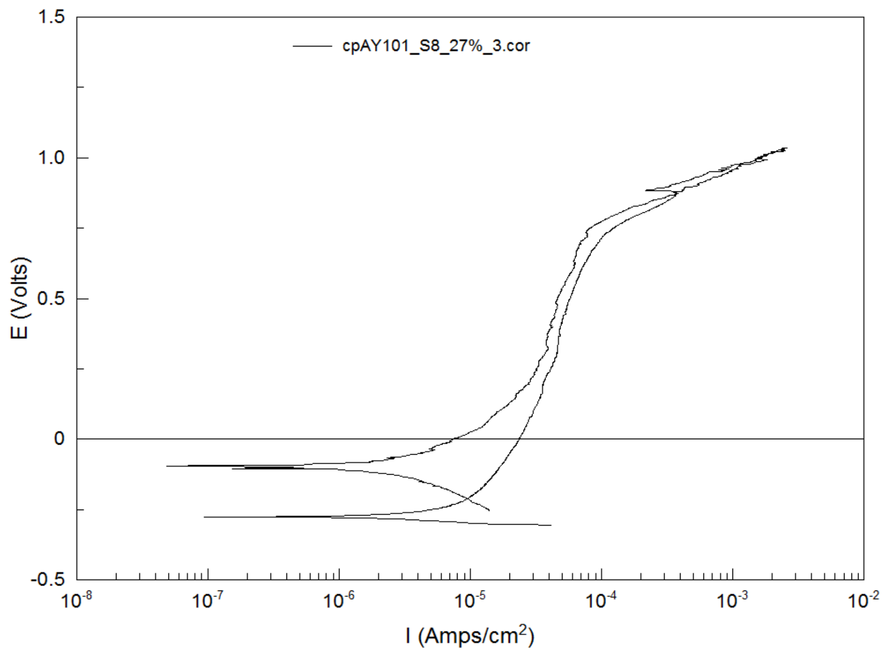

NO DATA

AY101 - Segment 8 – 27% Evaporation – 50 ppm NH_3
No Cover Gas – Sample 6

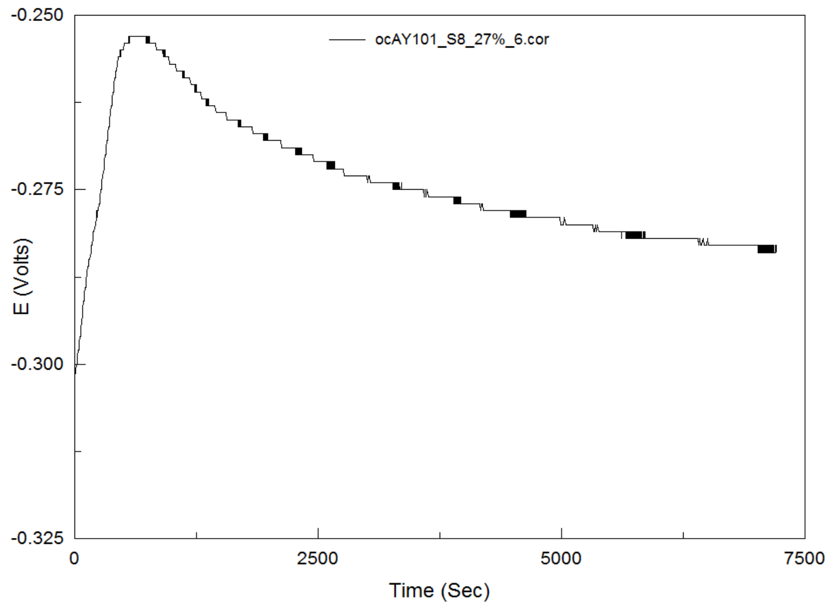

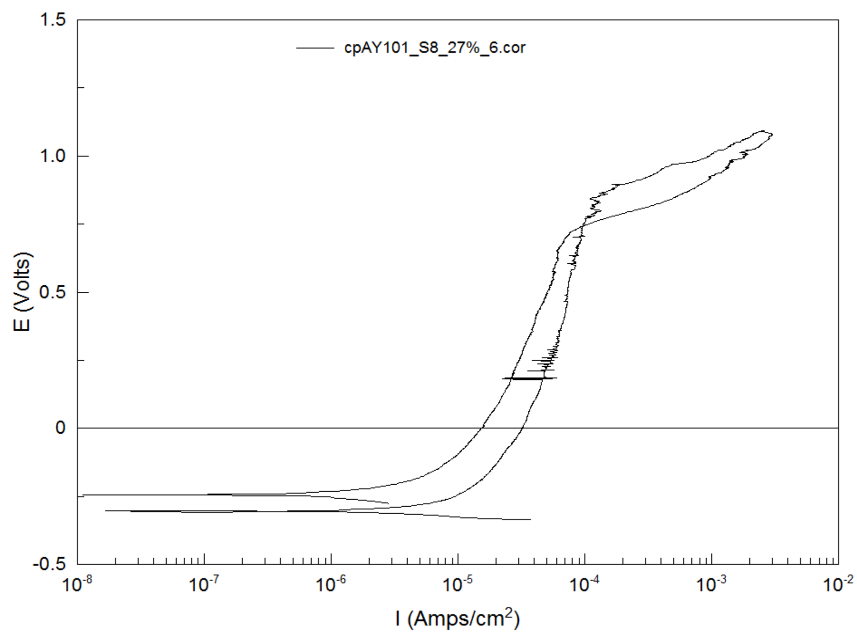

NO DATA

AY101 - Segment 8 – 27% Evaporation – 550 ppm NH_3
No Cover Gas – Sample 12

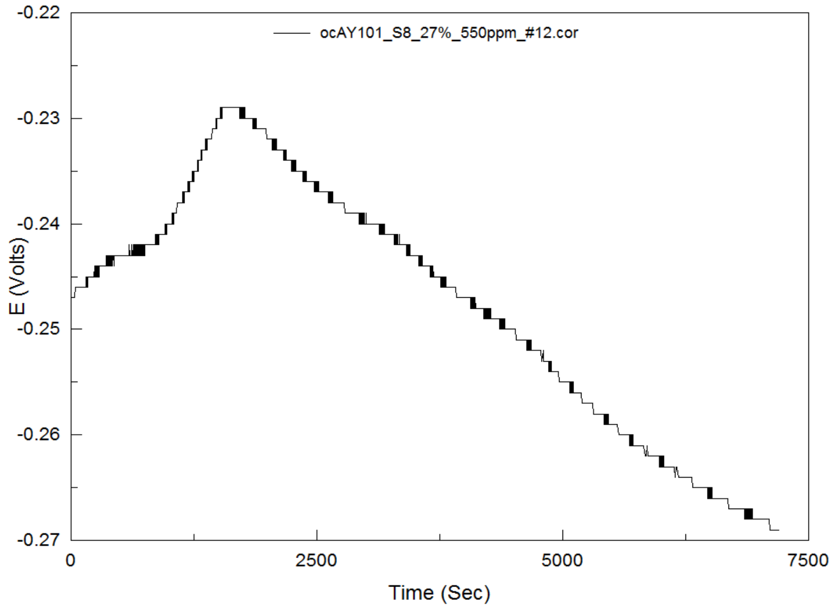

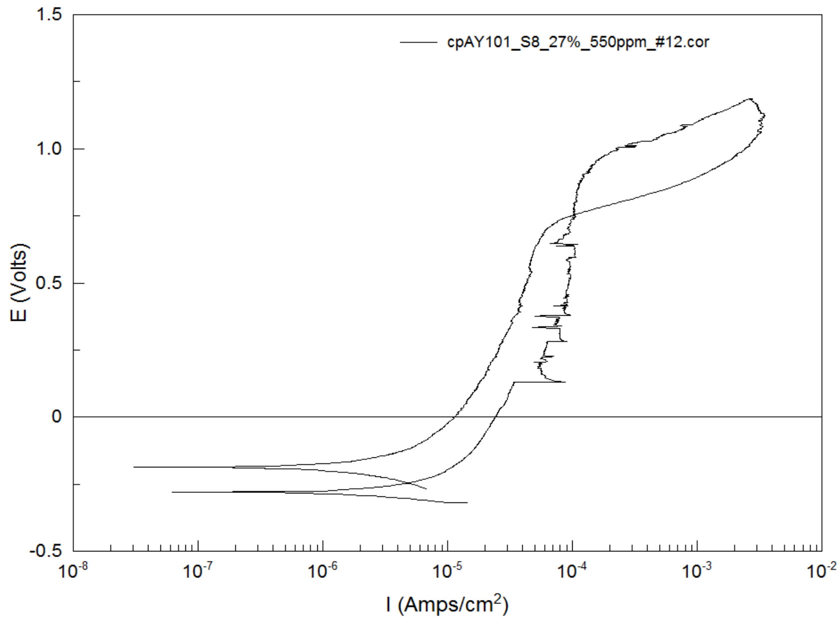

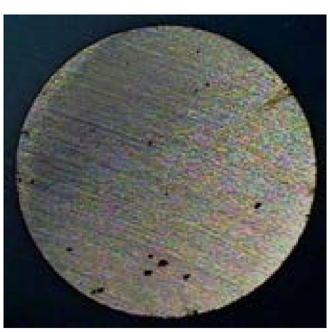
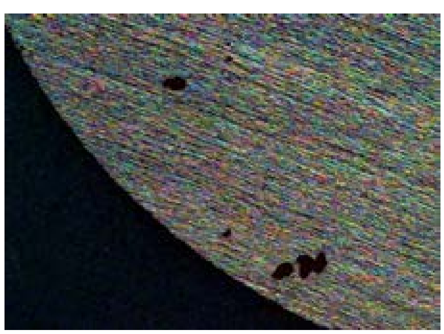
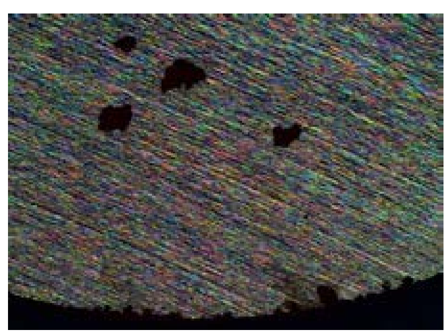

AY101 - Segment 8 – 27% Evaporation – 550 ppm NH_3
No Cover Gas – Sample 14

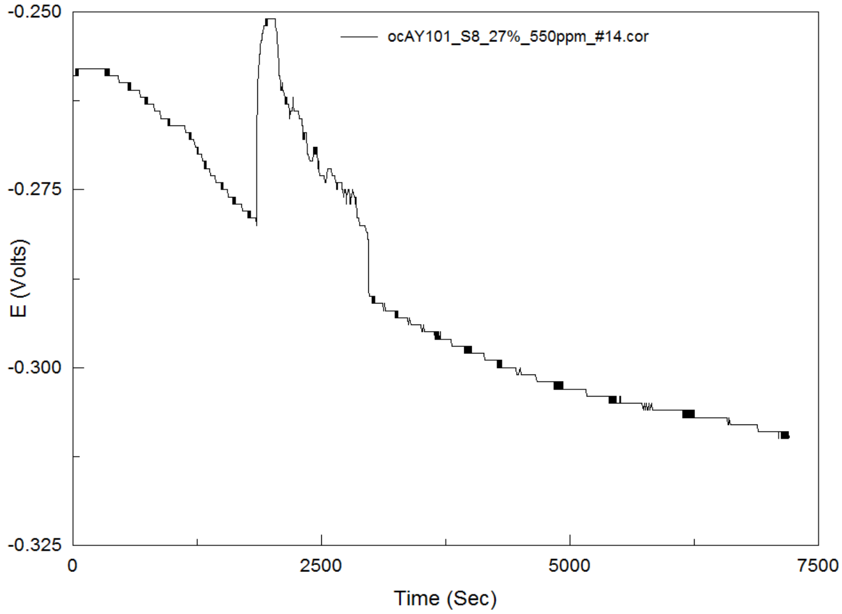

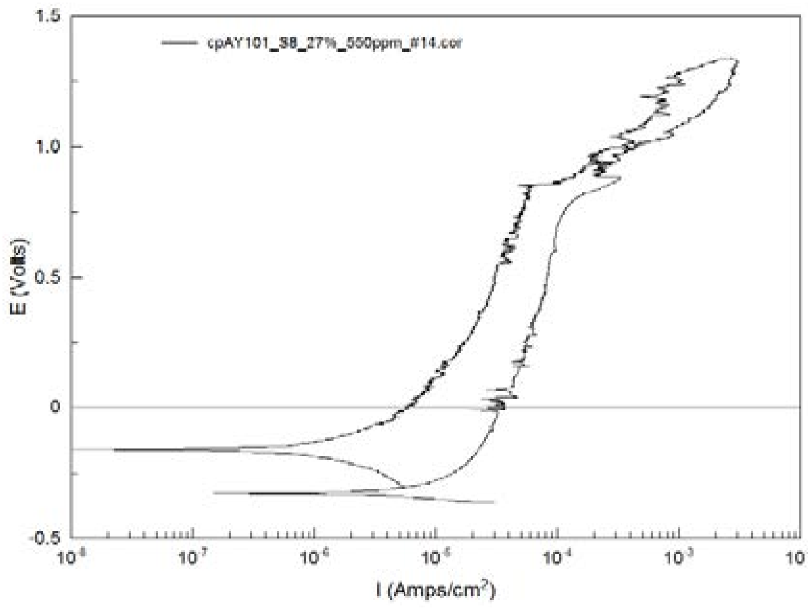

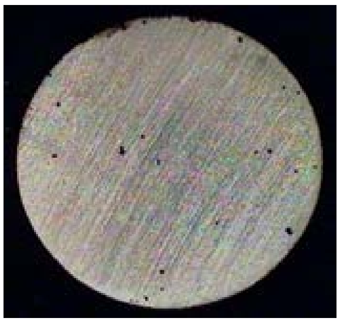
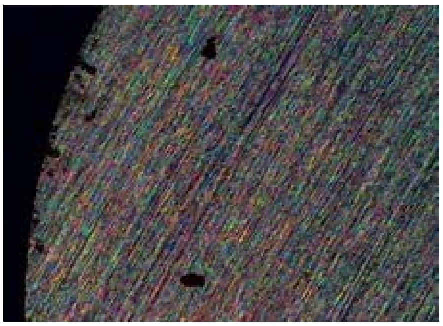
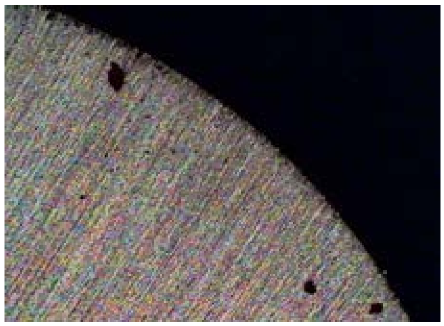

AY101 - Segment 8 – 68% Evaporation – 0 ppm NH_3
No Cover Gas – Sample 28

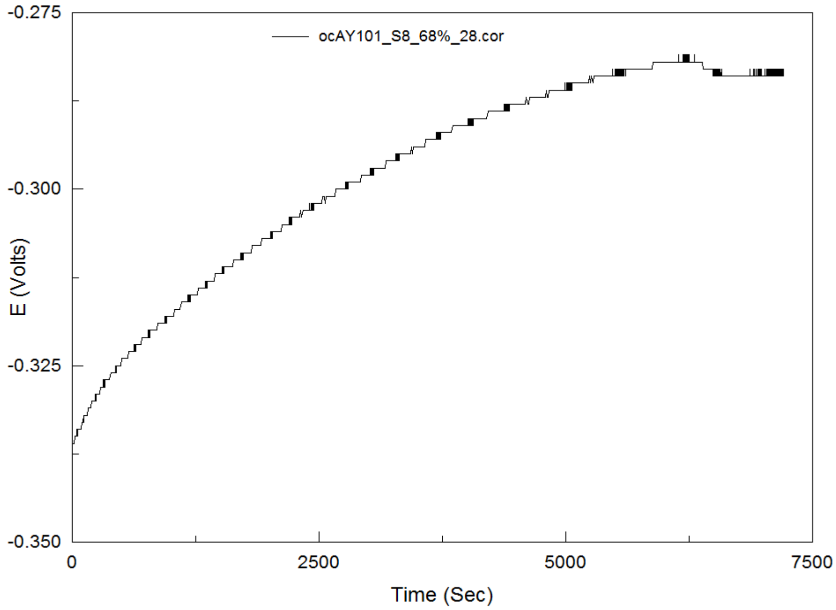

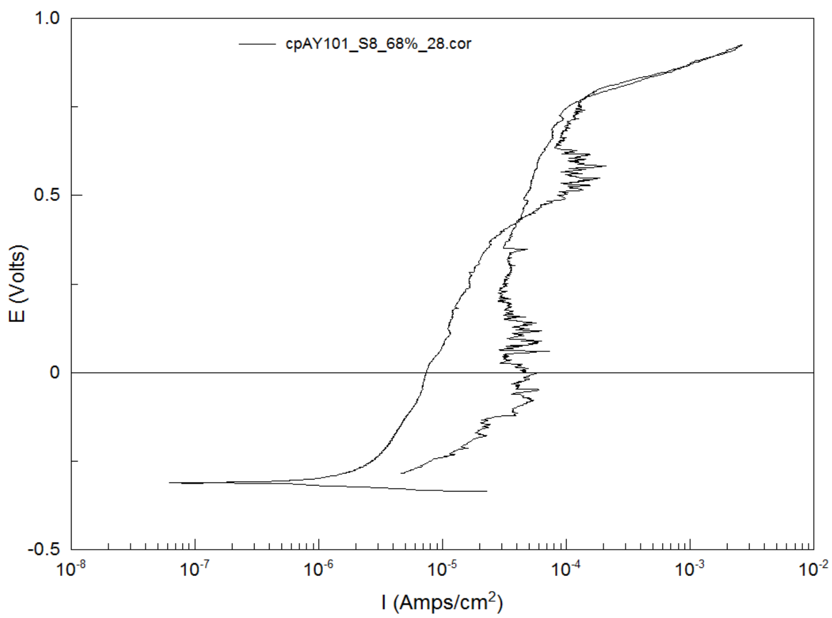

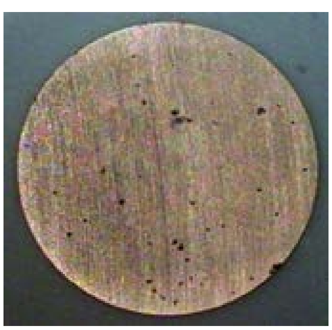

AY101 - Segment 8 – 68% Evaporation – 0 ppm NH_3
No Cover Gas – Sample 29

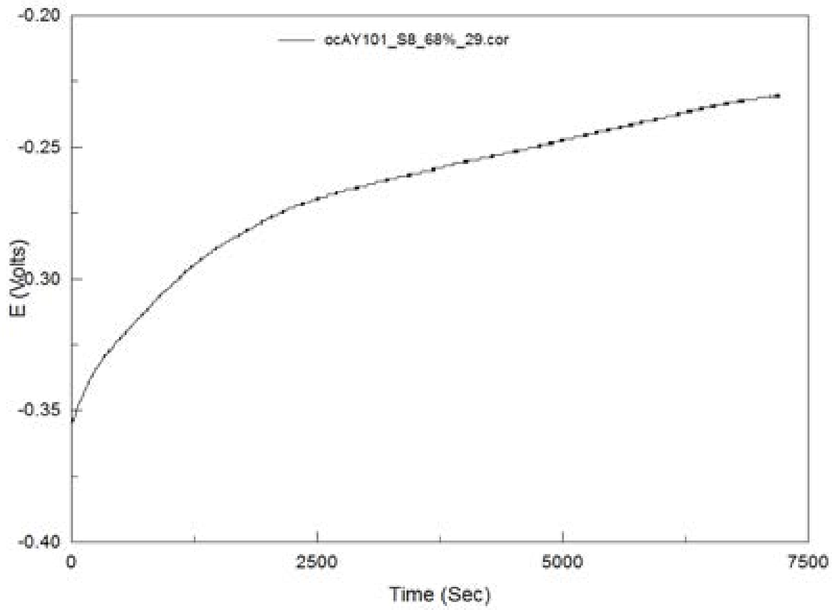

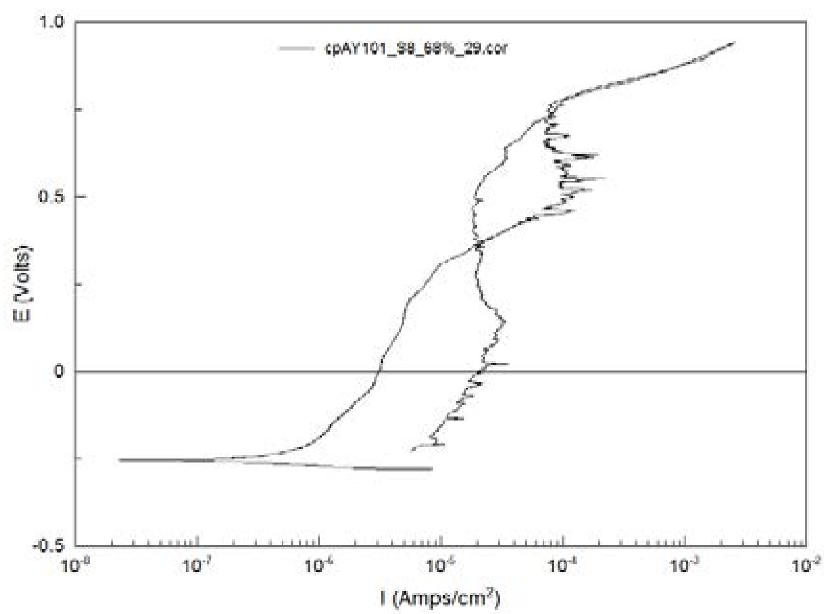

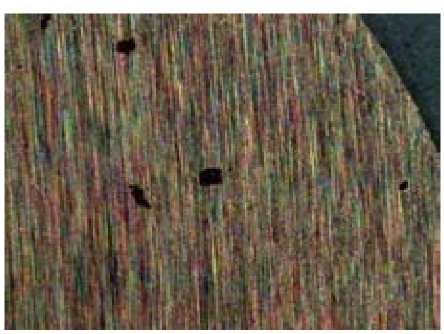

AY101 - Segment 8 – 68% Evaporation – 50 ppm NH_3
No Cover Gas – Sample 34

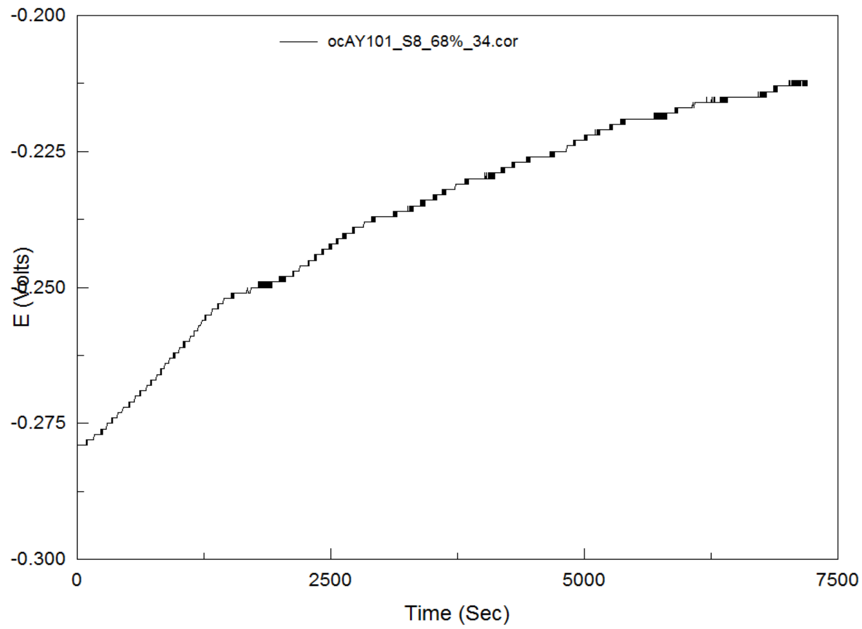

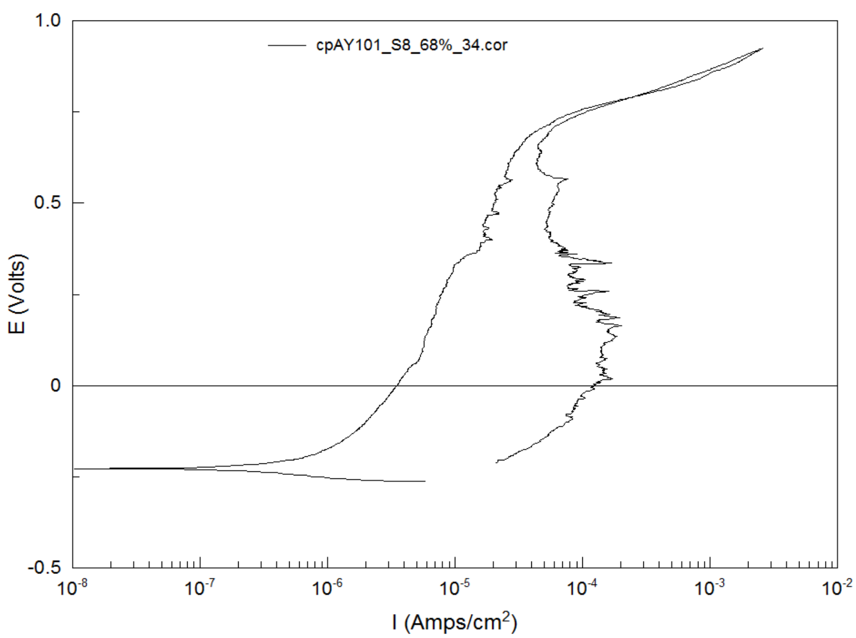

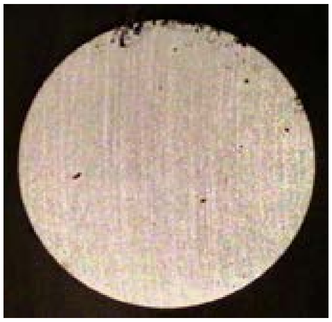

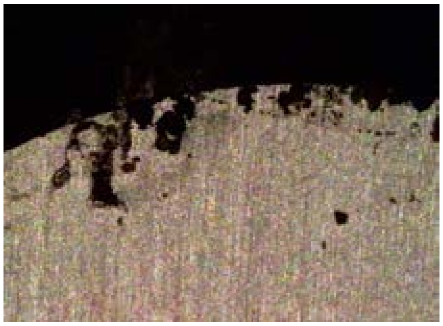

AY101 - Segment 8 – 68% Evaporation – 50 ppm NH_3
No Cover Gas – Sample 35

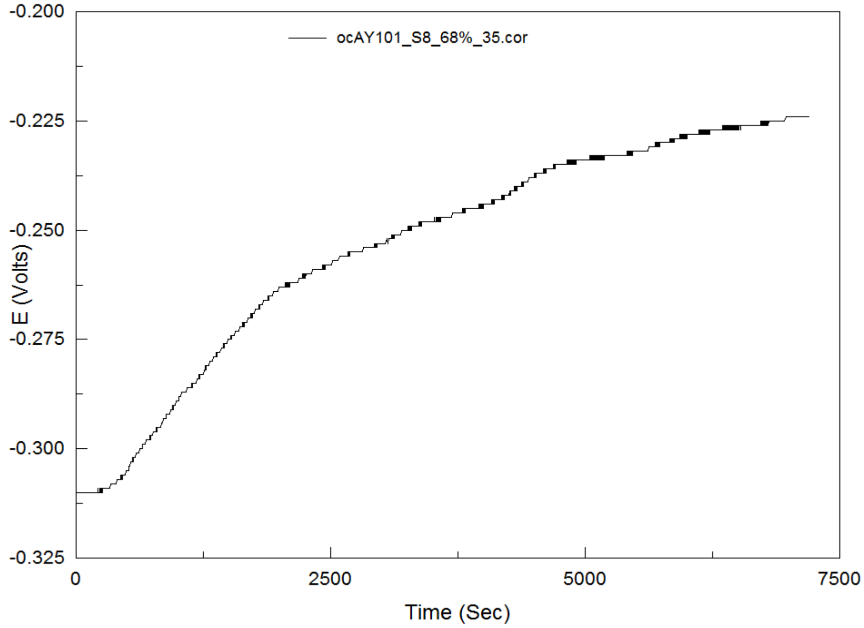

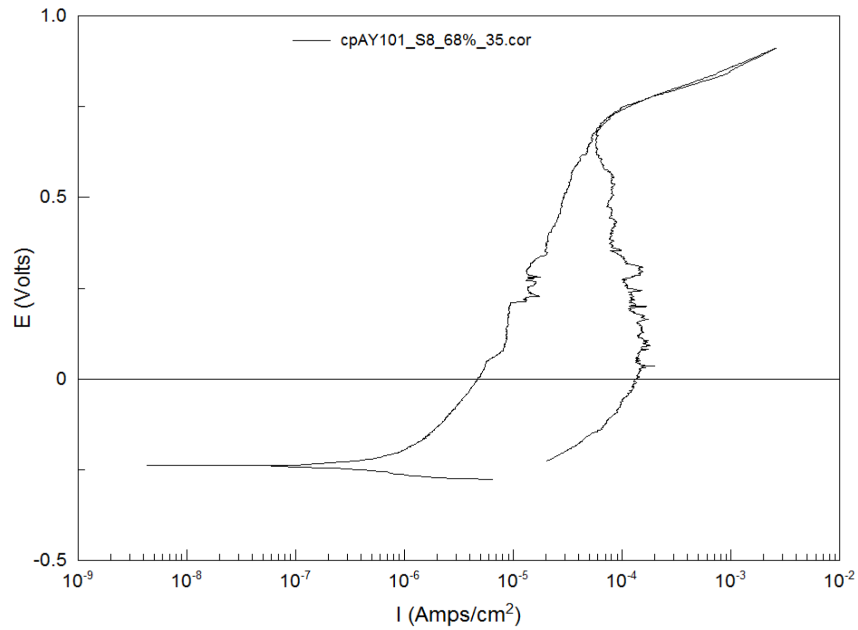

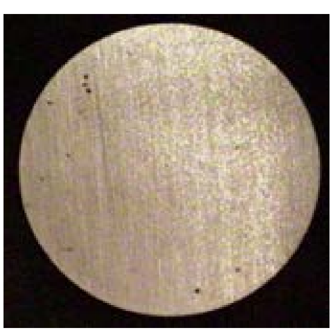

AY101 - Segment 8 – 68% Evaporation – 550 ppm NH_3
No Cover Gas – Sample 30

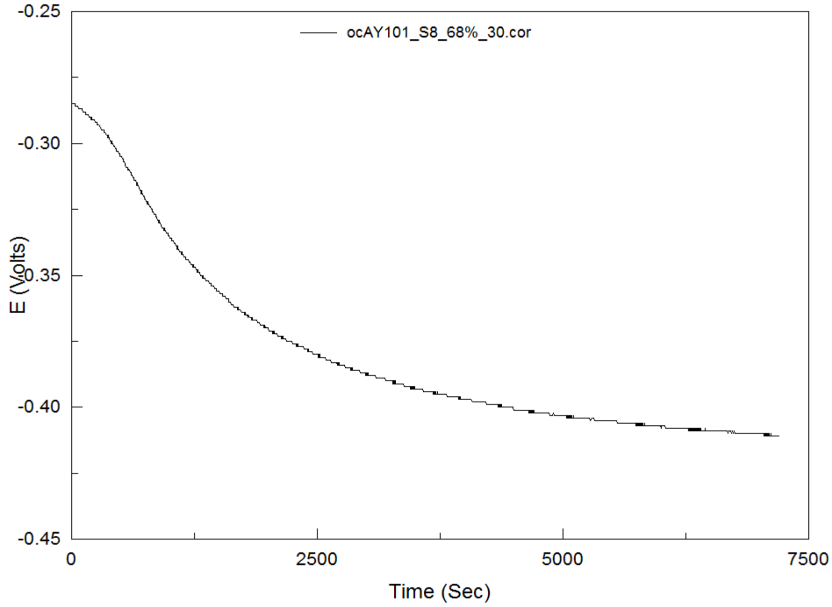

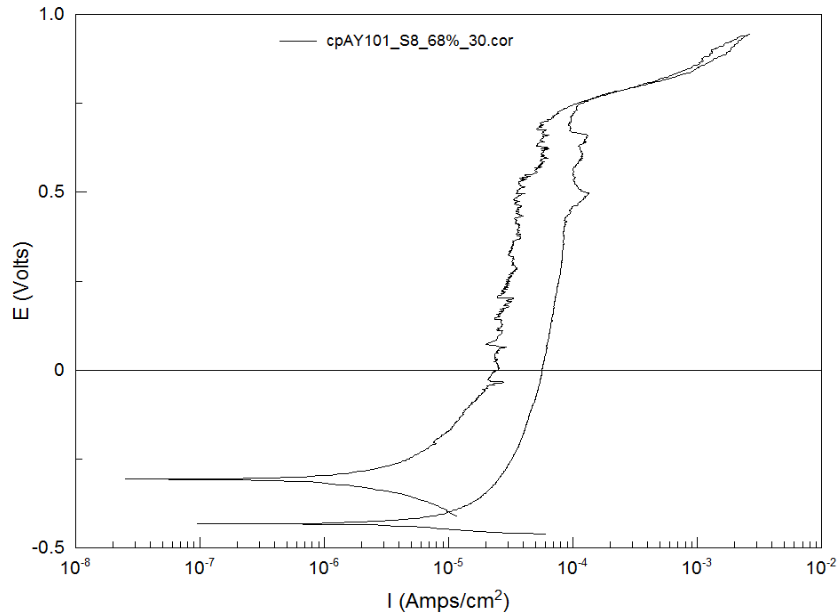

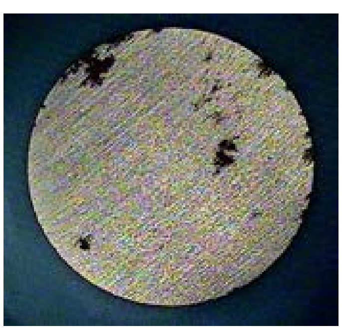

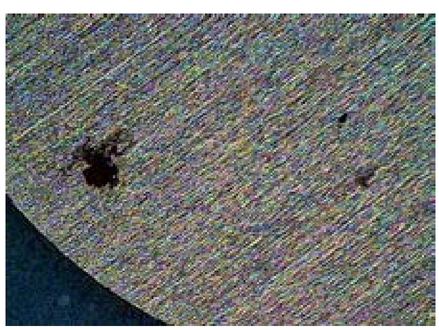

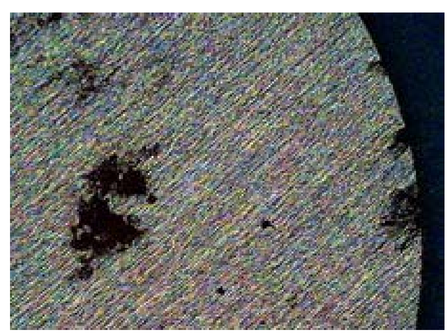

**AY101 - Segment 8 – 68% Evaporation – 550 ppm NH_3
No Cover Gas – Sample 31**

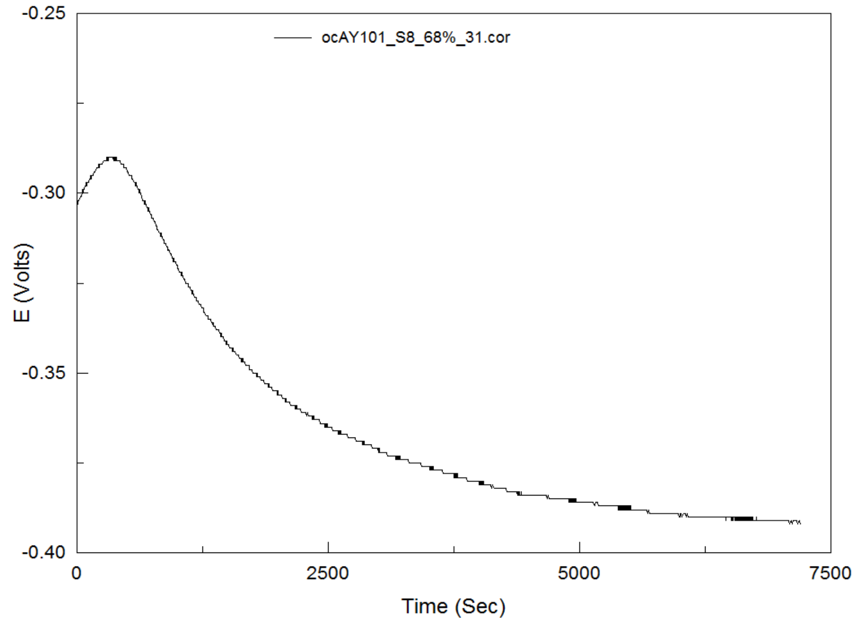

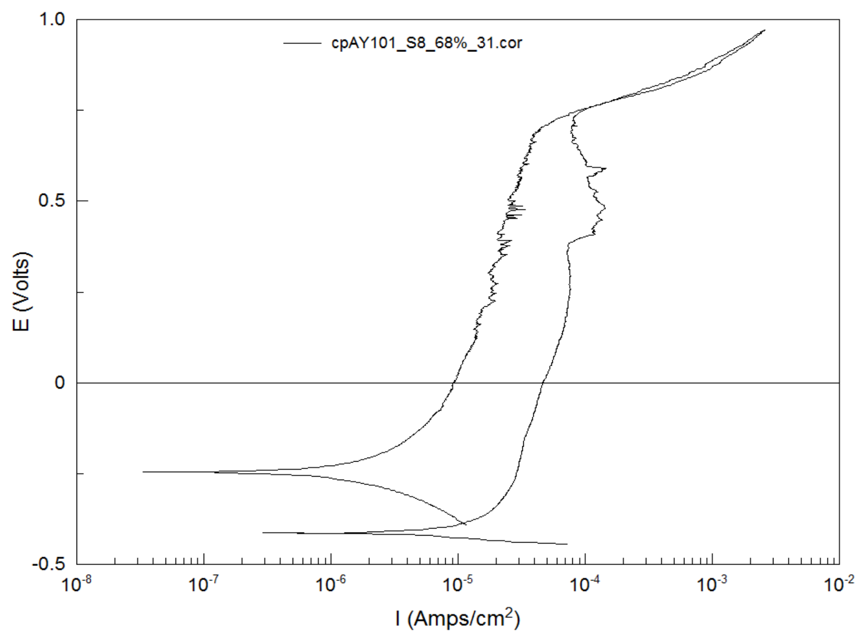

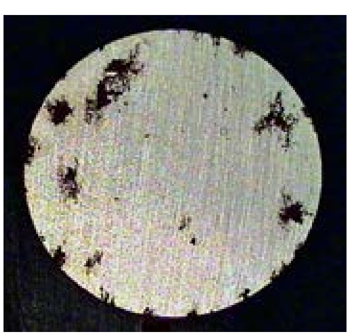

**SY102 – High Nitrate – 0% Evaporation – 0 ppm NH_3
No Cover Gas – Sample 30**

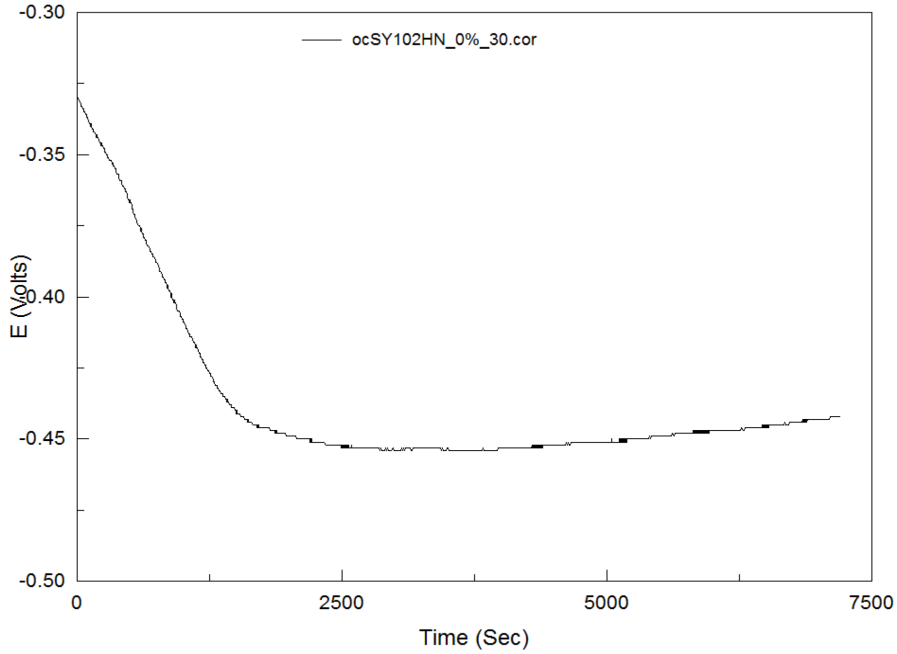

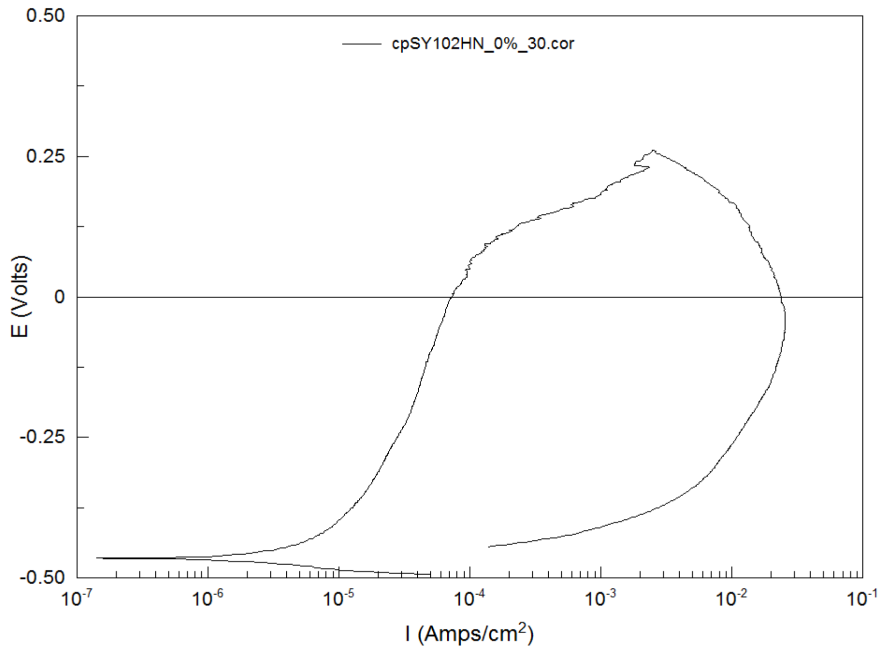

**SY102 – High Nitrate – 0% Evaporation – 0 ppm NH_3
No Cover Gas – Sample 31**

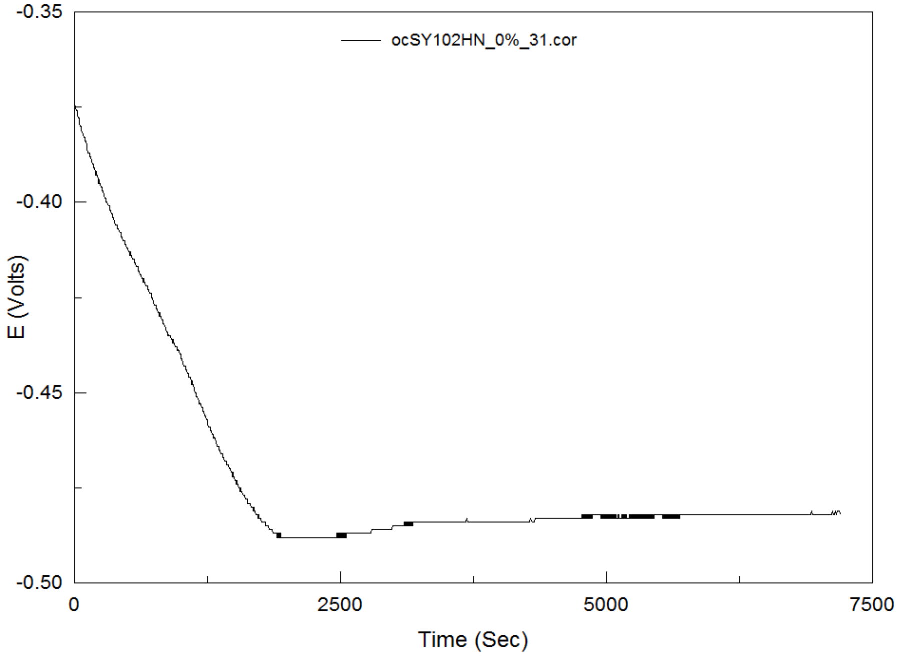

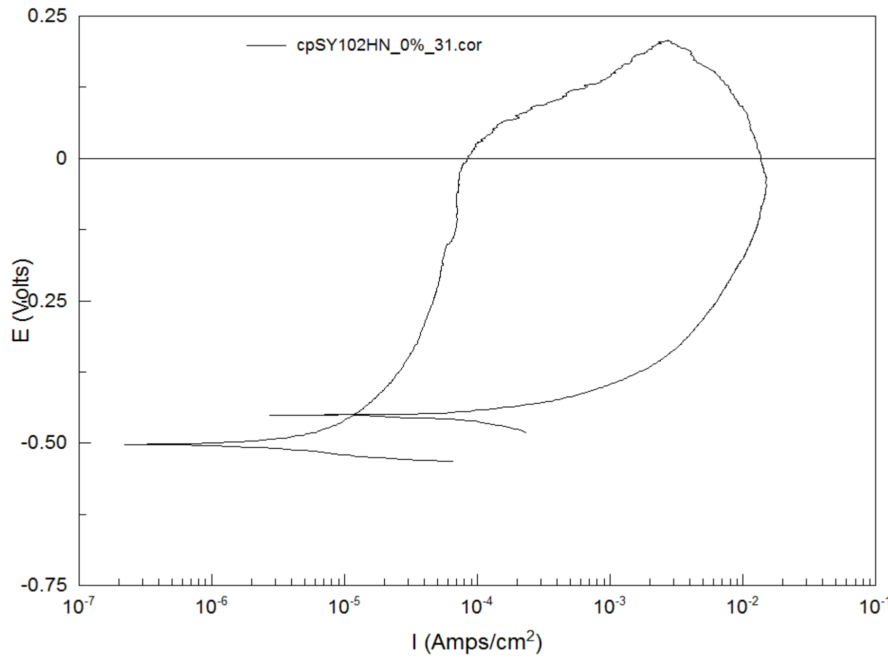

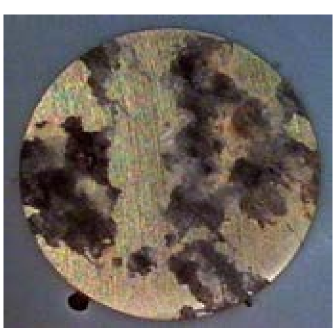

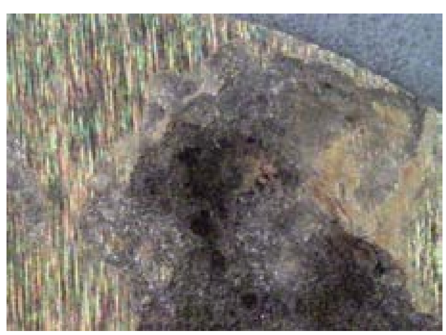

**SY102 – High Nitrate – 0% Evaporation – 50 ppm NH_3
No Cover Gas – Sample 3**

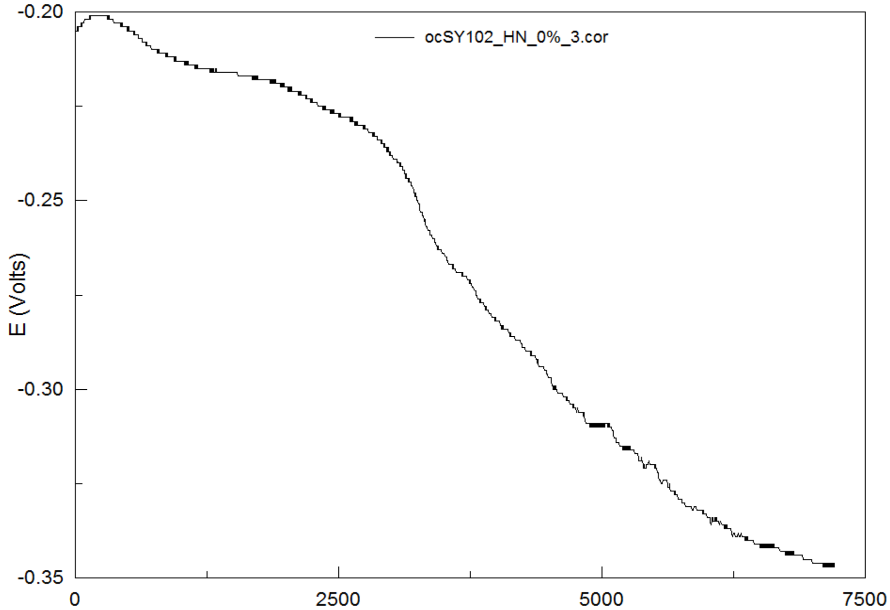

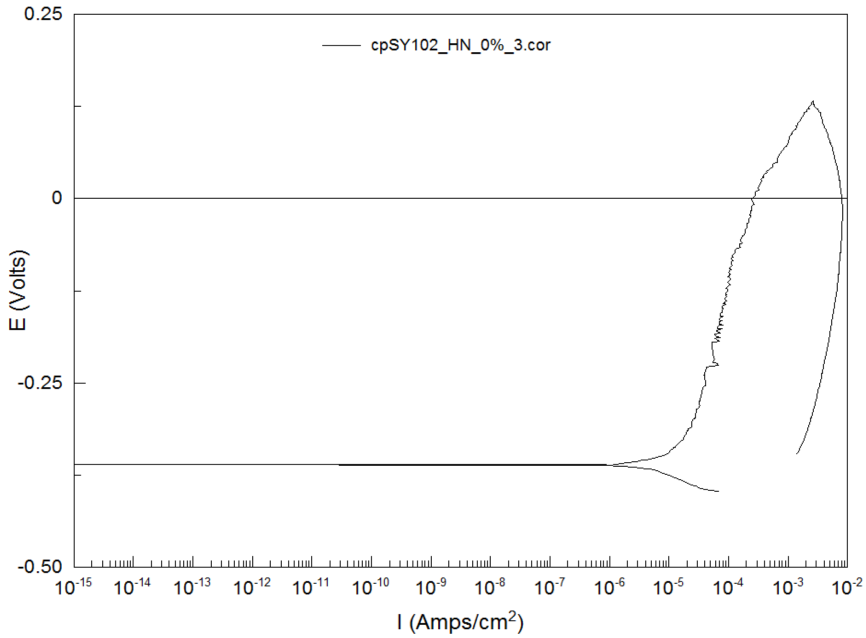

SY102 – High Nitrate – 0% Evaporation – 50 ppm NH_3
No Cover Gas – Sample 6

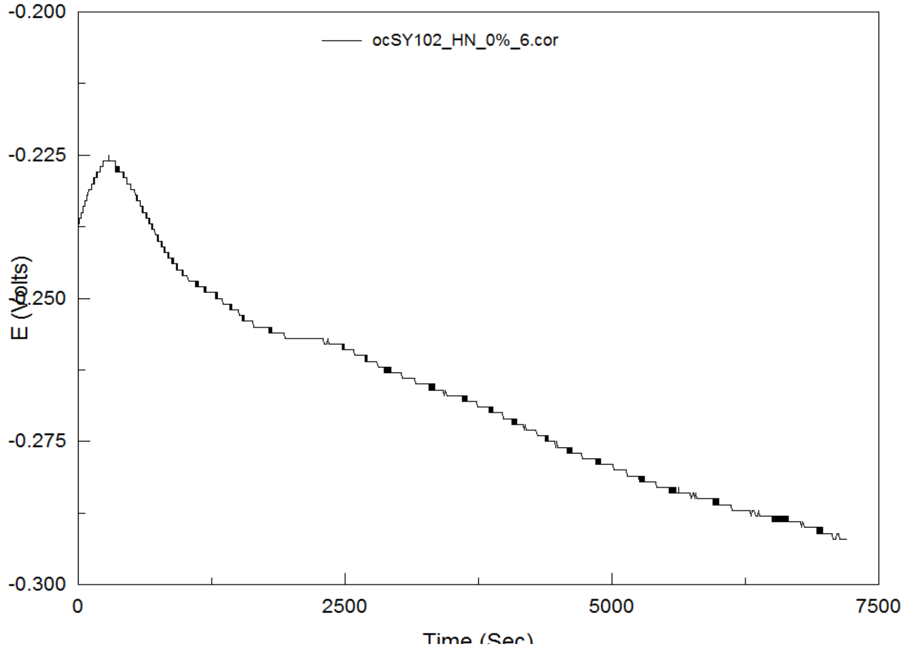

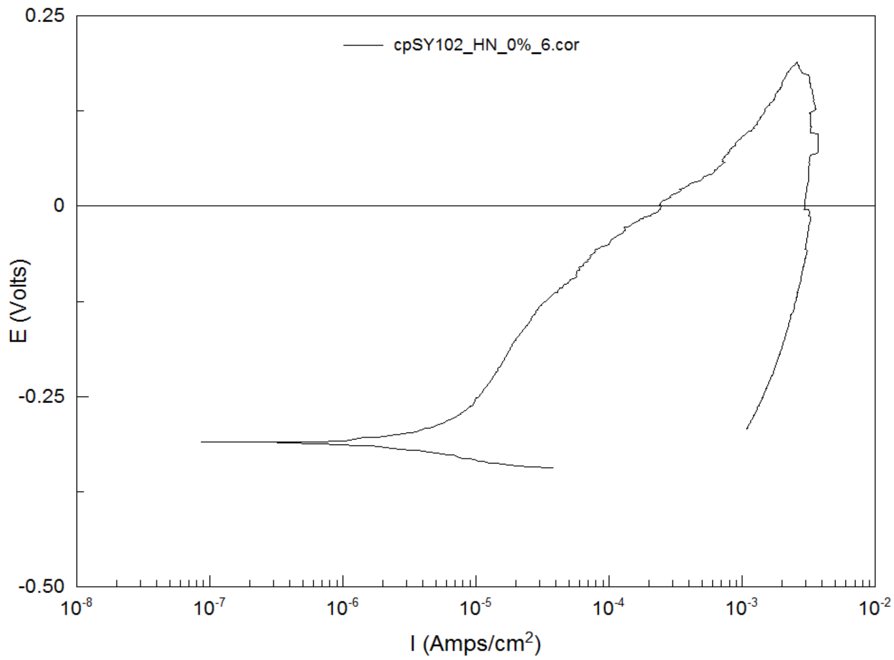

SY102 – High Nitrate – 0% Evaporation – 550 ppm NH_3
No Cover Gas – Sample 12

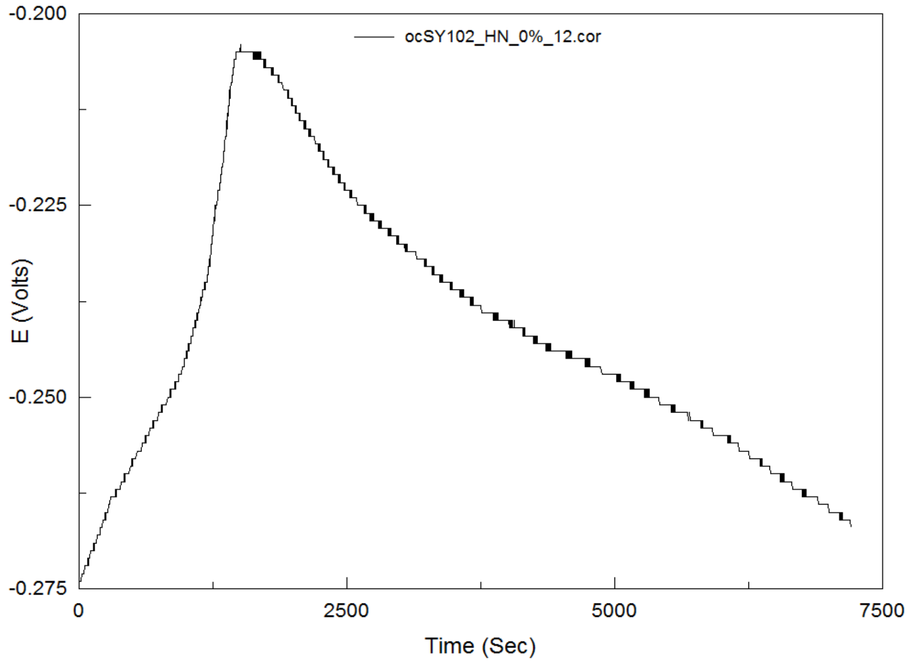

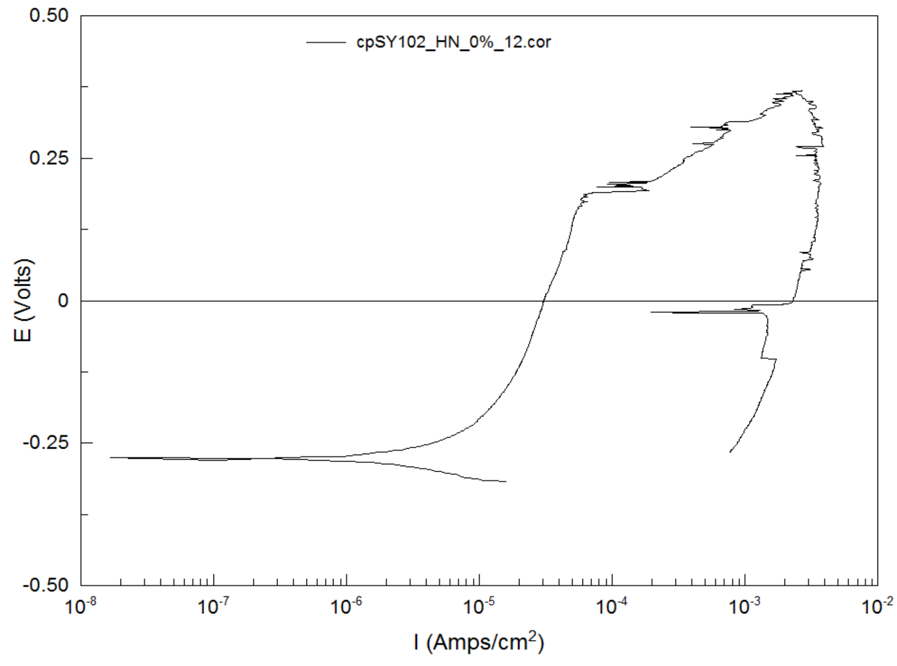

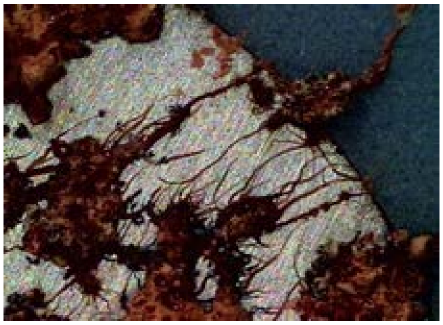

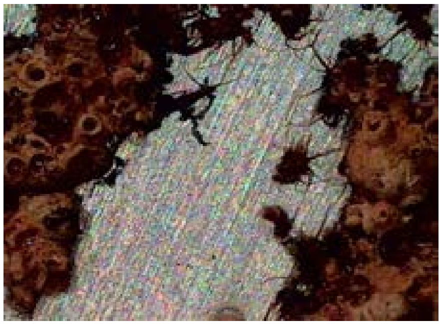

SY102 – High Nitrate – 0% Evaporation – 550 ppm NH_3
No Cover Gas – Sample 14

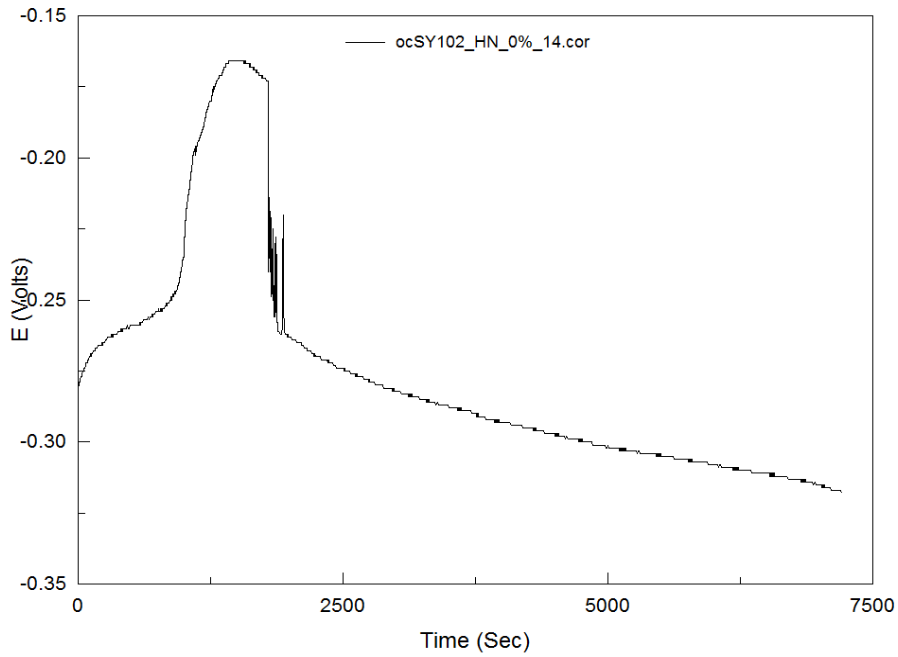

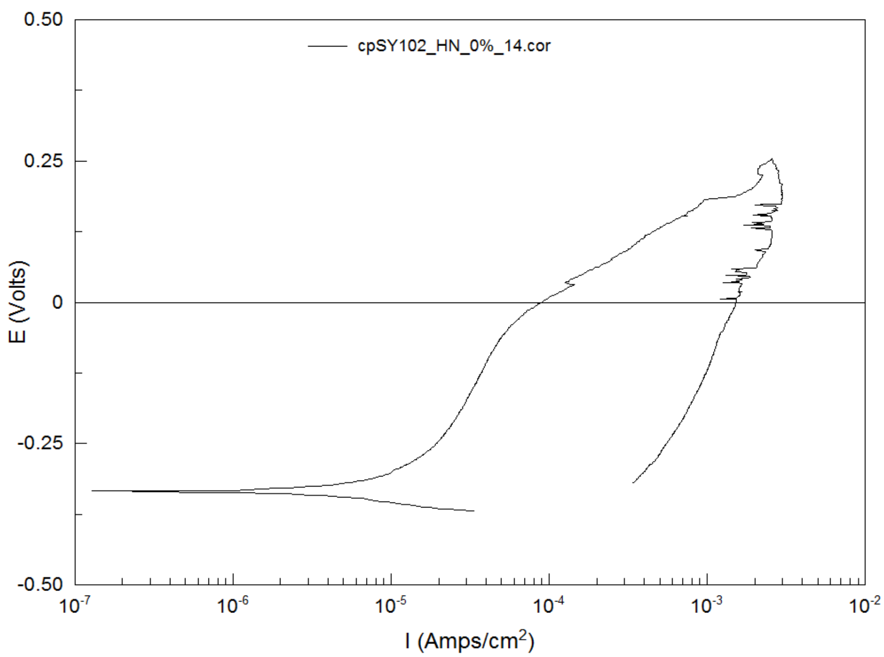


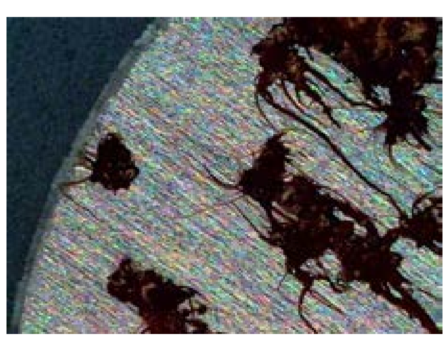
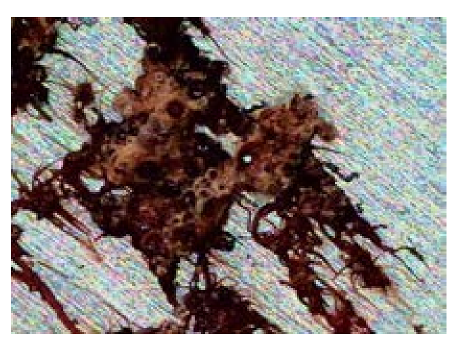

SY102 – High Nitrate – 33% Evaporation – 0 ppm NH_3
No Cover Gas – Sample 30

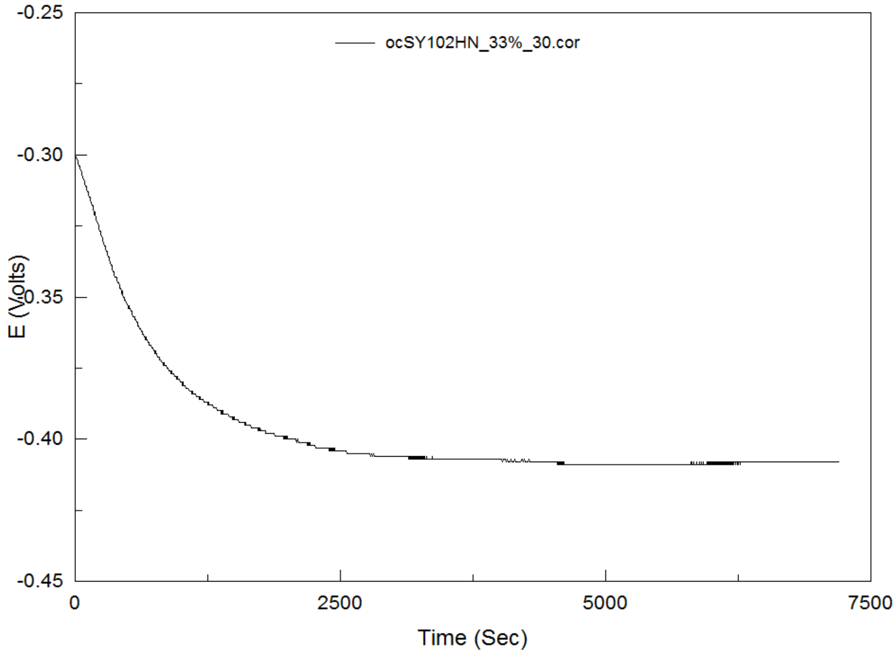

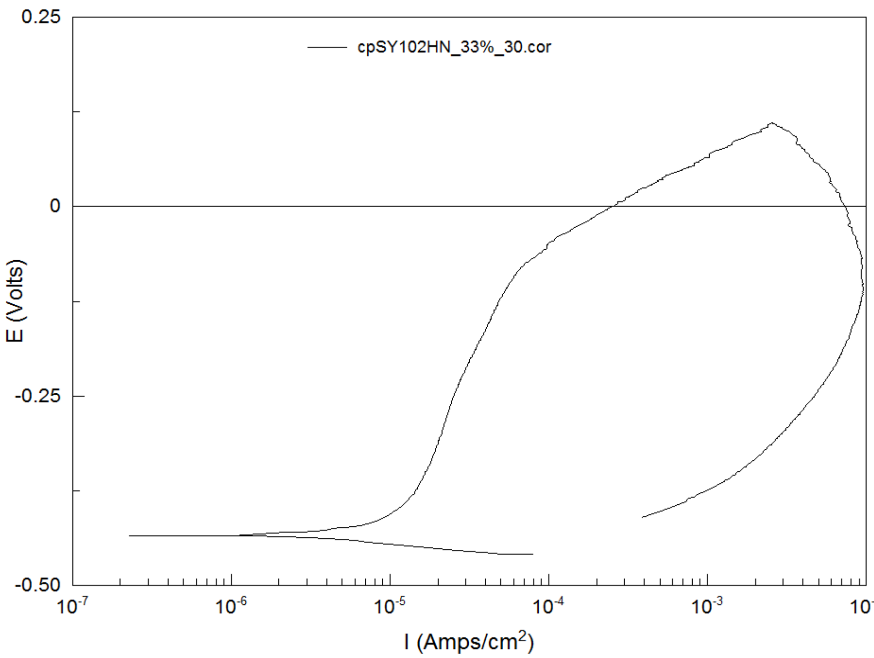

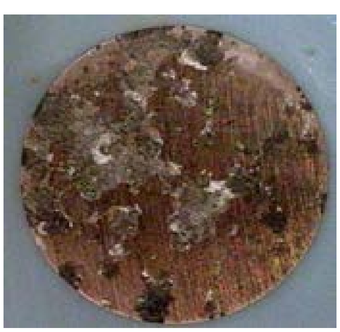

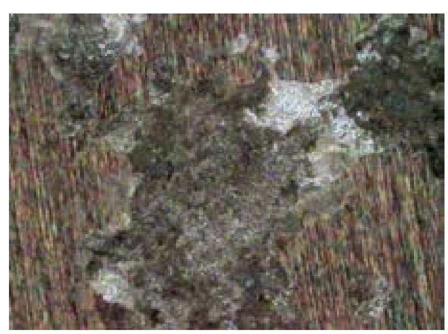

SY102 – High Nitrate – 33% Evaporation – 0 ppm NH_3
No Cover Gas – Sample 31

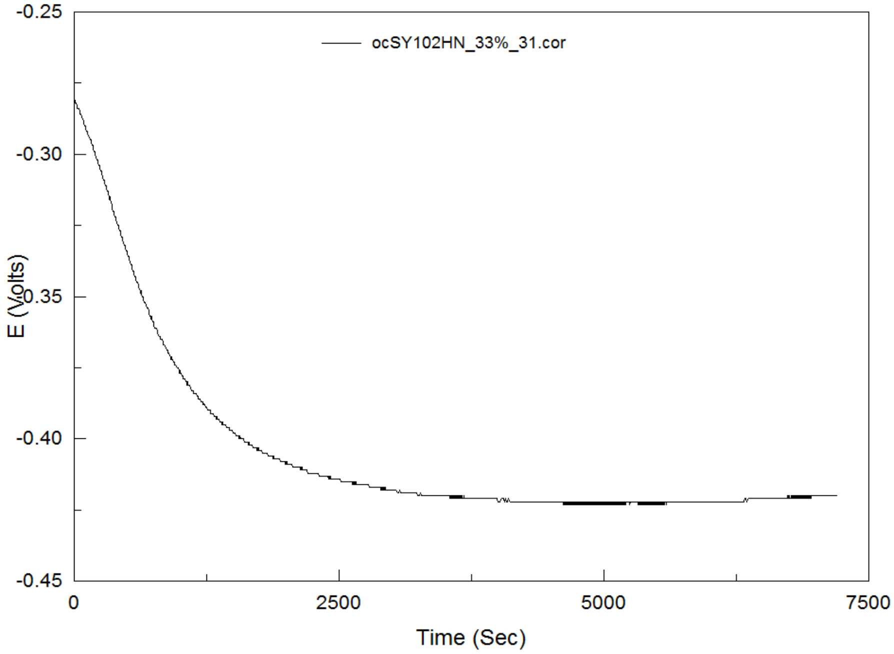

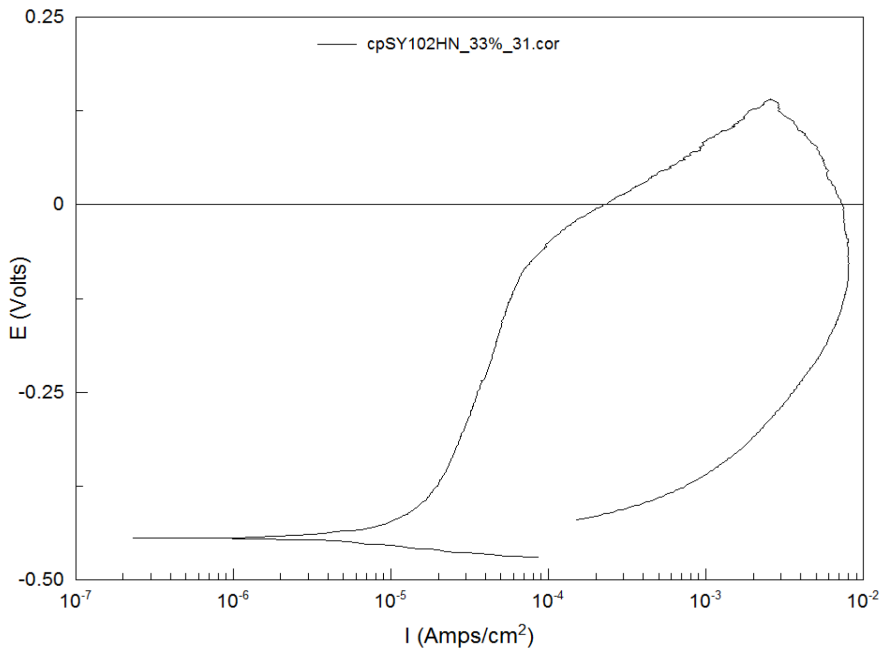

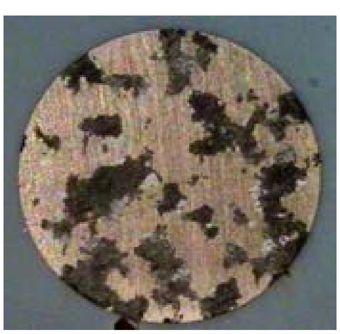

SY102 – High Nitrate – 33% Evaporation – 50 ppm NH_3
No Cover Gas – Sample 19

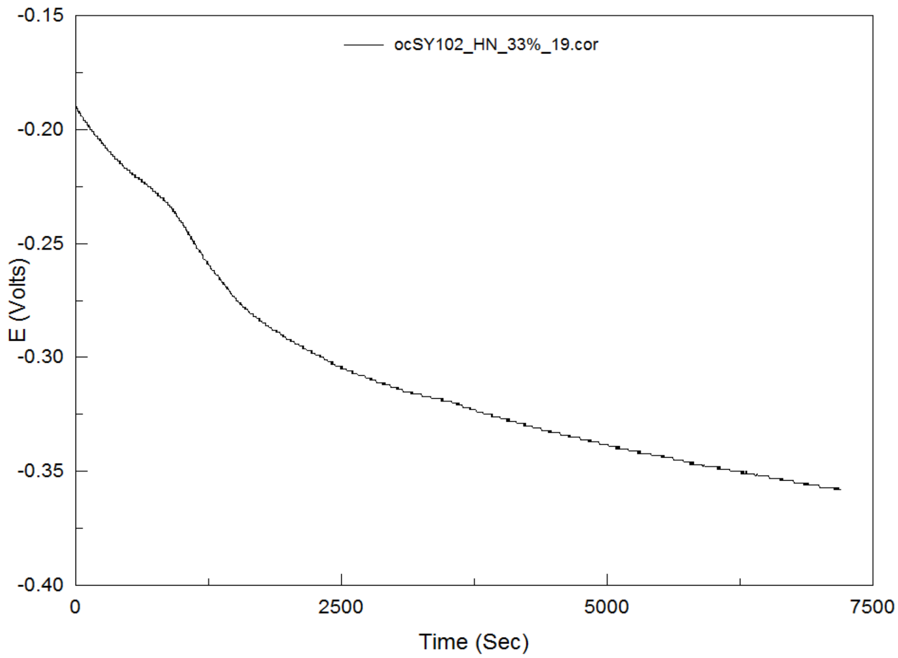

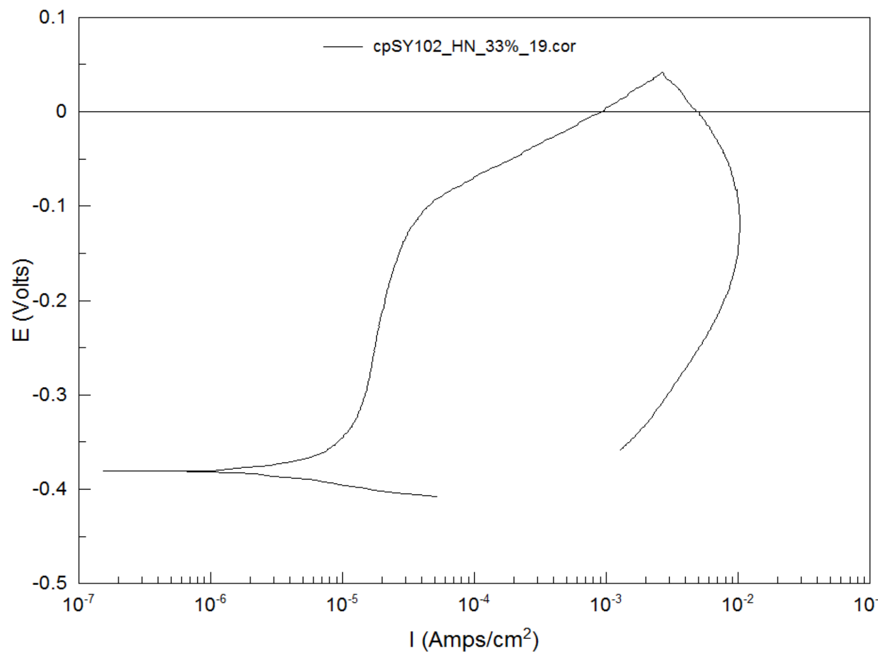

SY102 – High Nitrate – 33% Evaporation – 50 ppm NH_3
No Cover Gas – Sample 20

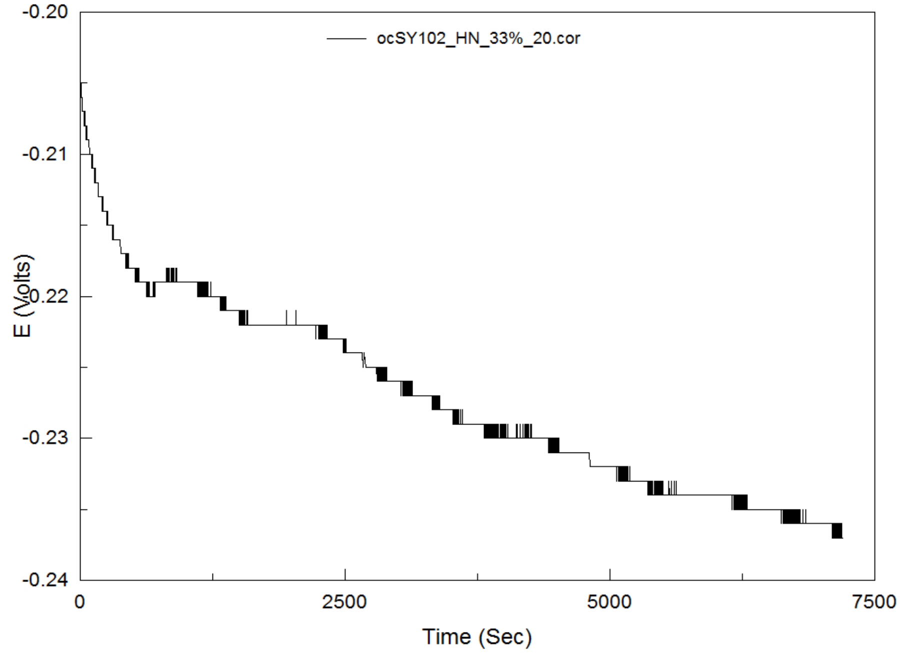

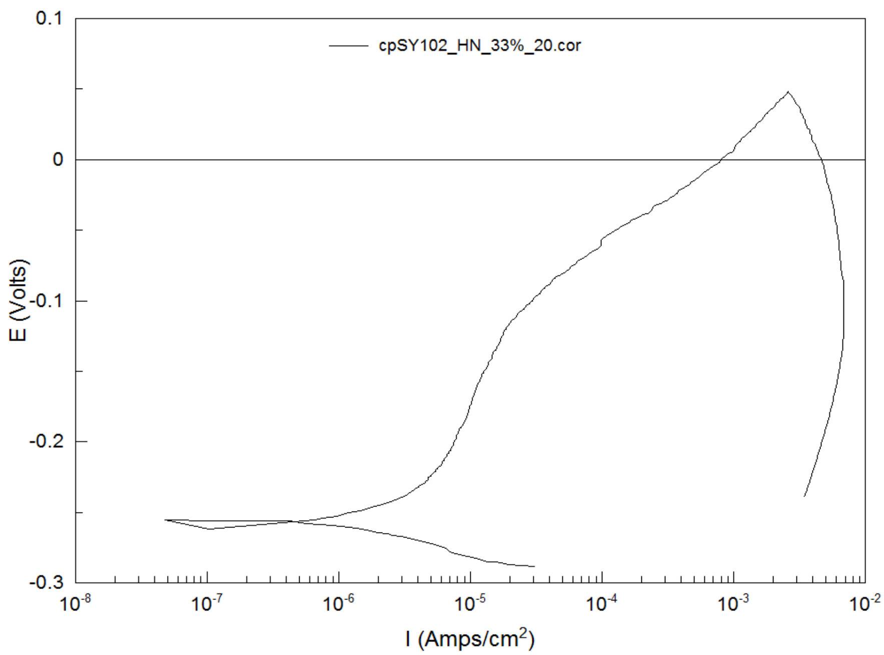

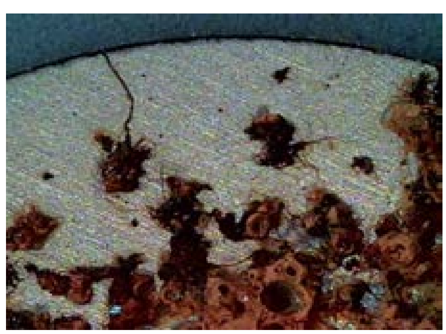

**SY102 – High Nitrate – 33% Evaporation – 550 ppm NH_3
No Cover Gas – Sample 12**

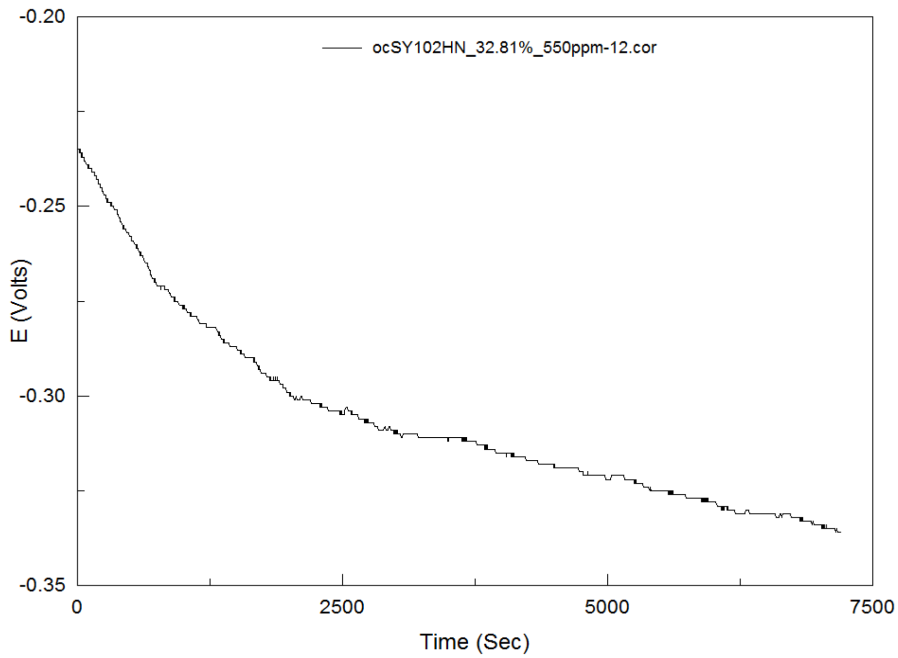

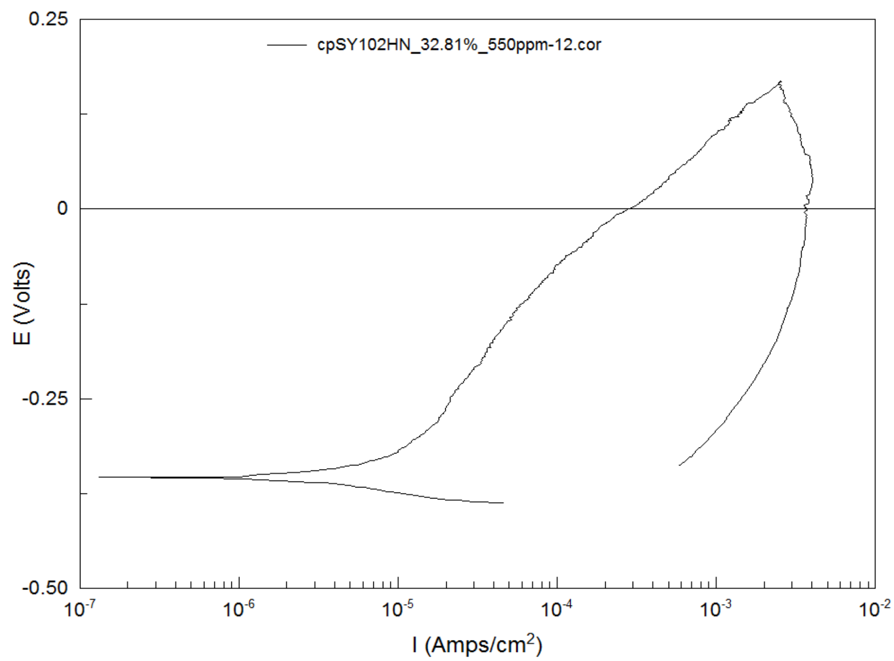

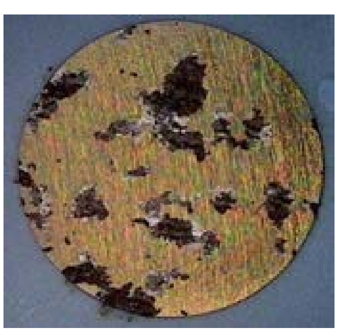
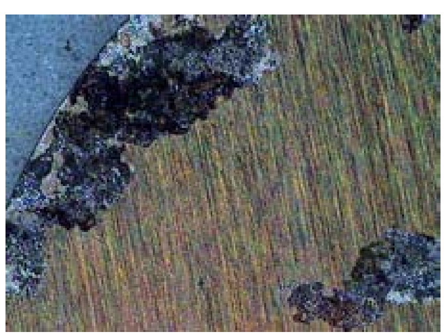


**SY102 – High Nitrate – 33% Evaporation – 550 ppm NH_3
No Cover Gas – Sample 14**

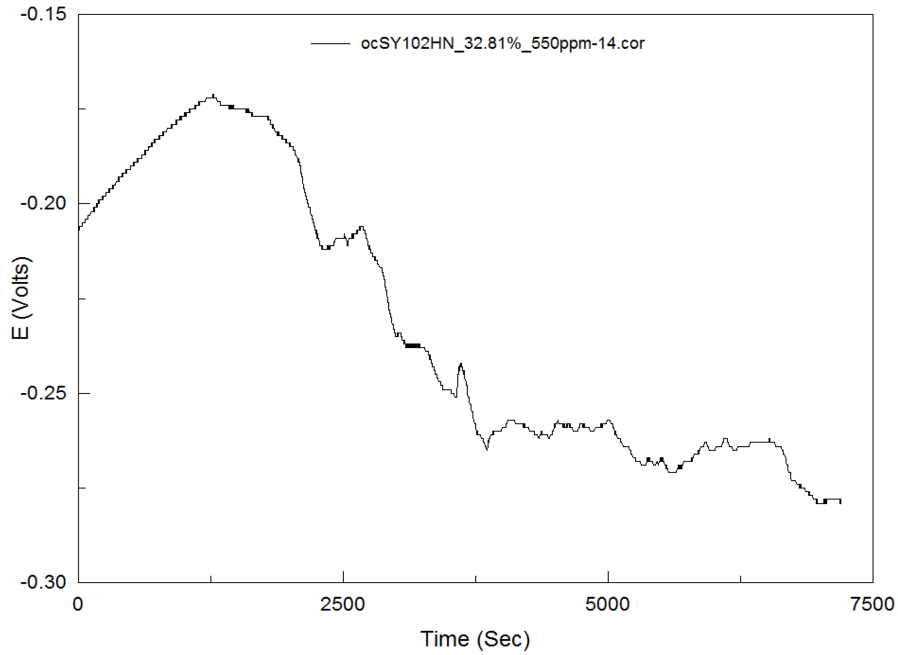

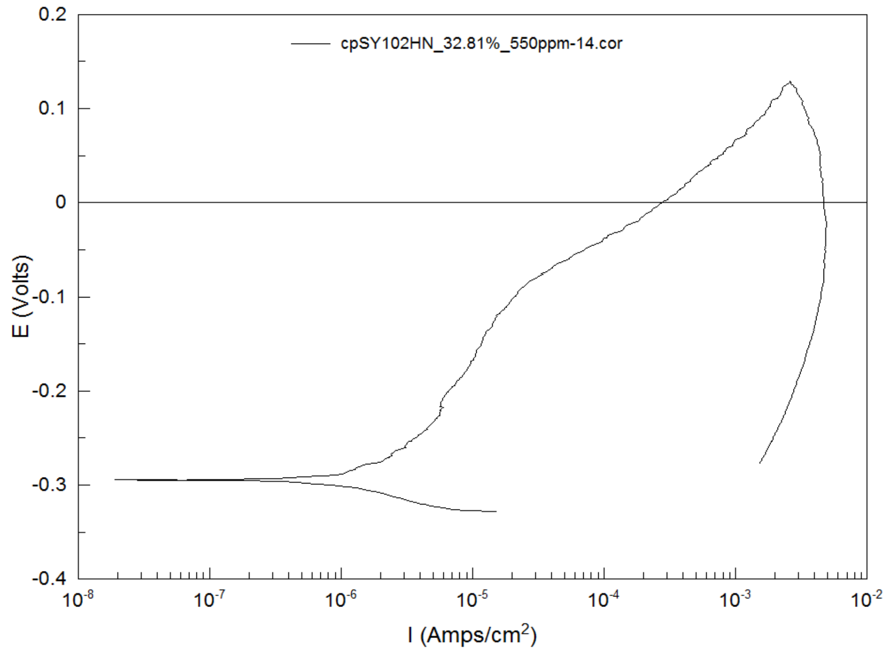

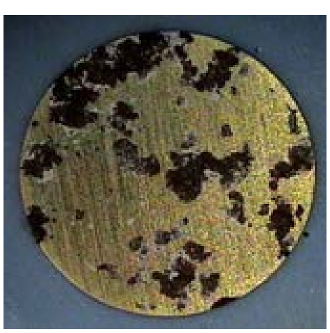

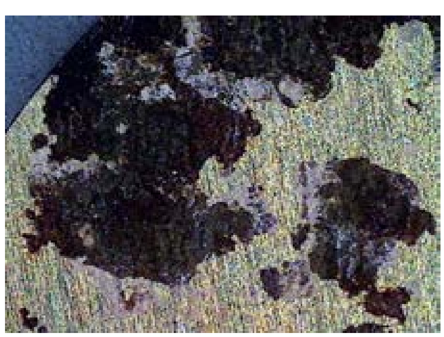

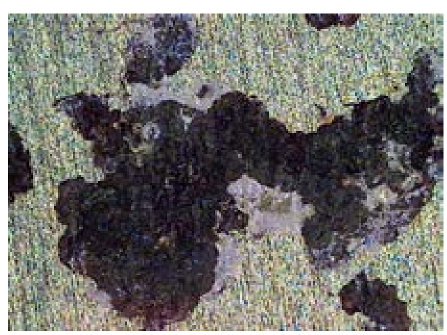

AY101 – Segment 3 – 0% Evaporation – 50 ppm NH_3
NH_3 Cover Gas – Sample 28

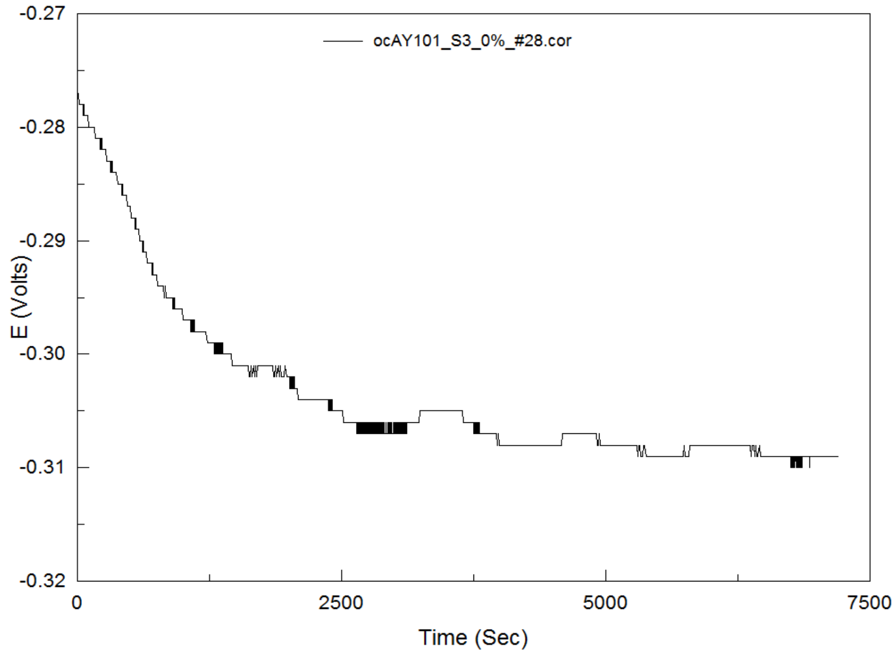

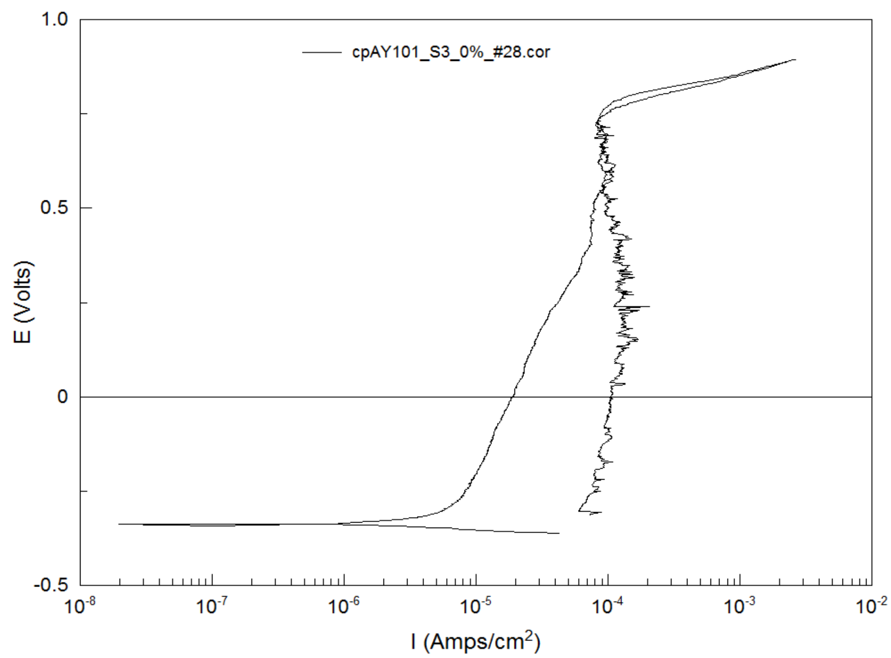

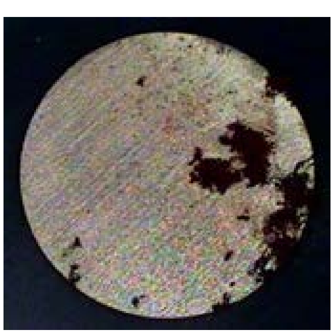

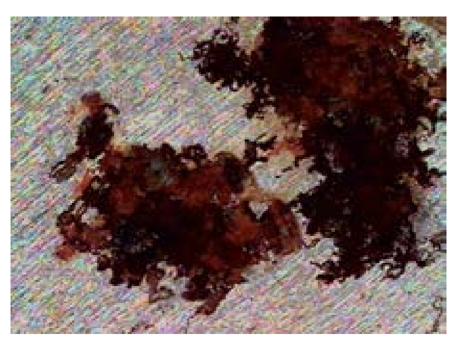

AY101 – Segment 3 – 0% Evaporation – 50 ppm NH_3
NH_3 Cover Gas – Sample 29

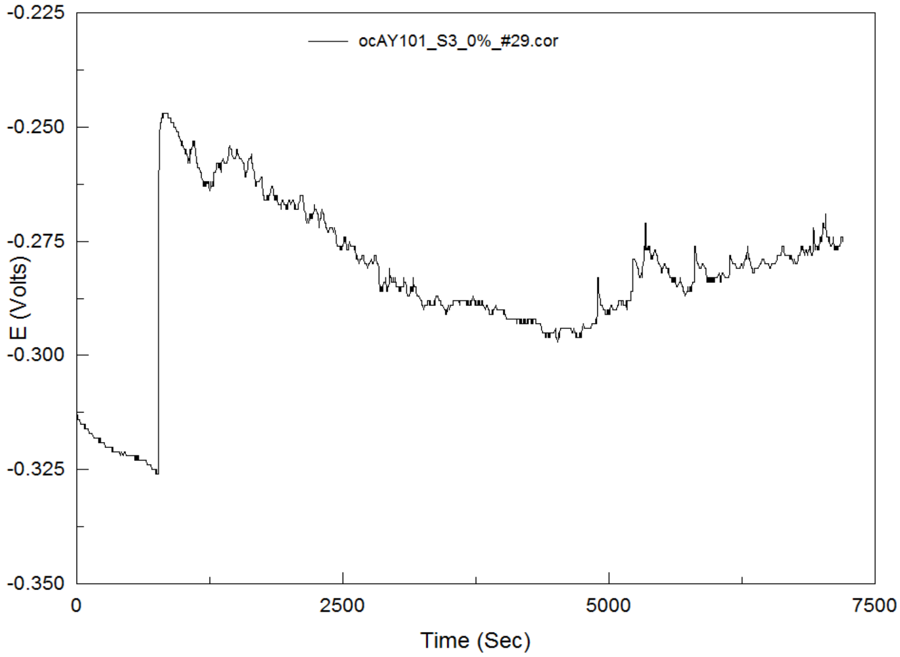

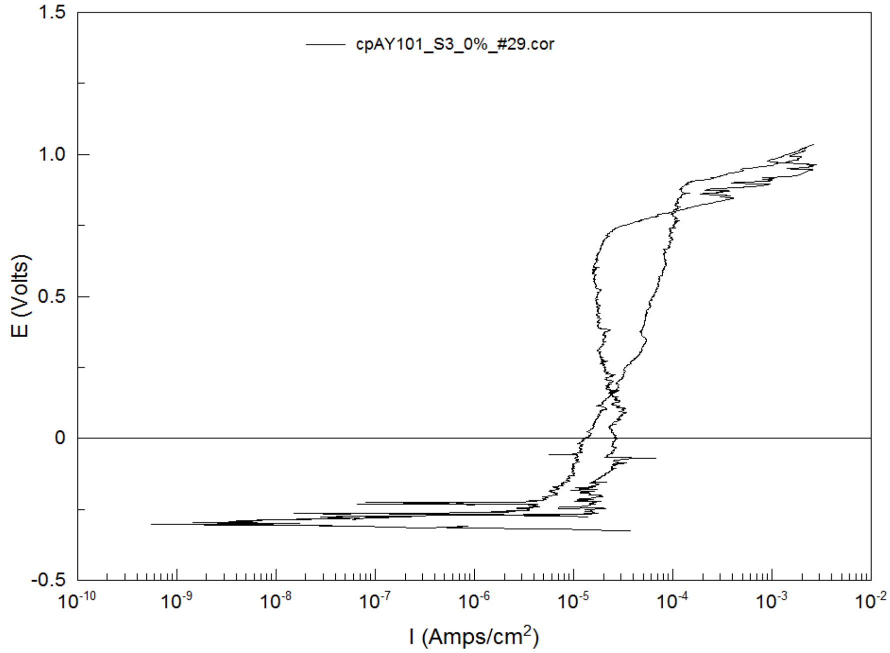

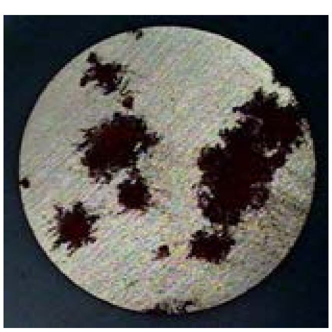
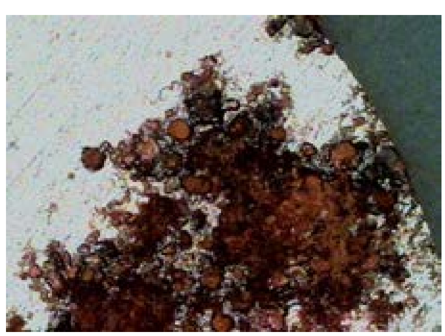
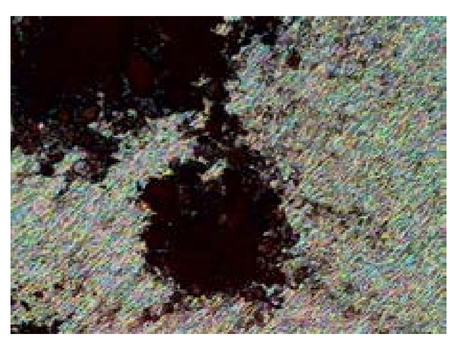

AY101 – Segment 8 – 0% Evaporation – 550 ppm NH_3
NH_3 Cover Gas – Sample 30

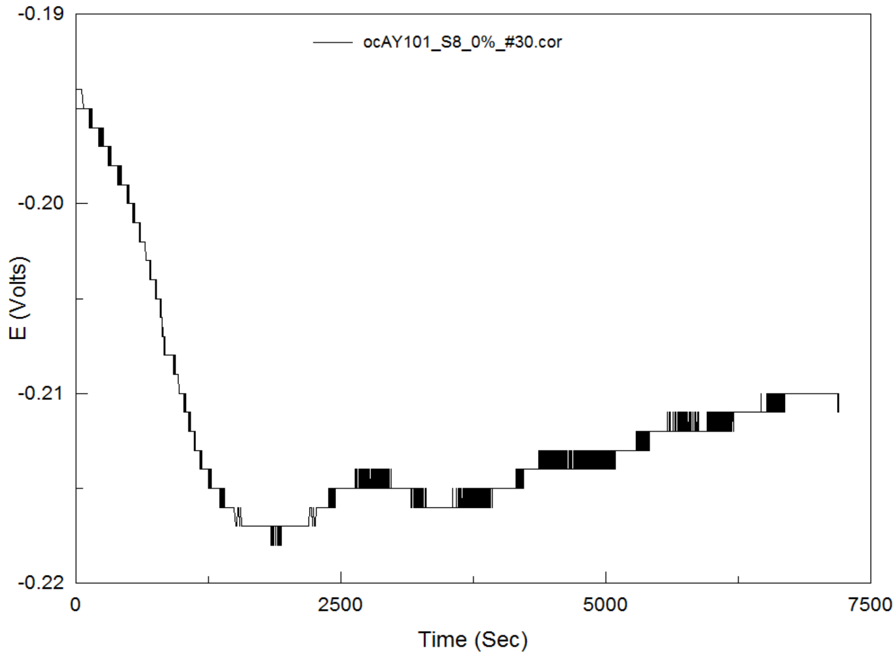

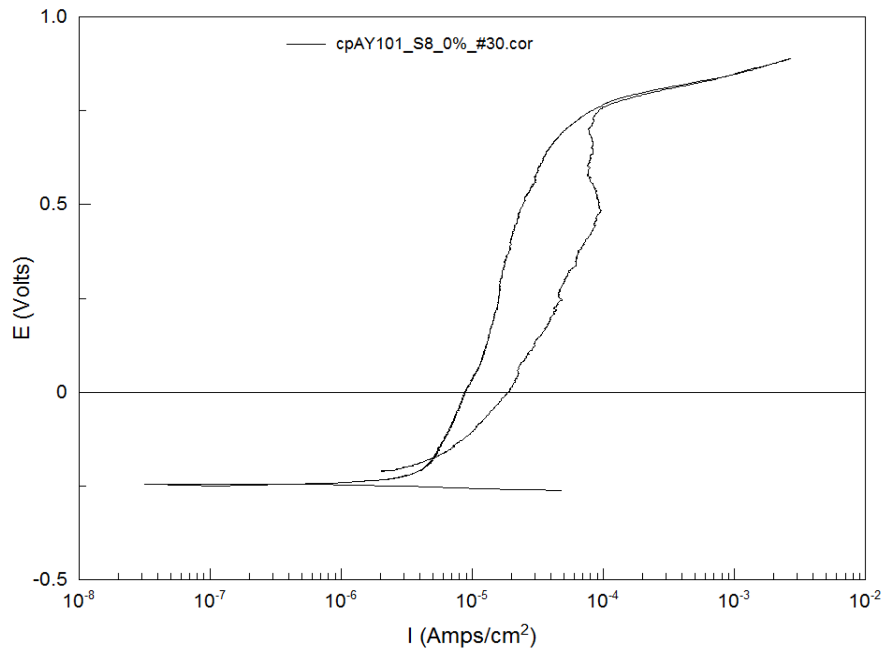

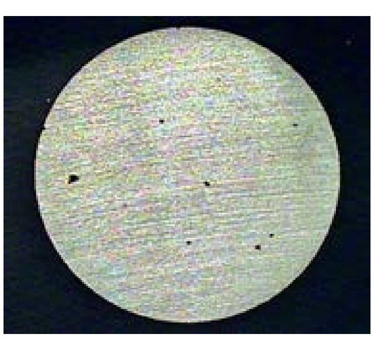

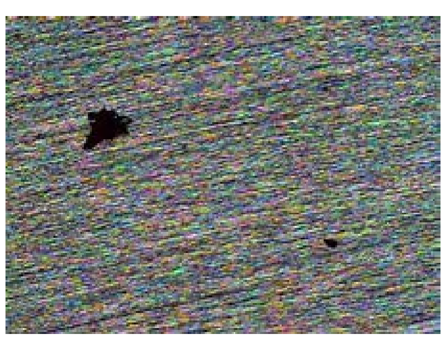

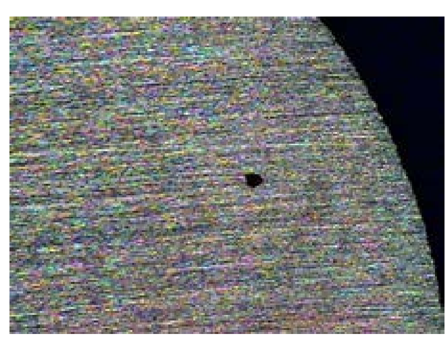

AY101 – Segment 8 – 0% Evaporation – 550 ppm NH_3
NH_3 Cover Gas – Sample 31

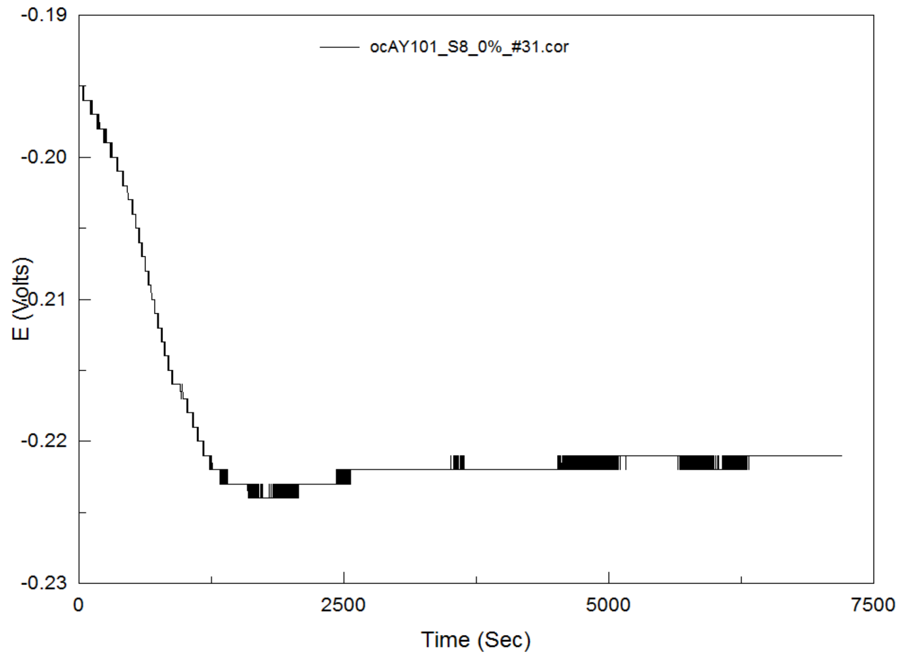

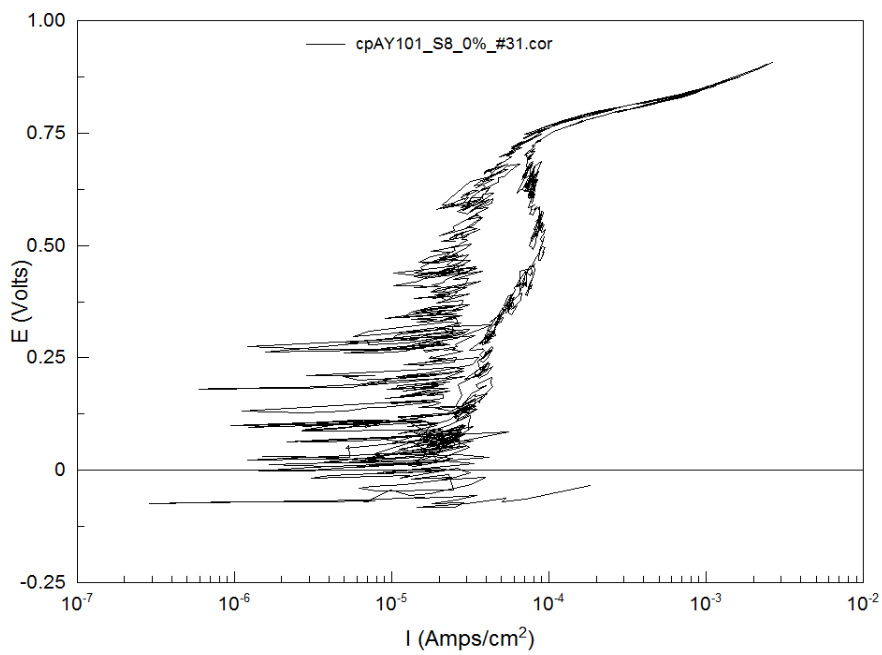

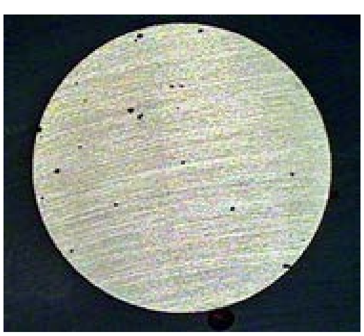

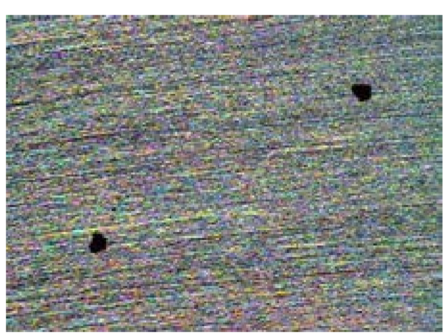

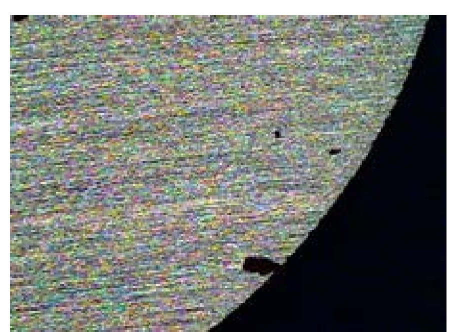

AY101 – Segment 8 – 67% Evaporation – 0 ppm NH_3
No Cover Gas – Bullet - Sample 146

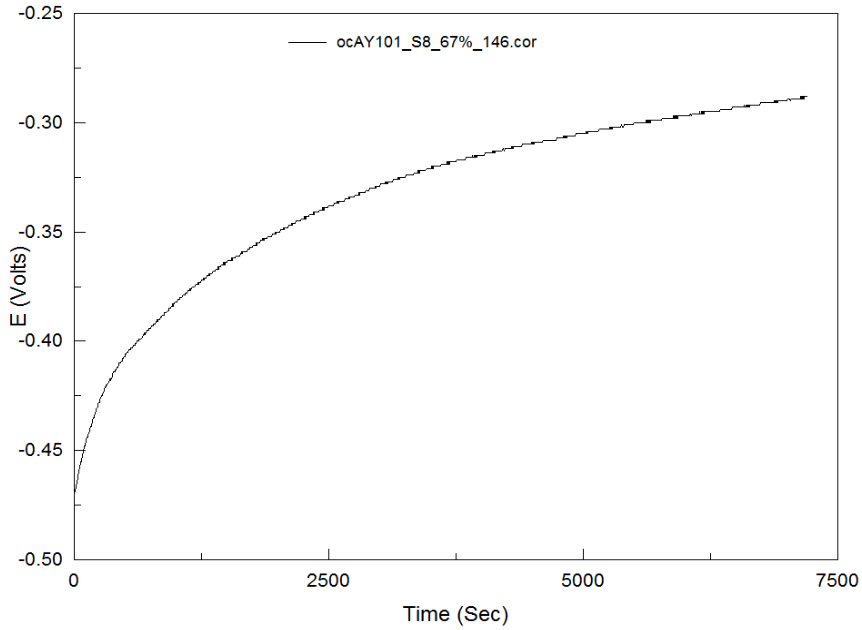

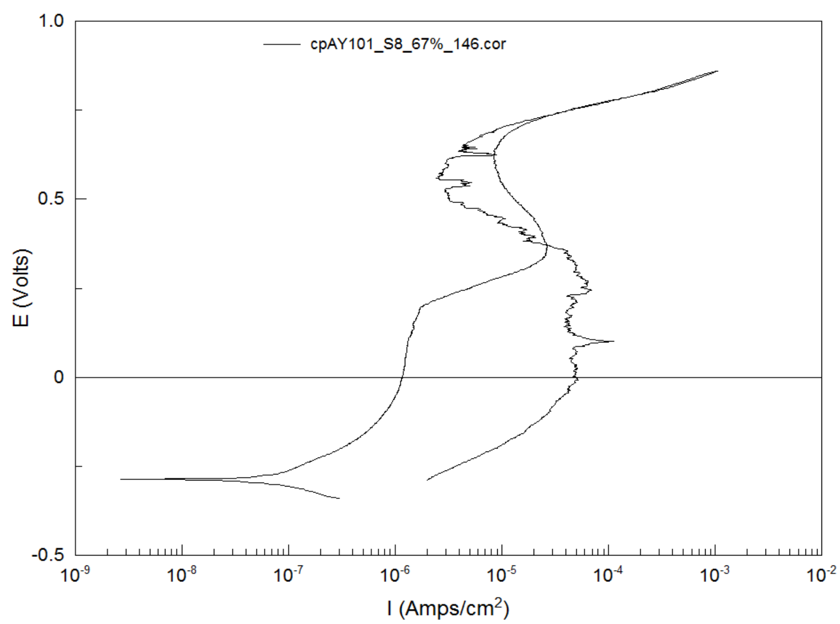

AY101 – Segment 8 – 67% Evaporation – 550 ppm NH_3
No Cover Gas – Bullet - Sample 148

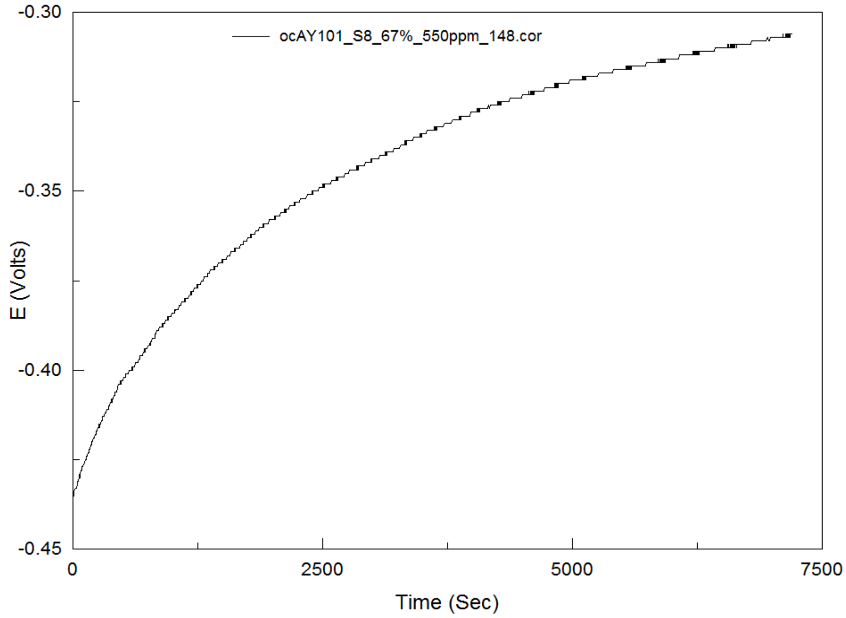

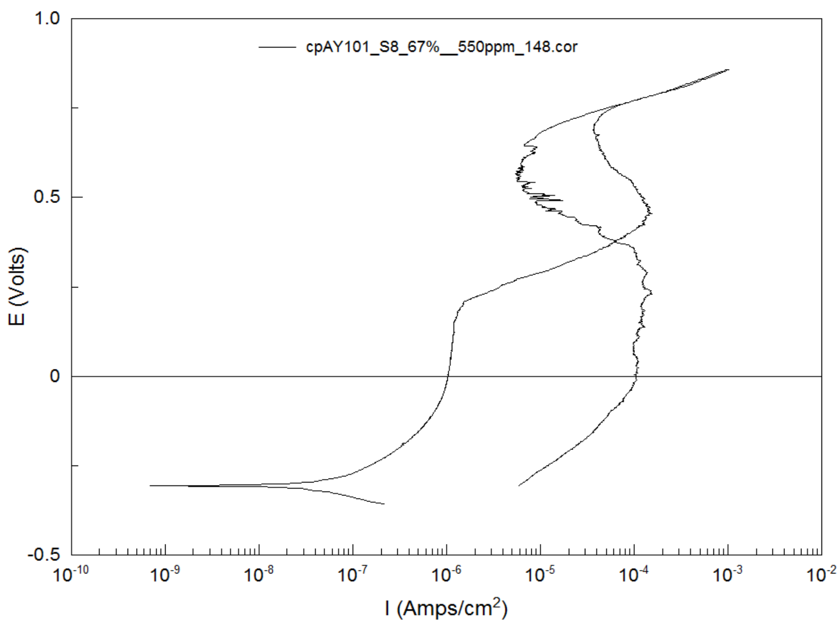

SY102 – High Nitrate – 0% Evaporation – 0 ppm NH_3
No Cover Gas – Bullet - Sample 147

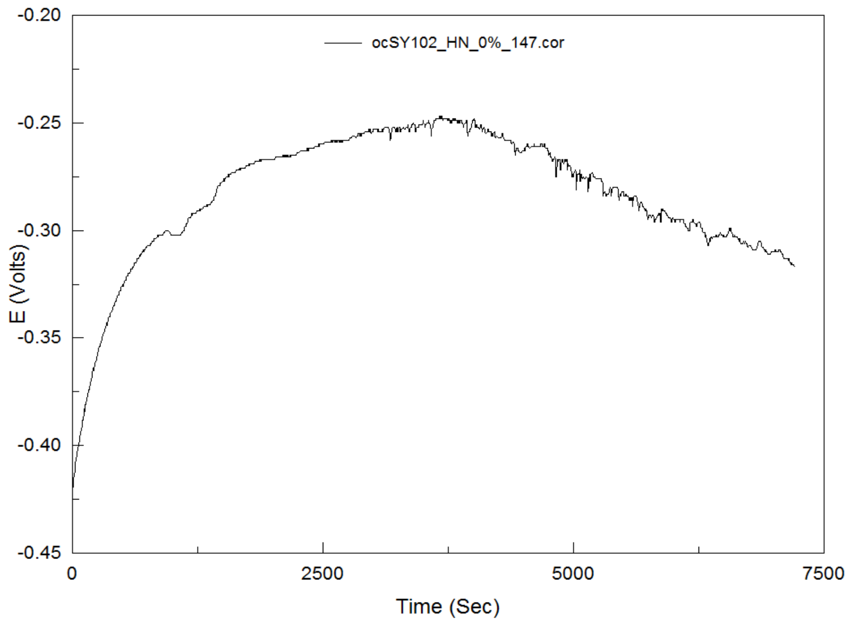

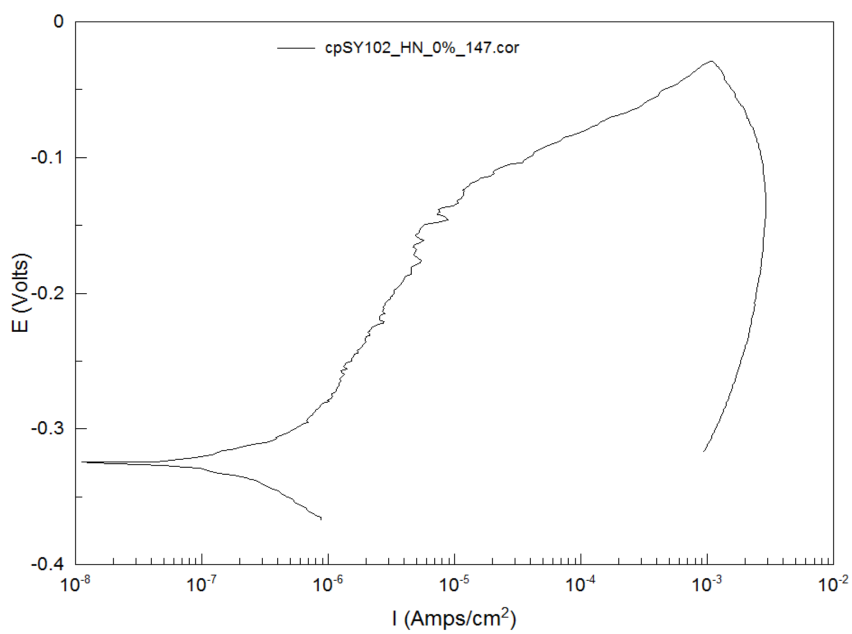

APPENDIX C

Ammonia Gas Coupon Test Data

SY102 – High Nitrate – 50 ppm NH_3 – 1 Month
Coupon #514

Before Cleaning

After Cleaning

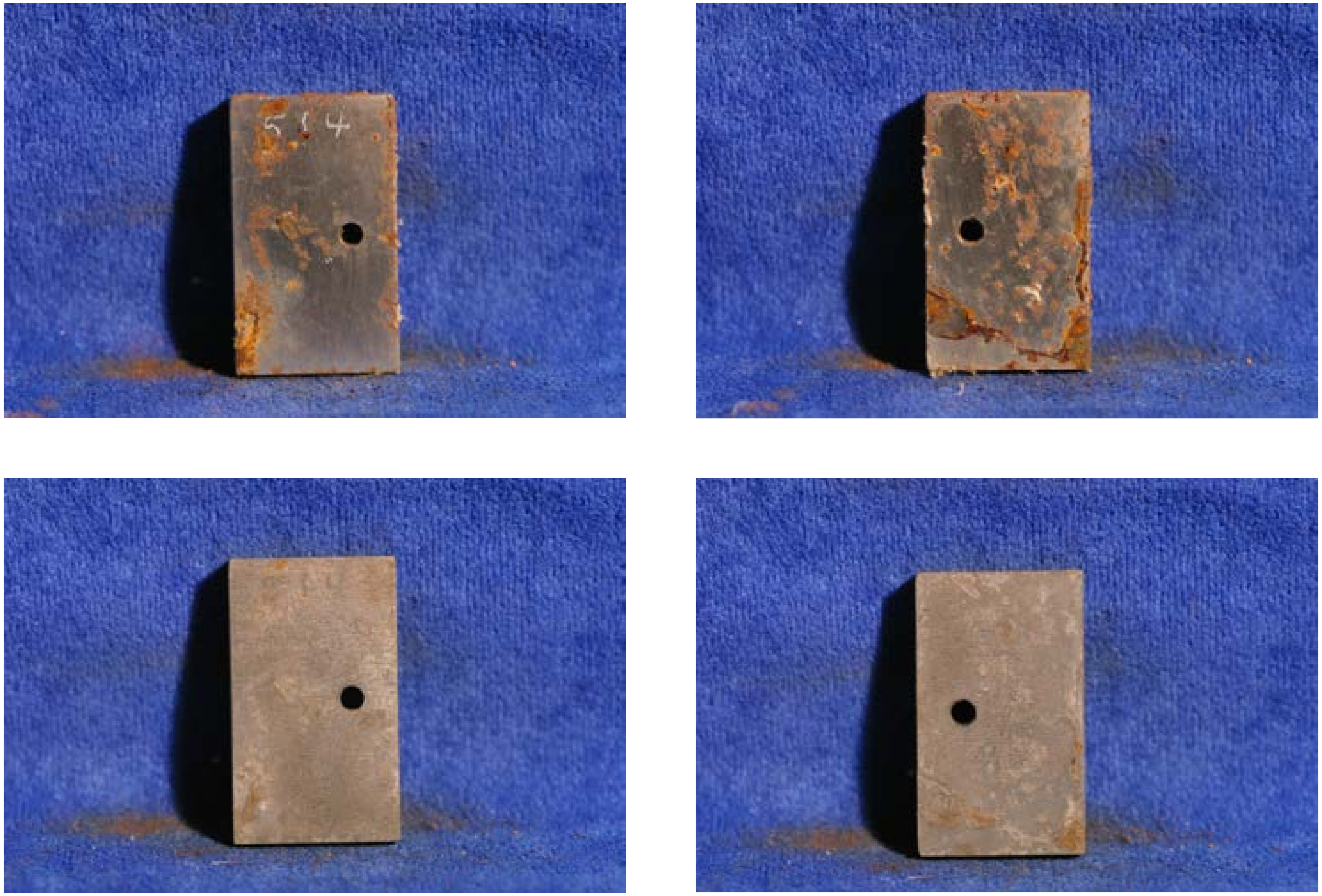

SY102 – High Nitrate – 50 ppm NH_3 – 1 Month
Coupon # 518

Before Cleaning

After Cleaning

SY102 – High Nitrate – 550 ppm NH_3 – 1 Month
Coupon # 506

Before Cleaning

No pictures available

No pictures available

After Cleaning

SY102 – High Nitrate – 550 ppm NH_3 – 1 Month
Coupon # 501

Before Cleaning

After Cleaning

SY102 – High Nitrate – 50 ppm NH_3 – 2 Months
Coupon # 517

Before Cleaning

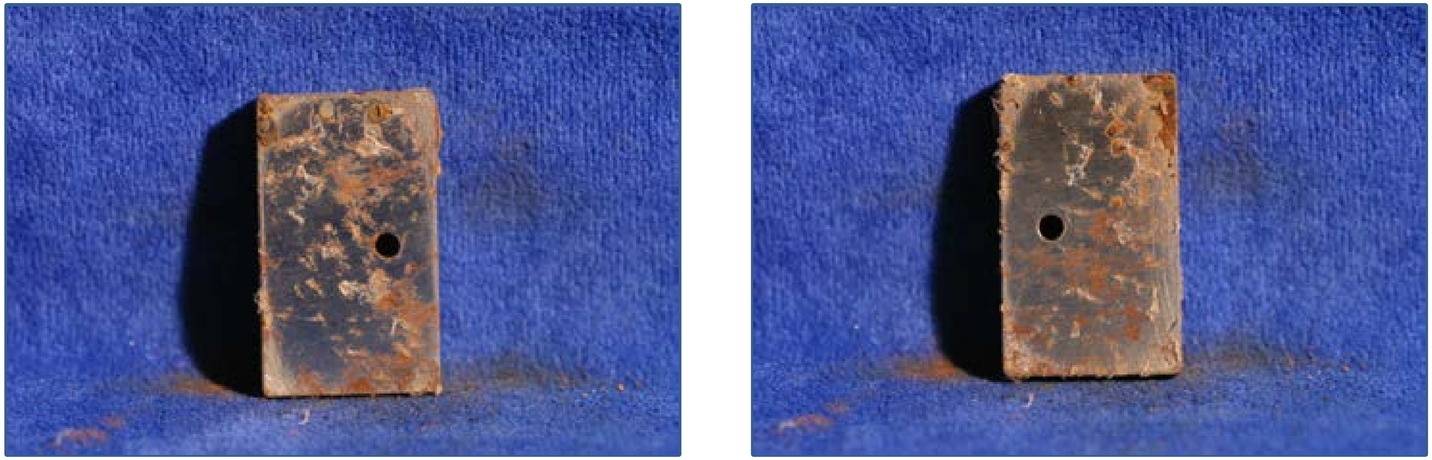

After Cleaning

SY102 – High Nitrate – 50 ppm NH_3 – 2 Months
Coupon # 522

Before Cleaning

After Cleaning

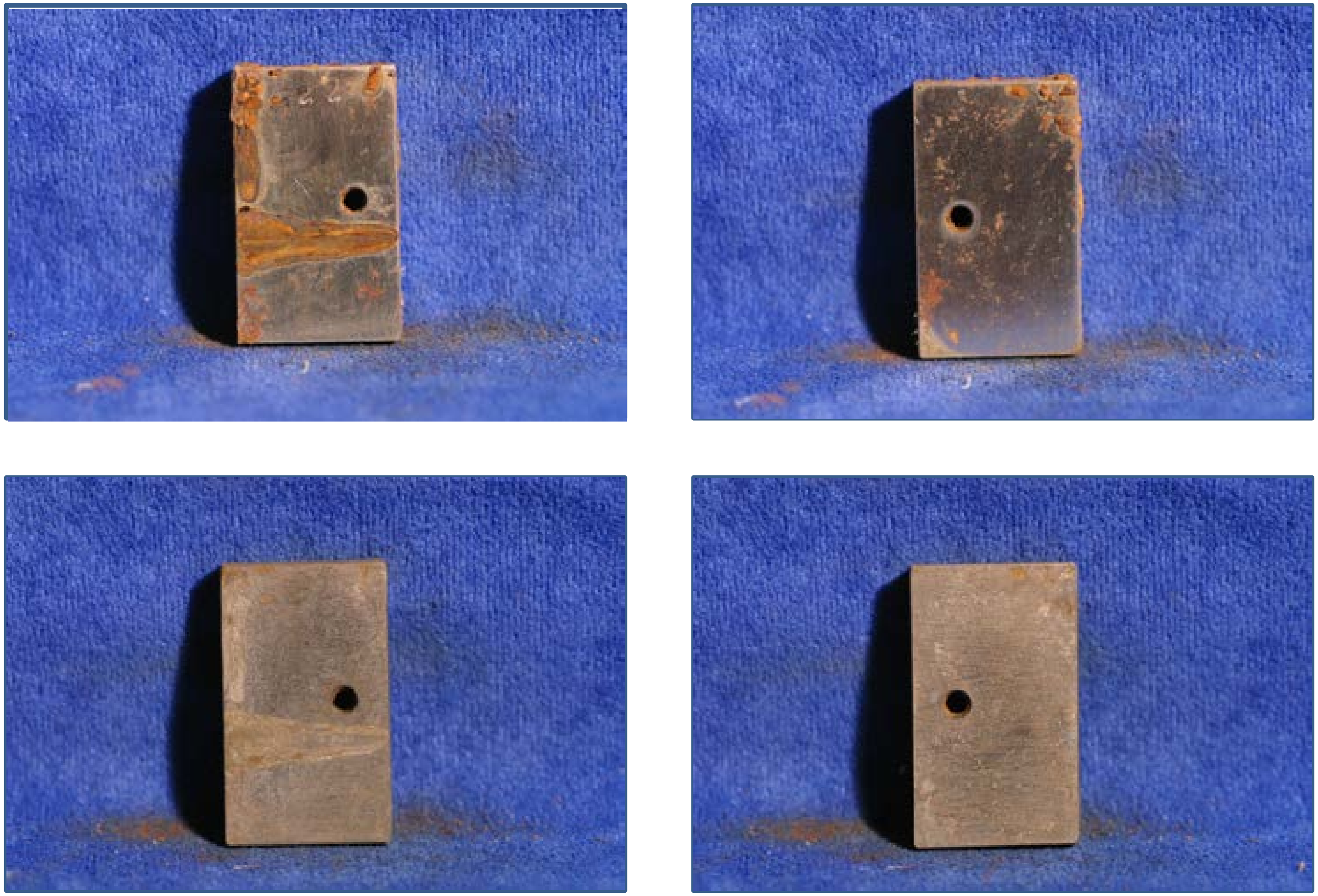

SY102 – High Nitrate – 550 ppm NH_3 – 2 Months
Coupon # 503

Before Cleaning

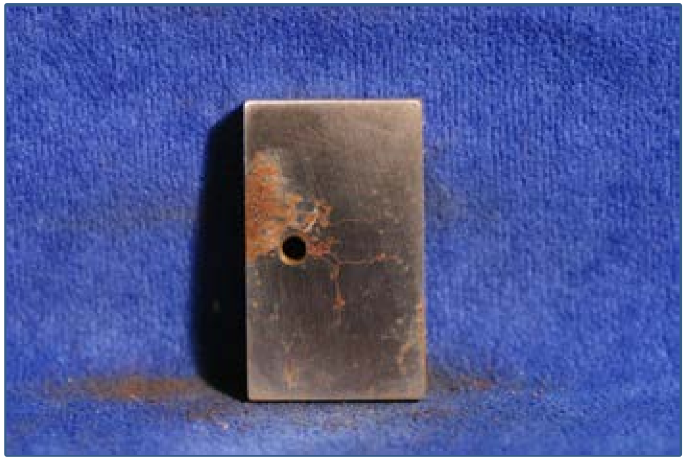

After Cleaning

SY102 – High Nitrate – 550 ppm NH_3 – 2 Months
Coupon # 507

Before Cleaning

After Cleaning

SY102 – High Nitrate – 50 ppm NH_3 – 3 Months
Coupon # 523

Before Cleaning

After Cleaning

SY102 – High Nitrate – 50 ppm NH_3 – 3 Months
Coupon # 524

Before Cleaning

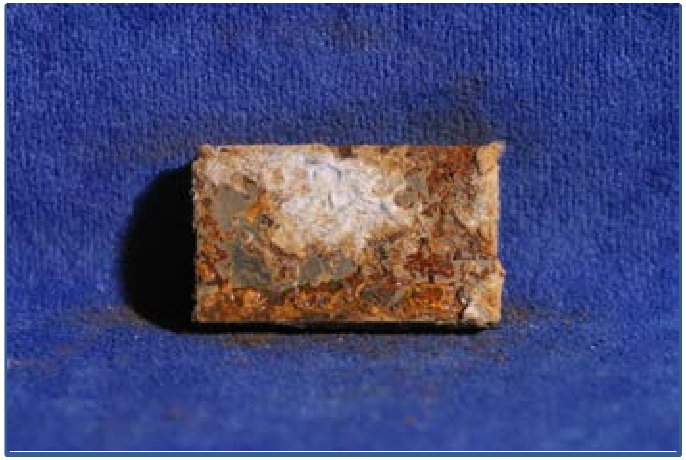

After Cleaning

SY102 – High Nitrate – 550 ppm NH_3 – 3 Months
Coupon # 502

Before Cleaning

After Cleaning

SY102 – High Nitrate – 550 ppm NH_3 – 3 Months
Coupon # 505

Before Cleaning

After Cleaning

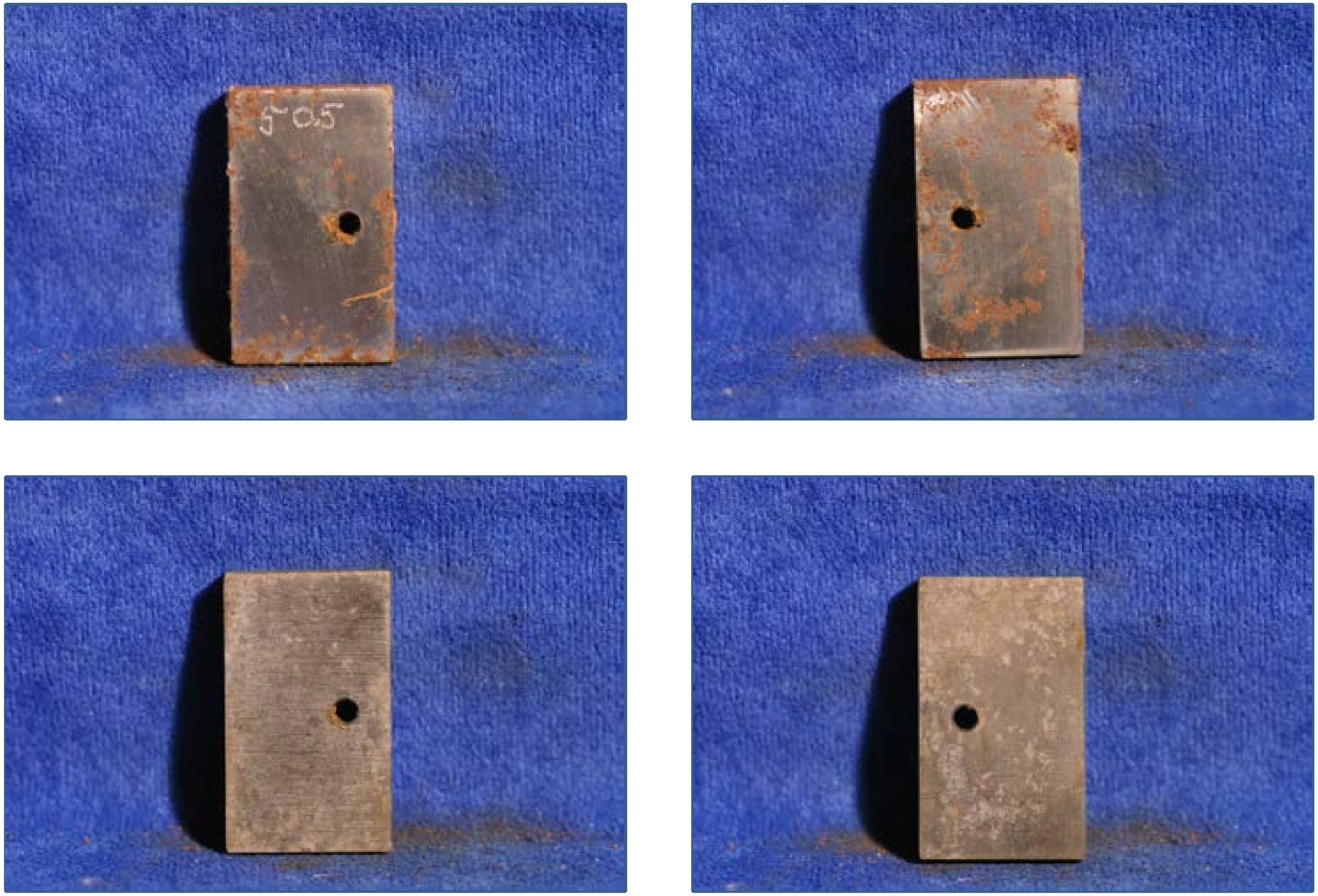

SY102 – High Nitrate – 50 ppm NH_3 – 4 Months
Coupon # 508

Before Cleaning

After Cleaning

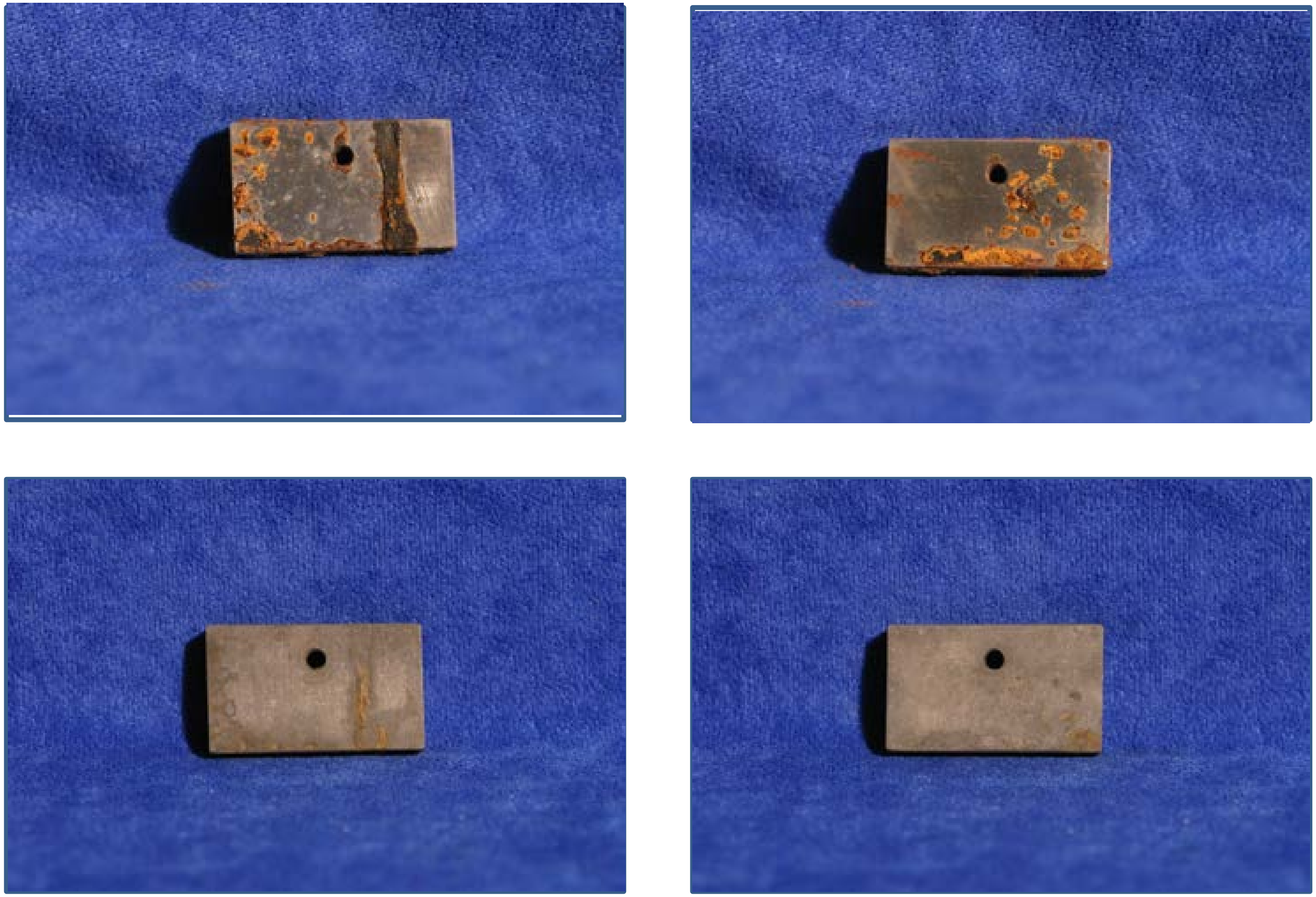

SY102 – High Nitrate – 50 ppm NH_3 – 4 Months
Coupon # 509

Before Cleaning

After Cleaning

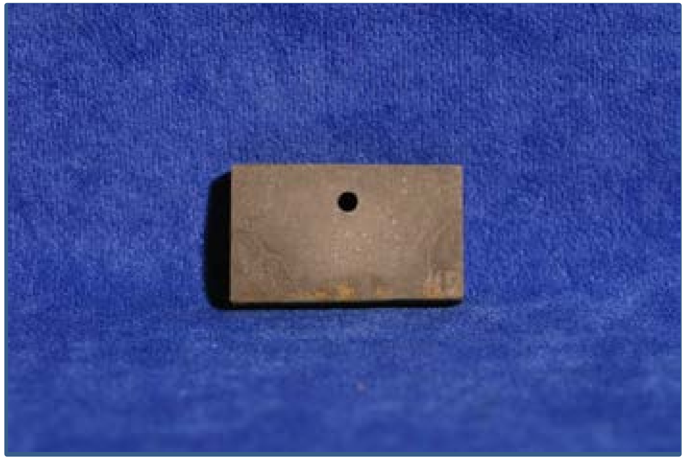

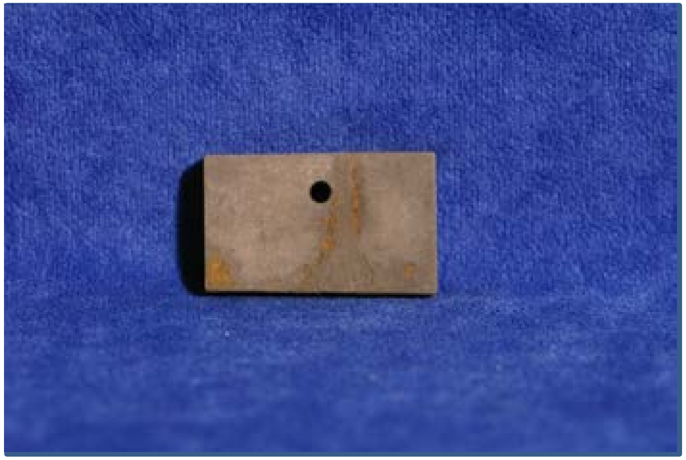

SY102 – High Nitrate – 550 ppm NH_3 – 4 Months
Coupon # 510

Before Cleaning

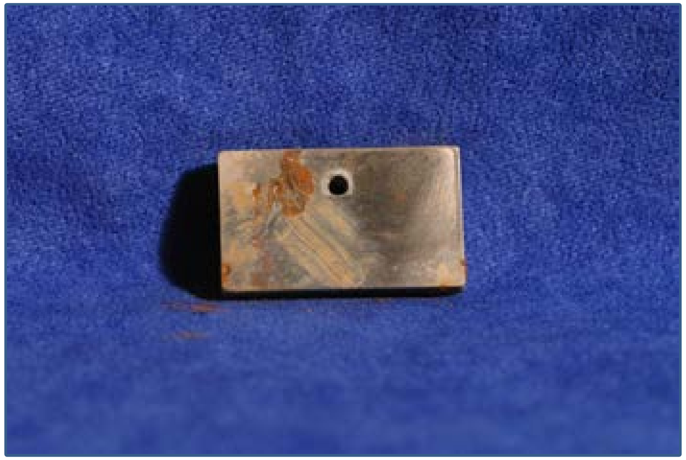

After Cleaning

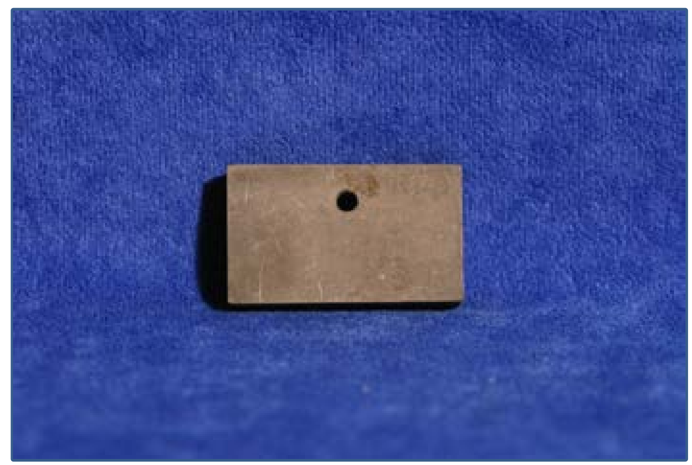

SY102 – High Nitrate – 550 ppm NH_3 – 4 Months
Coupon # 513

Before Cleaning

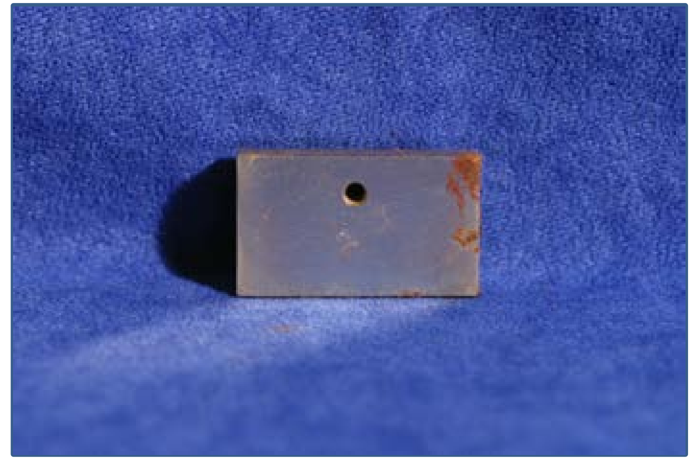

After Cleaning

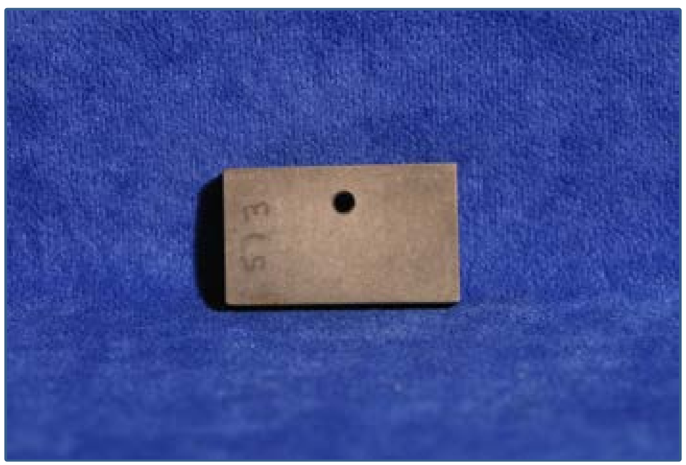

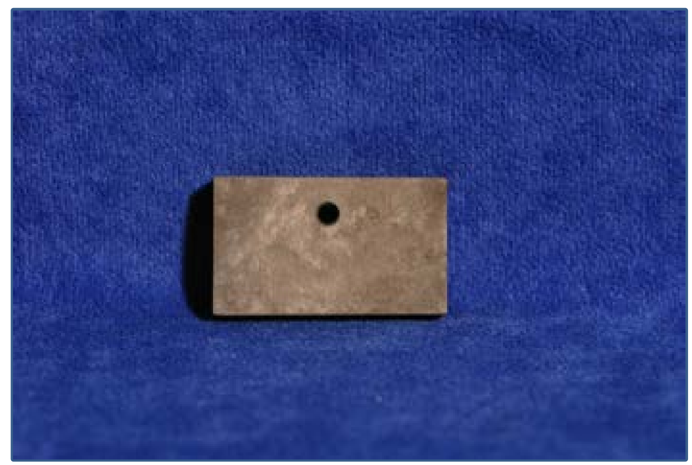

Visual Observations and Pit Measurements of Coupons*
SY102 – High Nitrate – 550 ppm NH_3

Time (mo.)	Coupon #	Weight Loss (g)	Depth (mils)	Diameter (mils)	Depth/Diameter	Qualitative Density Estimate
1	501	0.0103	NA	NA	NA	No Attack
	506	0.0406	NA	NA	NA	No Attack
2	503	0.0097	NA	NA	NA	No Attack
	507	0.0204	NA	NA	NA	No Attack
3	502	0.1061	NA	NA	NA	One small area of light surface attack. Less than 1 mil depth, less than 5% of surface area.
	505	0.0714	NA	NA	NA	No Attack
4	513	0.0974	NA	NA	NA	No Attack
	510	0.1223	NA	NA	NA	No Attack

* NA – no pitting observed

Visual Observations and Pit Measurements of Coupons*
SY102 – High Nitrate – 50 ppm NH_3

Time (mo.)	Coupon #	Weight Loss (g)	Depth (mils)	Diameter (mils)	Depth/Diameter	Qualitative Density Estimate
1	518	0.4323	NA	NA	NA	A couple of small areas of attack near edge (< 1 mil deep).
	514	0.1189	NA	NA	NA	No attack
2	517	0.075	NA	NA	NA	A couple of small areas near edge (< 1 mil deep). Less than 5% of area.
	522	0.0783	NA	NA	NA	A couple of small areas near edge (< 1 mil deep). Less than 10% of area.
3	523	0.1968	3.4	12	0.28	Some areas of localized general attack. Approximately 1-5 mils deep. Approximately 25% coupon is attacked.
			1.6	6.4	0.25	
			1.8	5.3	0.34	
			1.7	5.1	0.33	
			3.9	9.2	0.42	
			3.4	5.7	0.60	
			4.6	NA	NA	
	524	0.3435	2.5	NA	NA	Several areas of localized general attack. Approximately 1-3 mils deep. Approximately 25% of coupon attacked.
			2	6.4	0.313	
			1.8	7.3	0.247	
			5.9	NA	NA	
			3.5	12.1	0.289	
			2.5	9.7	0.258	
			2.9	5.4	0.537	

* NA – pits within locally attacked area and difficult to discern

Visual Observations and Pit Measurements of Coupons*
SY102 – High Nitrate – 50 ppm NH_3
continued

Time (mo.)	Coupon #	Weight Loss (g)	Depth (mils)	Diameter (mils)	Depth/Diameter	Qualitative Density Estimate
4	508	0.2581	NA	NA	NA	A few areas of localized general attack. Approximately 1-4 mils deep. Approximately 10% of coupon attacked. Several tiny pits approximately 1 mil or less deep. No discernable larger pits.
	509	0.3367	3.4	NA	NA	A few areas of localized general attack. Approximately 1-3 mils deep. Approximately 15% of coupon attacked. Several tiny pits approximately 1 mil or less deep.
			3.4	NA	NA	
			2.4	6.2	0.387	
			3	6.3	0.476	
			3.2	8.1	0.395	

* NA – pits within locally attacked area and difficult to discern

APPENDIX D

New Limits Coupon Test Data

Solution 1 – 1 Month
Coupon # 36

Before Cleaning

After Cleaning

Solution 1 – 1 Month
Coupon # 32

Before Cleaning

After Cleaning

Solution 1 – 2 Months
Coupon # 37

Before Cleaning

After Cleaning

Solution 1 – 2 Months
Coupon # 38

Before Cleaning

After Cleaning

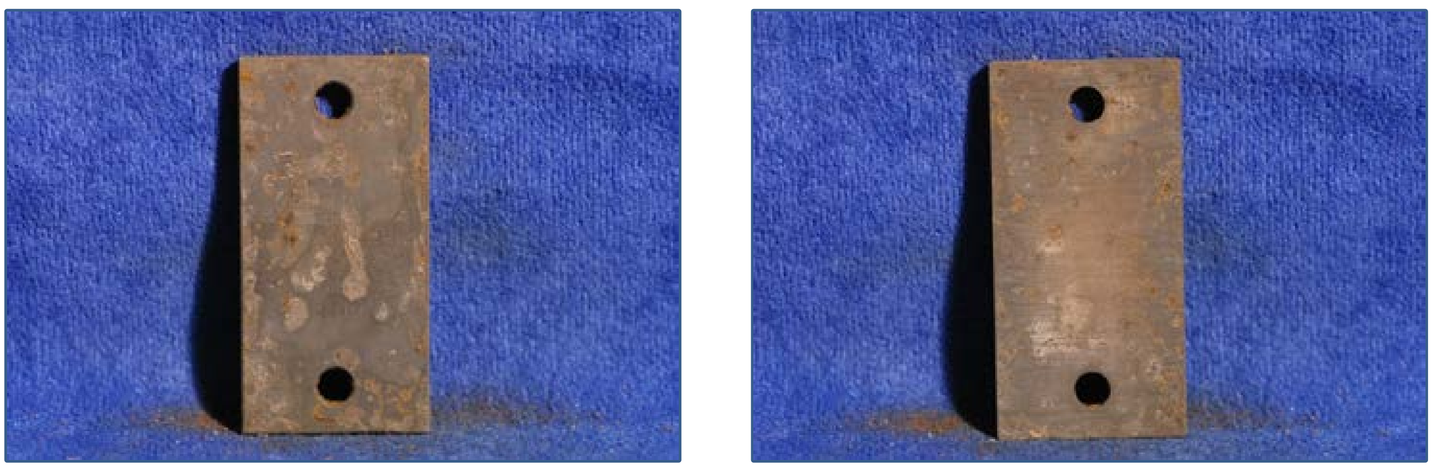

Solution 1 – 3 Months
Coupon # 09

Before Cleaning

After Cleaning

Solution 1 – 3 Months
Coupon # 10

Before Cleaning

After Cleaning

Solution 1 – 4 Months
Coupon # 15

Before Cleaning

After Cleaning

Solution 1 – 4 Months
Coupon # 16

Before Cleaning

After Cleaning

Solution 2 – 1 Month
Coupon # 408

Before Cleaning

After Cleaning

Solution 2 – 1 Month
Coupon #411

Before Cleaning

After Cleaning

Solution 2 – 2 Months
Coupon # 410

Before Cleaning

After Cleaning

Solution 2 – 2 Months
Coupon # 412

Before Cleaning

After Cleaning

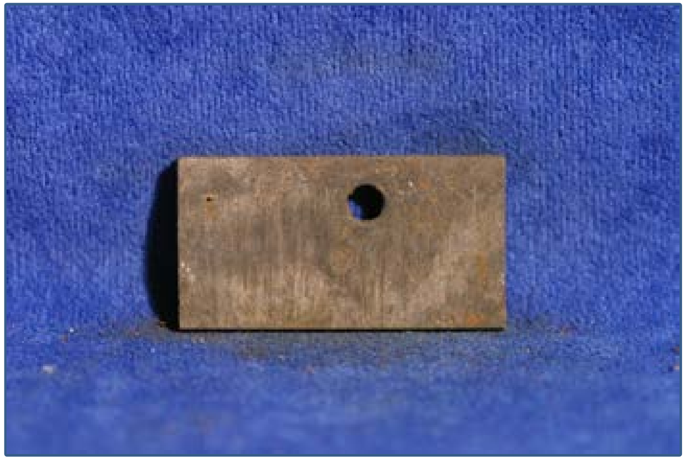

Solution 2 – 3 Months
Coupon # 453

Before Cleaning

After Cleaning

Solution 2 – 3 Months
Coupon # 458

Before Cleaning

After Cleaning

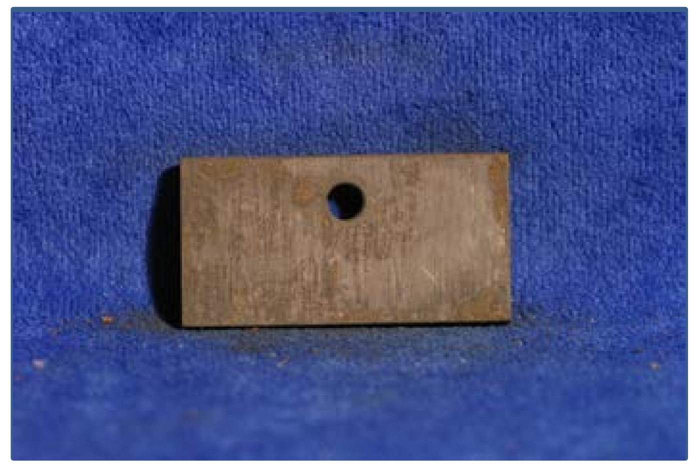

Solution 2 – 4 Months
Coupon # 457

Before Cleaning

After Cleaning

Solution 2 – 4 Months
Coupon # 459

Before Cleaning

After Cleaning

Solution 3 – 1 Month
Coupon #448

Before Cleaning

After Cleaning

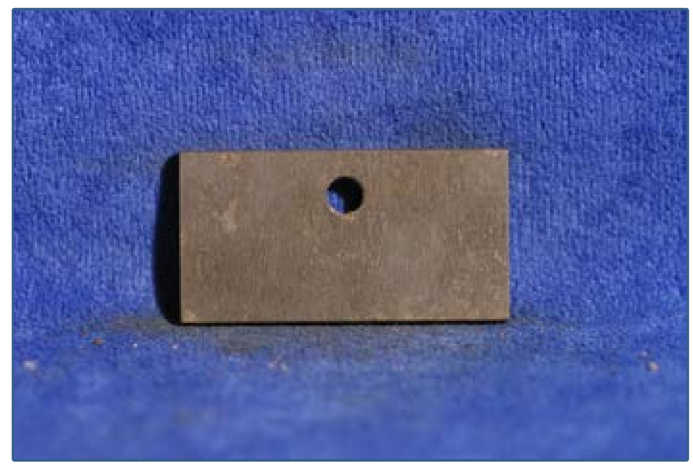

Solution 3 – 1 Month
Coupon # 451

Before Cleaning

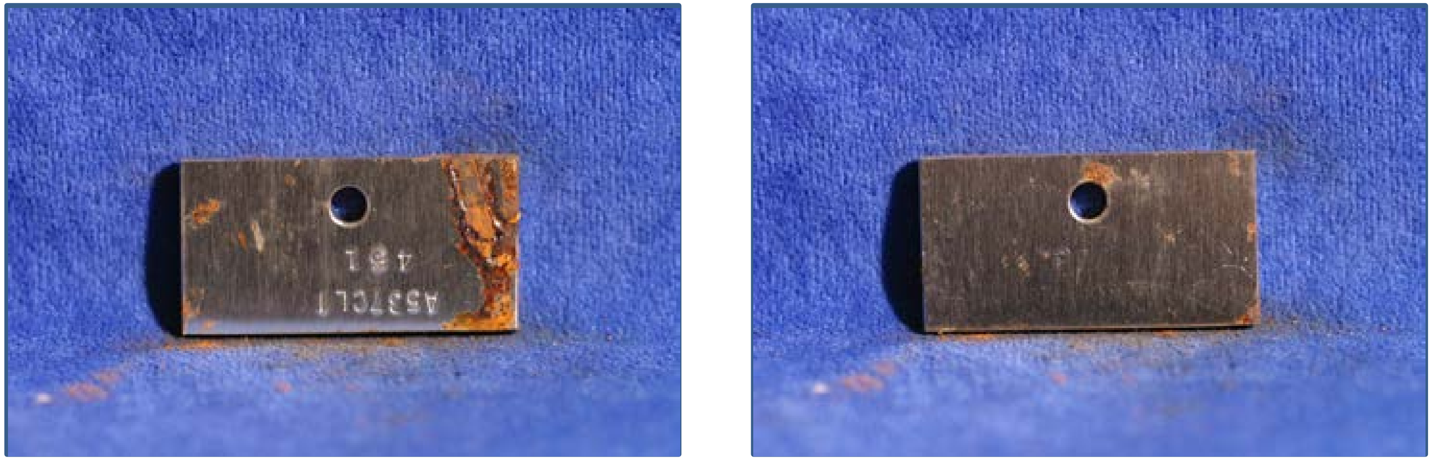

After Cleaning

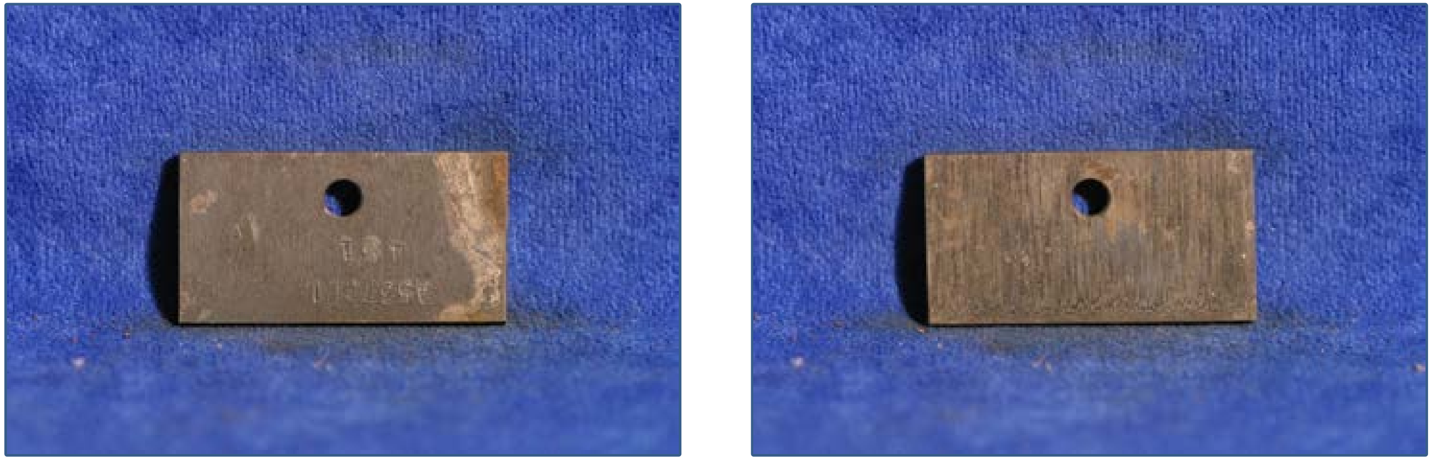

Solution 3 – 2 Months
Coupon # 406

Before Cleaning

After Cleaning

Solution 3 – 2 Months
Coupon # 407

Before Cleaning

After Cleaning

Solution 3 – 3 Months
Coupon # 405

Before Cleaning

After Cleaning

Solution 3 – 3 Months
Coupon # 409

Before Cleaning

After Cleaning

Solution 3 – 4 Months
Coupon # 449

Before Cleaning

After Cleaning

Solution 3 – 4 Months
Coupon # 450

Before Cleaning

After Cleaning

Visual Observations and Pit Measurements of Coupons*
Solution 1

Time (mo.)	Coupon #	Weight Loss (g)	Depth (mils)	Diameter (mils)	Depth/Diameter	Qualitative Density Estimate
1	36	0.1404	1.7	5.4	0.31	Several areas of localized general attack randomly oriented on sample. Small pits in and around areas noted.
			2	5	0.40	
			1.9	4	0.48	
			1.9	9	0.21	
			2.8	7.9	0.35	
	32	0.1586	2.1	6.2	0.34	A few areas of localized general attack randomly oriented on sample; not as many as 36. Small pits in and around areas noted.
			1.8	4.2	0.43	
			1.5	3.7	0.41	
			1.7	10.4	0.16	
			2	4.9	0.41	
2	38	0.2337	3.5	13.2	0.27	Several areas of localized general attack randomly oriented on sample. Attack is more intense than 1 month.
			1.9	7.9	0.24	
			2.1	9.8	0.21	
			2.7	NA	NA	
			1.8	6.5	0.28	
	37	0.2577	2.6	4.8	0.54	Several areas of localized general attack randomly oriented on sample. Attack is more intense than 1 month.
			2.5	NA	NA	
			2.6	NA	NA	
			2.8	NA	NA	
			2.3	NA	NA	

* NA – pits within locally attacked area and difficult to discern

Visual Observations and Pit Measurements of Coupons*
Solution 1
continued

Time (mo.)	Coupon #	Weight Loss (g)	Depth (mils)	Diameter (mils)	Depth/Diameter	Qualitative Density Estimate
3	10	0.3341	2.1	12.2	0.17	Several areas of localized general attack randomly oriented on sample. Attack on edges. Areas of localized corrosion 1-3 mils deep.
			2.7	NA	NA	
			2.4	NA	NA	
			2.6	NA	NA	
			2.6	9.2	0.28	
	9	0.2485	NA			Several areas of localized general attack randomly oriented on sample. Attack on edges. Areas of localized corrosion 1-3 mils deep.
4	15	0.361	2.5	23.2	0.11	Several areas of localized general attack. Areas are 1-4 mils deep. Some pits in and around areas.
			2	8.4	0.24	
			2.3	6.9	0.33	
			3.6	9.8	0.37	
			2	12.1	0.17	
	16	0.2863	2.8	8.8	0.32	Several areas of localized general attack. Areas are 2-4 mils deep. Areas are approximately 50 mils wide. Some pits in and around areas.
			2.7	5.9	0.46	
			2.4	6.8	0.35	
			2.3	11.6	0.20	
			2.8	5.6	0.50	

* NA – pits within locally attacked area and difficult to discern

Visual Observations and Pit Measurements of Coupons*
Solution 2

Time (mo.)	Coupon #	Weight Loss (g)	Depth (mils)	Diameter (mils)	Depth/Diameter	Qualitative Density Estimate
1	411	0.214	1.8	8.5	0.21	Several areas of localized general attack. Areas are approximately 1-3 mils deep. Pits within and around these areas.
			1.9	7.2	0.26	
			2.3	6.1	0.38	
			2.7	8.3	0.33	
			2.1	9.5	0.22	
	408	0.2603	1.5	5.6	0.27	Several areas of localized general attack. Particularly near edge. Areas are approximately 1-4 mils deep. Pits within and around these areas.
			1.4	2.7	0.52	
			1.8	5.3	0.34	
			2.6	4.7	0.55	
			2.4	8	0.30	
2	410	0.3394	2	7.8	0.26	Several areas of localized general attack. Particularly near edge. Areas are approximately 1-4 mils deep. Pits are difficult to discern.
	412	0.2429	2.6	NA	NA	Several areas of localized general attack. Particularly near edge. Areas are approximately 1-3 mils deep.
			2.5	NA	NA	
			2.6	NA	NA	
			2.4	4.6	0.52	
			1.6	4.9	0.33	

* NA – pits within locally attacked area and difficult to discern

Visual Observations and Pit Measurements of Coupons*
Solution 2
continued

Time (mo.)	Coupon #	Weight Loss (g)	Depth (mils)	Diameter (mils)	Depth/Diameter	Qualitative Density Estimate
3	453	0.1182	2.2	6.8	0.32	Several areas of localized general attack. Particularly near edge. Areas are approximately 1-3 mils deep.
			1.8	4.8	0.38	
			2.2	5.8	0.38	
			2.3	5.3	0.43	
	458	0.1563	1.9	6.3	0.30	Several areas of localized general attack. Particularly near edge. Areas are approximately 1-3 mils deep.
4	457	0.3043	4.1	NA	NA	Several areas of localized general attack. Particularly near edge. Areas are approximately 1-3 mils deep. Most severe attack for solution 2.
			2	5.3	0.38	
			1.5	6.5	0.23	
			1.8	6.5	0.28	
			2.5	NA	NA	
	459	0.2975	3.1	NA	NA	Several areas of localized general attack. Particularly near edge. Areas are approximately 1-3 mils deep. Most severe attack for solution 2. Approximately 1/3 of coupon attacked.
			4.3	NA	NA	
			3.8	NA	NA	
			3.9	7.9	0.49	

* NA – pits within locally attacked area and difficult to discern

Visual Observations and Pit Measurements of Coupons*
Solution 3

Time (mo.)	Coupon #	Weight Loss (g)	Depth (mils)	Diameter (mils)	Depth/Diameter*	Qualitative Density Estimate
1	448	-0.0012	3.3	10.57	0.31	Sample was clean with just a couple of spots of corrosion.
	451	0.045	3.1	13.3	0.23	Sample was clean with just a couple of small areas of localized general attack. Very low pit density.
			2	6.5	0.31	
			2.4	5.3	0.45	
			2.9	5.8	0.50	
			1.6	4.8	0.33	
2	406	0.052	NA	NA	NA	A couple of small areas of localized general attack. Some small pits, all less than 1 mil deep.
	407	0.0496	NA	NA	NA	A couple of small areas of localized general attack. Some small pits, all less than 1 mil deep.

* NA – pits within locally attacked area and difficult to discern

Visual Observations and Pit Measurements of Coupons*
Solution 3
continued

Time (mo.)	Coupon #	Weight Loss (g)	Depth (mils)	Diameter (mils)	Depth/Diameter	Qualitative Density Estimate
3	405	0.1209	1.3	5.7	0.23	A few more areas of localized general attack was observed. However attack is still very limited. Appears that pits are coalescing.
			1.3	5	0.26	
			3.1	10.1	0.31	
			1.6	7.7	0.21	
			2.8	5.9	0.47	
	409	0.0975	2.9	4.9	0.59	A few more areas of localized general attack was observed. However attack is still very limited. Appears that pits are coalescing.
			2.9	NA	NA	
			1.9	4.7	0.40	
			2.2	6.3	0.35	
			3.5	8.4	0.42	
4	449	0.1555	2.5	6.5	0.38	Areas of localized general corrosion intensified, however, much of coupon is still unattacked.
			3.5	6.1	0.57	
			2.4	5.1	0.47	
			2.2	10.8	0.20	
			3	7	0.43	
	450	0.122	2.3	4.6	0.50	Areas of localized general corrosion intensified, however, much of coupon is still unattacked. Less attack than was on 449
			2.2	5.8	0.38	
			3	6.7	0.45	
			2.3	4.3	0.53	
			2.5	8.2	0.30	

* NA – pits within locally attacked area and difficult to discern